MONITORING THERAPY RESISTANCE IN ADVANCED PROSTATE CANCER USING LIQUID BIOPSIES

Levi Groen

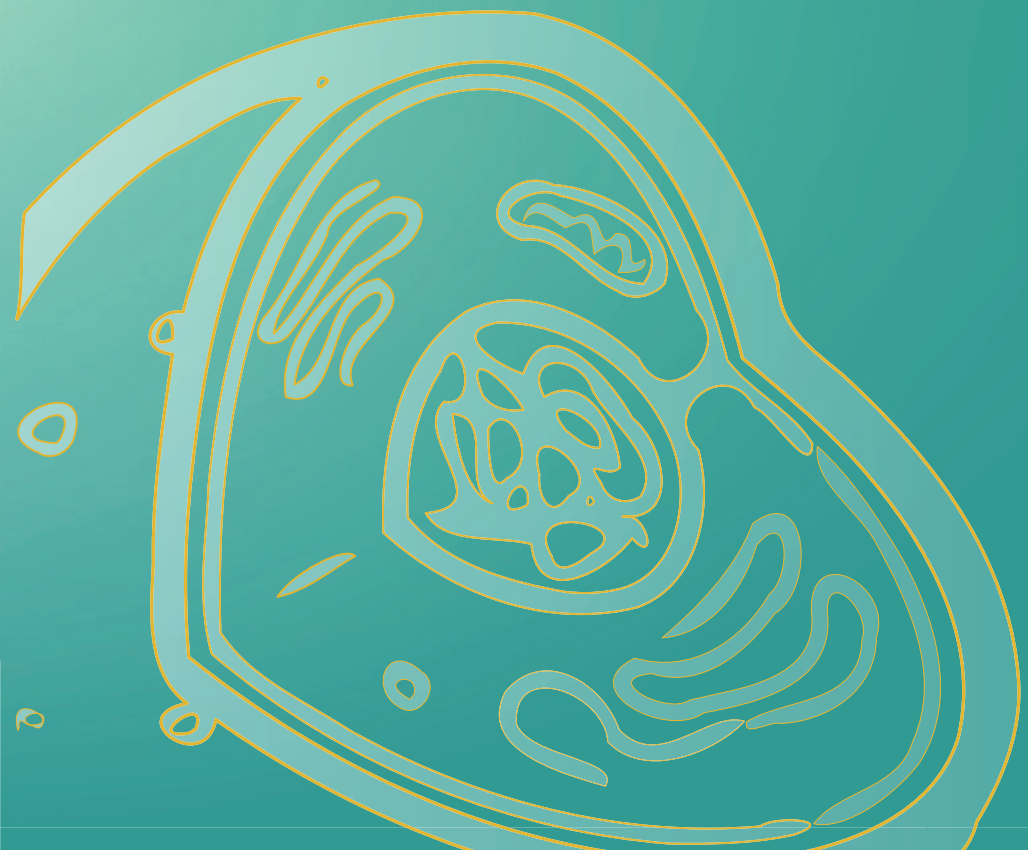

RADBOUD UNIVERSITY PRESS

Radboud Dissertation Series

Monitoring Therapy Resistance in Advanced Prostate Cancer Using Liquid Biopsies

Levi Naudin Groen

Monitoring Therapy Resistance in Advanced Prostate Cancer Using Liquid Biopsies
Levi Naudin Groen

Radboud Dissertation Series
ISSN: 2950-2772 (Online); 2950-2780 (Print)

Published by RADBOUD UNIVERSITY PRESS
Postbus 9100, 6500 HA Nijmegen, The Netherlands
www.radbouduniversitypress.nl

Design: Levi Naudin Groen
Cover: Charlotte Burgmans
Printing: DPN Rikken/Pumbo

ISBN: 9789465152417
DOI: 10.54195/9789465152417
Free download at: https://doi.org/10.54195/9789465152417

RADBOUD UNIVERSITY PRESS

Monitoring Therapy Resistance in Advanced Prostate Cancer Using Liquid Biopsies

Proefschrift ter verkrijging van de graad van doctor
aan de Radboud Universiteit Nijmegen
op gezag van de rector magnificus prof. dr. J.M. Sanders,
volgens besluit van het college voor promoties
in het openbaar te verdedigen op

maandag 13 april 2026

om 16.30 uur precies

door

Levi Naudin Groen

geboren op 9 mei 1992
te Leusden

Promotoren:

Prof. dr. J.A. Schalken

Prof. dr. P.F.A. Mulders

Dr. N. Mehra

Manuscriptcommissie:

Dr. W.J.G. Melchers

Prof. dr. G. Jenster (Erasmus MC)

Prof. dr. L.W.M.M. Terstappen (Universiteit Twente)

Monitoring Therapy Resistance in Advanced Prostate Cancer Using Liquid Biopsies

Dissertation to obtain the degree of doctor
from Radboud University Nijmegen
on the authority of the Rector Magnificus prof. dr. J.M. Sanders,
according to the decision of the Doctorate Board
to be defended in public on

Monday, April 13, 2026

at 4.30 pm

by

Levi Naudin Groen

born on May 9, 1992
in Leusden (the Netherlands)

Supervisors:

Prof. dr. J.A. Schalken

Prof. dr. P.F.A. Mulders

Dr. N. Mehra

Manuscript Committee:

Dr. W.J.G. Melchers

Prof. dr. G. Jenster (Erasmus MC)

Prof. dr. L.W.M.M. Terstappen (University of Twente)

"*How can one capture genes that behave like ghosts influencing cells from behind some dark curtain?*"

Robert Weinberg

Contents

List of Figures

List of Tables

List of Abbreviations

ADT androgen deprivation therapy

AI artificial intelligence

AKT protein kinase B

ALK anaplastic lymphoma kinase

AR androgen receptor

ARSI androgen receptor signaling inhibitor

ARSIs androgen receptor signaling inhibitors

ARv7 androgen receptor splice variant 7

BCT blood collection tube

BMI body mass index

BPH benign prostatic hyperplasia

CEA carcinoembryonic antigen

cfDNA cell-free DNA

CK cytokeratin

CNA copy-number alteration

CNAs copy-number alterations

CRPC castration-resistant prostate cancer

csPCa clinically significant prostate cancer

CTC circulating tumor cell

CTCs circulating tumor cells

CI confidence interval

ctDNA circulating tumor DNA

CZ central zone

DAPI 4',6-diamidino-2-phenylindole

DDR DNA damage repair

DRE digital rectal examination

EGFR epidermal growth factor receptor

EMT epithelial-to-mesenchymal transition

EpCAM epithelial cell adhesion molecule

FAIR Findable, Accessible, Interoperable, and Reusable

FDA Food and Drug Administration

FZ anterior fibromuscular zone

GTEx Genotype-Tissue Expression

GSV genomic structural variant

HER2 human epidermal growth factor receptor 2

HR hazard ratio

HRR homologous recombination repair

HyCEAD Hybrid Capture Enrichment Amplification and Detection

IJMS International Journal of Molecular Sciences

lncRNA long non-coding RNA

lncRNAs long non-coding RNAs

LoD limit of detection

mCRPC metastatic castration-resistant prostate cancer

MET mesenchymal-to-epithelial transition

mPCa metastatic prostate cancer

mRNA messenger RNA

mpMRI multiparametric magnetic resonance imaging

MRI magnetic resonance imaging

MPS MyProstateScore

MSI microsatellite instability

NEPC neuroendocrine prostate cancer

NPV negative predictive value

OS overall survival

PARP poly(ADP-ribose) polymerase

PARPi poly(ADP-ribose) polymerase inhibitor(s)

PBMC peripheral blood mononuclear cell

PCa prostate cancer

PCA3 prostate cancer antigen 3

PD-L1 programmed death-ligand 1

PET positron emission tomography

PET/CT positron emission tomography / computed tomography

PFS progression-free survival

PI3K phosphatidylinositol 3-kinase

PI3K/AKT/mTOR phosphatidylinositol 3-kinase / protein kinase B / mechanistic target of rapamycin

PPAR peroxisome proliferator-activated receptor

PRAD prostate adenocarcinoma

PSA prostate-specific antigen

PSMA prostate-specific membrane antigen

PSMA PET/CT prostate-specific membrane antigen positron emission tomography / computed tomography

PZ peripheral zone

qPCR quantitative polymerase chain reaction

RCT randomized controlled trial

RNA-FISH RNA-fluorescent in situ hybridization

siRNA small interfering RNA

SOC standard of care

sPSA serum prostate-specific antigen

TCGA The Cancer Genome Atlas

TMB tumor mutational burden

TSS transcription start site

TZ transition zone

USPSTF United States Preventive Services Task Force

AUC area under the (receiver operating characteristic) curve

AS2 *NAALADL2-AS2* (shorthand used in figure captions)

CE-IVD European Conformity–in vitro Diagnostics

CLIA Clinical Laboratory Improvement Amendments

CSS charcoal-stripped serum

DepMap Cancer Dependency Map

FPKM fragments per kilobase of transcript per million mapped reads

GEPIA2 Gene Expression Profiling Interactive Analysis 2

GRCh37/hg19 Genome Reference Consortium Human Build 37 / human genome 19

GRCh38/hg38 Genome Reference Consortium Human Build 38 / human genome 38

GS Gleason score

h hour(s)

KD knockdown

LDT laboratory-developed test

MALAT1 Metastasis Associated Lung Adenocarcinoma Transcript 1

NAALADL2-AS2 N-Acetylated Alpha-Linked Acidic Dipeptidase Like 2 Antisense Transcript 2

PDF portable document format

pPCa primary prostate cancer

RC transfection reagent control

R1881 synthetic androgen (methyltrienolone)

SCR scrambled control (e.g., scrambled GapmeR)

UCSC University of California, Santa Cruz

Chapter 1

General Introduction

Adapted from:
Groen, L. & Schalken, J. Liquid Biopsy for Prostate and Bladder Cancer: Progress and Pitfalls. European Urology Focus (2022).

1.1 The Prostate

The prostate is a small, walnut-sized gland located below the bladder that functions as an accessory organ of the male reproductive system. Its secretions contribute essential nutrients and proteins to seminal fluid, supporting the production of viable ejaculate. The prostate consists of smooth muscle tissue and glandular tissue. It can be divided into several anatomical zones: a transition zone (TZ), a central zone (CZ), a peripheral zone (PZ), and an anterior fibromuscular zone (FZ) (Figure 1.1).

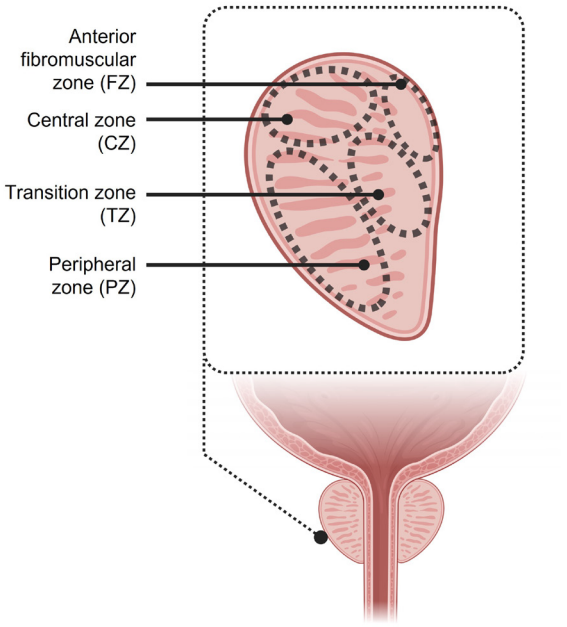

Figure 1.1: The anatomy of the prostate.

TZ comprises the smallest volume of the prostate (5%) but can expand significantly with age, primarily due to benign prostatic hyperplasia (BPH). As the TZ expands, it causes urinary problems by compressing the urethra, making urination difficult. The CZ surrounds the TZ, makes up approximately 25% of the gland, and is typically not associated with BPH or other forms of

neoplasia. The PZ comprises approximately 65% of the prostate, with the FZ forming the remaining 5%. The prostatic ducts of the PZ are the most susceptible to cancer and consist of epithelial, basal, and neuroendocrine cells that surround a lumen (Figure 1.2). Almost all prostate tumors (95%) arise from epithelial cells in the PZ, neuroendocrine cells are responsible for approximately 1%, and the remaining 4% arise from several rare carcinomas, such as small cell carcinoma [1].

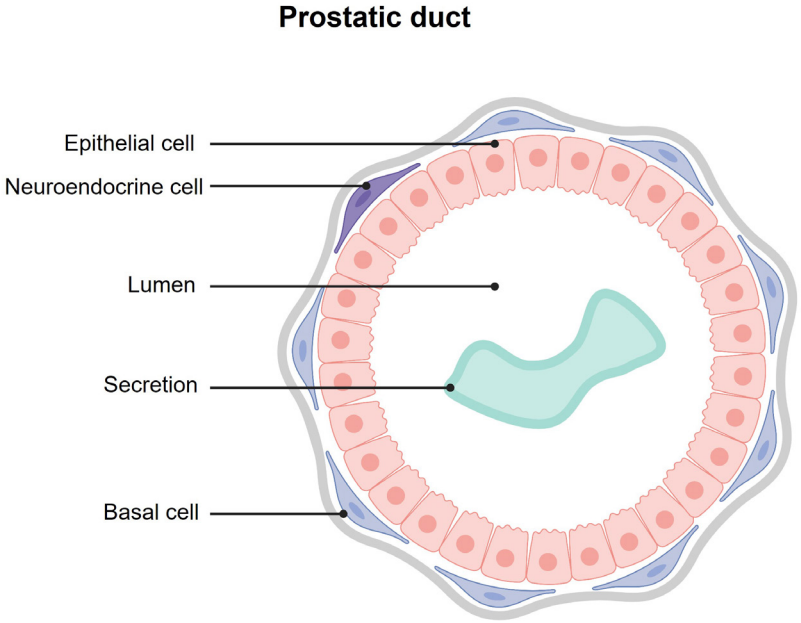

Figure 1.2: Cross section of the prostatic duct.

1.2 Challenges in the Treatment of Prostate Cancer

Prostate cancer (PCa) constituted 27% of new cancer cases in men in the United States during 2021, ranking first in this cohort [2]. The response to PCa therapy can be dichotomous, with localized disease highly responsive to surgical and systemic therapy, while advanced disease often becomes

resistant to first-line therapy [3, 4]. Until recently, nearly all available therapeutic strategies were based on antagonizing the androgen receptor (AR). This idea was conceived in the first half of the twentieth century when Charles Huggins *et al.* discovered that medical castration, through the administration of estrogens, inhibited tumor growth in metastatic PCa (mPCa) [5]. Estrogens inhibit testicular androgen production via negative feedback on the hypothalamic-pituitary axis, which effectively reduces AR signaling in the prostate and inhibits tumor growth. This form of androgen deprivation therapy (ADT) is comparable to orchiectomy (surgical removal of the testes) and became the gold standard for the treatment of mPCa until the 1970s [3, 5]. Although effective, estrogenic medical castration is associated with cardiovascular stress and has been shown to induce cardiac events and excess mortality. The study of antiandrogenic compounds in the late 1960s and early 1970s led to the development of several novel androgenic hormone therapies with similar efficacy and fewer side effects than estrogen-based therapy [5].

Following PCa diagnosis, biopsy tissue is graded to estimate tumor aggressiveness by assessing how differentiated the cancer cells appear under a microscope. This grading method, known as the Gleason classification system, was developed by Dr. Donald Gleason in the 1960s and remains central to guiding prognosis and treatment decisions in PCa [6]. Many of the clinical tools used to manage PCa find their origins in the twentieth century (Figure 1.3).

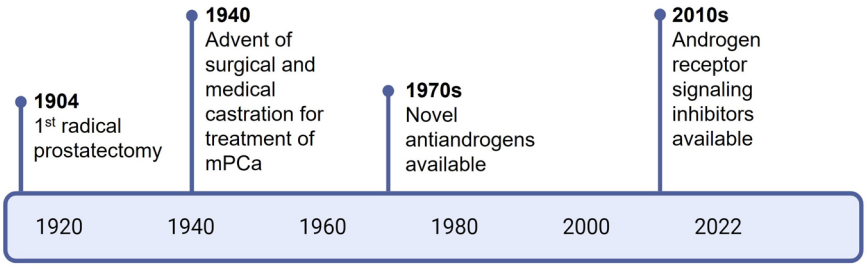

Figure 1.3: Key developments in PCa therapeutics.

First-line hormone therapy is remarkably successful for patients with localized and metastatic PCa. However, resistance to ADT and progression to castration-resistant prostate cancer (CRPC) develops in nearly 20% of patients with metastatic disease within five years of treatment [7]. Metastatic CRPC (mCRPC) is the leading cause of PCa-related death and is characterized by substantial morbidity, with a median survival of 24–36 months despite the availability of several second-line therapeutic approaches [8].

The continued reliance on solid tissue biopsies to identify drug-resistant alterations may limit progress. Conventional biopsies do not capture clonal heterogeneity and are limited by their invasive nature and the inaccessibility of certain lesions [9]. Inadequate insight into dynamic spatiotemporal alterations in PCa tumors has restricted the overall clinical benefit of novel therapies. Furthermore, the detection limit of traditional diagnostic imaging techniques is currently approximately 1 billion cells; below this threshold, malignant lesions are undetectable [10]. Together, these lesions can represent a significant tumor burden, exhibit a high degree of heterogeneity, and harbor genetic aberrations associated with resistance to therapy [11].

Liquid biopsies are a relatively non-invasive and less complex alternative to traditional biopsies. They allow clinicians to assess PCa in real time, which is useful in both diagnostic and disease management settings.

1.3 Liquid Biopsies in PCa

The history of liquid biopsies in PCa dates back to the late nineteenth century, when Australian pathologist Thomas Ashworth reported epithelial cells in the blood of a man with metastatic disease. He proposed that these circulating cells could contribute to metastasis, an early description of what are now known as circulating tumor cells (CTCs) [12]. The discovery of cell-free DNA (cfDNA) in 1948, nearly a century later, was another key development in the field of liquid biopsy research. This discovery, particularly the observation that cfDNA levels were elevated in patients with leukemia, renewed interest

in the field. The subsequent decades witnessed numerous discoveries that were instrumental in realizing the clinical potential of liquid biopsies in PCa.

The discovery of carcinoembryonic antigen (CEA) as a biomarker of colon cancer in the 1960s led to several studies exploring its diagnostic and prognostic utility as a blood or urine biomarker for PCa in the 1970s [13]. Several years later, in 1975, prostate-specific antigen (PSA) was purified [14]. The clinical utility of PSA would be realized in the 1990s when population screening of serum PSA levels revolutionized PCa diagnostics. Rapid adoption of PSA testing in the 1990s reduced the prevalence of advanced PCa at diagnosis by 80% and decreased PCa mortality by more than 42% in US men [15]. Although highly effective, PSA is not cancer-specific, and its use in the diagnosis of PCa is prone to produce false positives. Furthermore, prostatic PSA secretion is governed by the AR, which limits the clinical utility of PSA for androgen-sensitive PCa. Interestingly, CEA is used to monitor recurrence in patients with androgen-insensitive primary neuroendocrine prostate cancer (NEPC) [16].

For most diagnoses ($\approx$ 80%), PCa is not the primary cause of mortality. Hence, many men diagnosed with PCa are more likely to suffer than benefit from treatment. The overdiagnosis and treatment of PCa led the United States Preventive Services Task Force (USPSTF) to advise against PSA screening in 2012. This recommendation reduced the occurrence of localized PCa in men of all ages. However, it also increased the incidence of metastatic PCa (mPCa) in men 75 years and older [17] (Figure 1.4). As the use of diagnostic PSA screening decreases, the primary challenge in diagnosing PCa is to differentiate between clinically significant and indolent disease. In the 2000s, several urine biopsy tests were developed that have been shown to be highly sensitive and specific for detecting clinically significant PCa (csPCa) [18]. As a result, these urine-based tests can reduce overtreatment and improve the detection of csPCa. However, these tests are not commonly used in standard clinical practice [4]. The lack of standardization in preanalytical variables in liquid biopsy platforms makes it difficult to conduct effective

validation studies and hinders their implementation as tools to diagnose PCa in daily clinical practice [4, 19, 20]. This has led to a steady increase in the incidence of de novo mPCa since the USPSTF recommended against PSA screening in 2012.

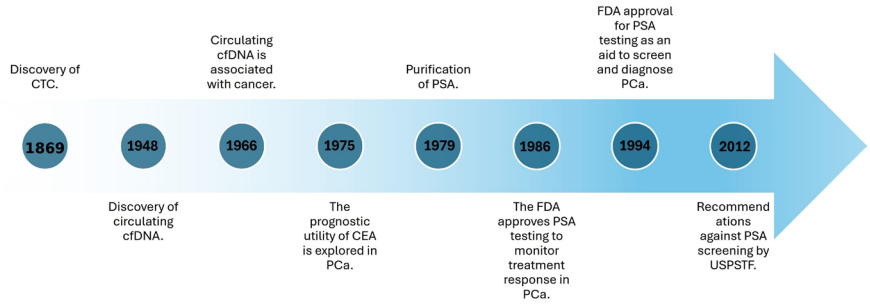

Figure 1.4: Milestones in PCa liquid biopsy research.

1.4 Outline of this Thesis

Chapter 2 centers on the clinical utility of emerging biomarkers in prostate cancer through the use of liquid biopsies. Traditional diagnostic methods, such as prostate-specific antigen (PSA) monitoring and tumor biopsies, are contrasted with liquid biopsies, highlighting their clinical utility and future potential. Various types of biomarkers derived from urine and blood are explored for their diagnostic and prognostic capabilities.

Chapter 3 focuses on the role of the long non-coding RNA (lncRNA) *NAALADL2-AS2* in promoting tumor cell survival in prostate cancer. It highlights how traditional use of ADT can lead to castration resistance, which remains a significant challenge in the treatment of PCa. The chapter contrasts the emerging role of lncRNAs in driving resistance to therapies.

Chapter 4 underscores the prognostic value of the subtypes of the PCa transcriptome, highlighting several clinically distinct epithelial subtypes.

The association between *NAALADL2-AS2* expression and PCa epithelial subtypes is explored.

Chapter 5 focuses on the use of circulating tumor cell transcriptome profiling to predict clinical outcomes in castration-resistant metastatic prostate cancer. The chapter explores how label-free enrichment and targeted transcriptome profiling of CTCs can stratify patients with clinical outcomes. This chapter underscores the ability of CTC profiling to improve precision diagnostics and personalized treatment strategies in mCRPC, highlighting the need to integrate advanced molecular profiling techniques into clinical practice.

References

1. Oh, W. K., Hurwitz, M., D'Amico, A. V., Richie, J. P. & Kantoff, P. W. in *Holland-Frei Cancer Medicine. 6th edition* (BC Decker, 2003).
2. Siegel, R. L., Miller, K. D., Fuchs, H. E. & Jemal, A. Cancer statistics, 2022. *CA: A Cancer Journal for Clinicians* 72, 7–33 (Jan. 2022).
3. Schröder, F., Crawford, E. D., Axcrona, K., Payne, H. & Keane, T. E. Androgen deprivation therapy: past, present and future. *BJU international* 109 Suppl 6, 1–12 (June 2012).
4. Groen, L. & Schalken, J. Liquid Biopsy for Prostate and Bladder Cancer: Progress and Pitfalls. *European Urology Focus* 8, 904–906 (July 2022).
5. Crawford, E. D. Hormonal Therapy in Prostate Cancer: Historical Approaches. *Rev Urol* 6, S3–S11 (2004).
6. Montironi, R. *et al.* Prostate cancer: from Gleason scoring to prognostic grade grouping. *Expert Review of Anticancer Therapy* 16, 433–440 (Apr. 2, 2016).
7. Mansinho, A., Macedo, D., Fernandes, I. & Costa, L. in *Advances in Experimental Medicine and Biology* 117–133 (Springer New York LLC, 2018).
8. Toren, P. J. & Gleave, M. E. Evolving landscape and novel treatments in metastatic castrate-resistant prostate cancer. *Asian Journal of Andrology* 15, 342–349 (May 2013).
9. Gilson, P., Merlin, J. L. & Harlé, A. Deciphering Tumour Heterogeneity: From Tissue to Liquid Biopsy. *Cancers* 14 (Mar. 1, 2022).
10. Frangioni, J. V. New technologies for human cancer imaging. *Journal of Clinical Oncology* 26, 4012–4021 (2008).
11. Braun, S. *et al.* A Pooled Analysis of Bone Marrow Micrometastasis in Breast Cancer. *New England Journal of Medicine* 353, 793–802 (Aug. 25, 2005).

12. Ashworth, T. A case of cancer in which cells similar to those in the tumours were seen in the blood after death. *The Medical Journal of Australia* 14, 146–147 (1869).
13. Guinan, P., Dubin, A., Bush, I., Alsheik, H. & Ablin, R. J. *The CEA Test in Urologie Cancer: an Evaluation and a Review* Publication Title: Oncology Volume: 32 (1975), 158–168.
14. Wang, M. C., Valenzuela, L. A., Murphy, G. P. & Chu, T. M. Purification of a human prostate specific antigen1. *Journal of Urology* 167, 1226–1230 (Mar. 2002).
15. Catalona, W. J. History of the discovery and clinical translation of prostate-specific antigen. *Asian Journal of Urology* 1, 12–14 (Oct. 2014).
16. Bray, A. W. *et al.* Elevated serum CEA is associated with liver metastasis and distinctive circulating tumor DNA alterations in patients with castration-resistant prostate cancer. *The Prostate* 82, 1264–1272 (2022).
17. Jemal, A. *et al.* Prostate Cancer Incidence and PSA Testing Patterns in Relation to USPSTF Screening Recommendations. *JAMA* 314, 2054–2061 (Nov. 17, 2015).
18. Matuszczak, M., Schalken, J. A. & Salagierski, M. Prostate cancer liquid biopsy biomarkers' clinical utility in diagnosis and prognosis. *Cancers* 13 (July 1, 2021).
19. Ignatiadis, M., Sledge, G. W. & Jeffrey, S. S. Liquid biopsy enters the clinic — implementation issues and future challenges. *Nature Reviews Clinical Oncology* 18. Number: 5, 297–312 (May 2021).
20. Oey, O., Ghaffari, M., Li, J. J. & Hosseini-Beheshti, E. Application of extracellular vesicles in the diagnosis and treatment of prostate cancer: Implications for clinical practice. *Critical Reviews in Oncology/Hematology* 167, 103495 (Nov. 1, 2021).

Chapter 2

Liquid Biopsies in Prostate Cancer

Adapted from:
Boerrigter, E., Groen, L. N., Van Erp, N. P., Verhaegh, G. W. & Schalken, J. A. Clinical utility of emerging biomarkers in prostate cancer liquid biopsies. Expert Review of Molecular Diagnostics 20, 219–230 (2020).

2.1 Urine Biomarkers in PCa

Tumors, like all tissues, require access to capillaries for the exchange of nutrients and the removal of metabolic waste products. Capillaries also enable the release of tumor-derived materials into the bloodstream, making blood an ideal candidate for liquid biopsies. However, blood contains a mixture of biomarkers from both healthy and malignant cells, which can make it more challenging to detect cancer-specific signals. In contrast, urine presents an additional and often cleaner source of effective biomarkers for urological cancers because it typically contains fewer non-cancerous cells, reducing background noise and potentially improving the accuracy of cancer detection. The glandular anatomy of the prostate facilitates the release of tumor material into urine, both through the excretion of prostatic fluid and as urine passes through the urethra. Despite these advantages, most biofluids, including urine, require upfront enrichment of tumor content to achieve a sufficient signal-to-background ratio for molecular analysis.

Digital rectal examination (DRE), commonly used to diagnose PCa, significantly raises tumor-derived molecule levels in urine compared to samples taken before DRE. Consequently, several urine biomarkers discovered around the 2000s have established their clinical relevance for the diagnosis of PCa, resulting in four commercial tests: Progensa® PCA3, SelectMDx™, MyProstateScore (MPS; formerly MiPS), and ExoDx™ Prostate (IntelliScore). These tests address key issues in PCa diagnostics, such as overtreatment and excessive biopsies due to reliance on sPSA, which is a surrogate of prostate size and is not cancer-specific. The Progensa PCA3 test, introduced in 2006, was the first available post-DRE urine liquid biopsy test. Although able to detect PCa with decent sensitivity and specificity, it did not show improvement above the standard of care (SOC) (that is, DRE and sPSA screening). By including additional biomarkers such as the *TMPRSS2-ERG* fusion gene, the sensitivity and specificity significantly improved the performance of the Progensa test. The MPS test implements a similar strategy that

increases the detection of csPCa and reduces unnecessary biopsies by 32% compared to SOC. Another post-DRE test, SelectMDx, is highly sensitive and specific in detecting csPCa. This test measures RNA transcripts of two oncogenes and supplemented with *KLK3* (the PSA gene) resulting in a reduction of 53% of avoidable biopsies. Unfortunately, specialized facilities and the reliance on DRE for PCa diagnostics are needed, which restricts accessibility to people living in underdeveloped, rural, and poverty-stricken regions. However, recently, the ExoDx test was shown to remain effective in detecting csPCa without a DRE, preventing unnecessary biopsies by 26% [1]. The urine liquid biopsy tests mentioned above have a high negative predictive value (NPV), as is evident from their ability to avoid unnecessary biopsies (Table 2.1). SelectMDx, MPS, and ExoDX tests have a particularly high sensitivity and NPV for csPCa (Gleason score ≥ 7). The clinical utility of these four liquid biopsy tests was extensively reviewed in a 2017 publication by Hendriks et al. [2]. One key limitation is their restricted utility in the localized setting, as prostatectomies make urine biopsies unsuitable for clinical management in advanced PCa.

Table 2.1: Clinically available urinary biomarker tests for PCa.

Biomarkers	Test	Predictive value*	Cert.	Ref.
PCA3, *KLK3*	Progensa PCA3	NPV=90%, AUC=0.71	CE-IVD, FDA	[3–5]
DLX1, *HOXC6*	SelectMDx	NPV=95%, AUC=0.85	CLIA, LDT, CE-IVD	[6, 7]
PCA3, *TMPRSS-ERG*	MyProstateScore	NPV=97%, AUC=0.77	CLIA, LDT	[8–10]
Exosomal RNA	ExoDx	NPV=94%, AUC=0.74	CLIA, LDT	[11]

AUC: Area Under the (Receiver Operating Characteristic) Curve. CE-IVD: European Conformity-in vitro Diagnostics. CLIA-certified LDT: Clinical Laboratory Improvement Amendments-based clinical laboratory-developed test. FDA: US Food and Drug Administration. NPV: Negative Predictive Value. Most tests, such as the SelectMDx test, factor in clinical parameters such as age, DRE, family history of PCa, prostate volume, and serum PSA. Predictive value* is defined as the ability of a test to detect clinically significant disease (GS$\geq$7).

2.2 Circulating Biomarkers in Prostate Cancer

Unfortunately, 20% of patients with advanced PCa have resistance to first-line androgen receptor signaling inhibitors (ARSIs), increasing with exposure to subsequent lines of ARSI therapy [12]. Clinical biomarkers are lacking to stratify this cohort, which has limited the potential of novel targeted and immune therapies in advanced PCa compared to other malignancies [13]. Tumor-derived material in the bloodstream provides a unique opportunity to characterize both localized and metastatic lesions. As such, liquid biopsies could be used to optimize treatment strategies and improve therapy response and survival outcomes in mCRPC. In the following sections, the prognostic utility of circulating tumor DNA, RNA, and cells is discussed.

2.2.1 Circulating Biomarkers

The discovery of novel circulating biomarkers continues to advance and holds significant potential for improving the diagnosis and prognosis of various cancers. In contrast to urinary biomarkers, circulating biomarkers are more suitable for monitoring therapeutic response due to their origins from both primary tumors and distant metastatic sites, thereby supporting precision medicine strategies. Tumors release viable cells, nucleic acids, tumor-educated platelets, exosomes, and cell-free nucleic acids into the circulation (Figure 2.1). These emerging biomarkers are increasingly being evaluated as surrogate endpoints in clinical trials and may be nearing clinical adoption [14, 15]. Additionally, tumor-associated proteins and metabolites have demonstrated potential as biomarkers for managing PCa; however, their integration into clinical practice remains in the early stages [16].

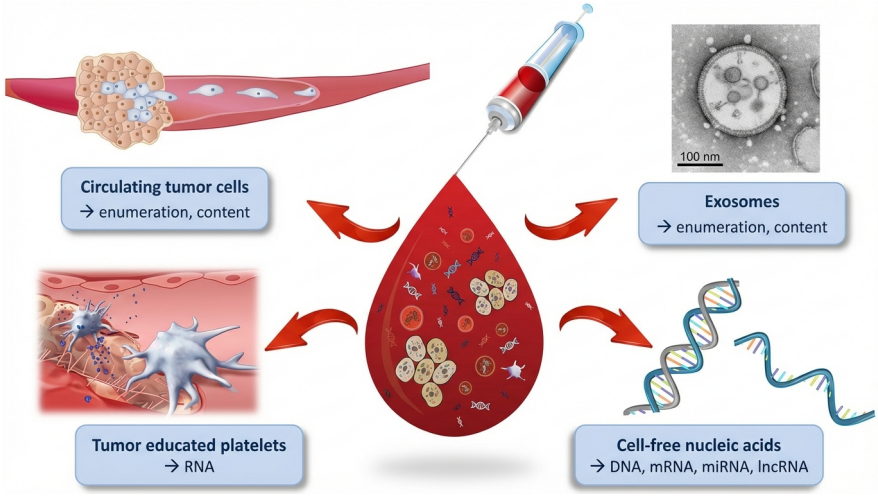

Figure 2.1: Circulating biomarkers.

Liquid biopsies contain a variety of clinically informative components. Blood samples can be analyzed for CTCs, tumor-educated platelets, exosomes, and cell-free nucleic acids, each providing valuable information. Adapted with permission from: Mader & Pantel [17].

Circulating DNA

Tumor-derived cfDNA, also known as circulating tumor DNA (ctDNA), is an emerging biomarker in PCa. Apoptosis followed by necrosis of nucleated cells is considered the primary source of cfDNA in blood. Active secretion of cfDNA is typically associated with malignancy [18]. Circulating DNA molecules are highly fragmented (150–200 base pairs) and are rapidly cleared from the bloodstream [19, 20]. Background levels of cfDNA in healthy individuals typically range from one to ten nanograms per milliliter. However, these levels can increase due to physiological stressors such as intense exercise, trauma, infection, and inflammation [20]. Clearance of low-molecular-weight cfDNA is possible through the kidneys, but its utility as a urine biomarker would depend on the glomerular filtration rate, as highlighted in a study by Siravegna et al. [21]. Tumor-derived cfDNA is relatively rare compared to other sources, which poses a significant challenge to its prognostic utility, especially in the context of early-stage disease. At low concentrations (ctDNA$\leq$1%), ultrasensitive methods are needed that severely limit qualitative analysis [22, 23]. In advanced stage disease, tumor-derived cfDNA concentrations are often sufficient for cost-effective targeted sequencing (ctDNA$\geq$2%) [23]. ctDNA is associated with tumor burden and is an independent prognosticator of overall survival (OS) in PCa [23]. Combined, ctDNA emerges as a promising multifaceted biomarker for prognostication in advanced-stage PCa. The rapid clearance and molecular breakdown of circulating DNA present a distinct opportunity to characterize tumor somatic profiles in real time. Due to the swift degradation of cfDNA, the application of specialized blood collection tubes such as BCT® and CellSave™ is required, posing challenges for routine clinical implementation [24]. Several prognostic ctDNA liquid biopsy assays are currently available for lung, colon, and prostate cancers [25, 26]. Circulating DNA is increasingly utilized as a response marker in clinical trials, whereas its adoption in diagnostic settings remains less prevalent [25, 26].

Quantification of Circulating DNA As initially described in 1977, cfDNA levels are often increased in patients with cancer [27]. The quantification of cfDNA is a relatively simple approach to diagnosing and assessing cancer. cfDNA concentrations are positively correlated with tumor burden, and high levels in therapy-naive patients could be indicative of aggressive disease [23]. In two phase III clinical trials, a decrease in cfDNA levels was positively correlated with radiographic progression-free survival (PFS) and OS in mCRPC patients treated with taxane-based chemotherapy [28]. Furthermore, decreased cfDNA is associated with a favorable response to therapy. In a separate study, high levels of cfDNA before chemotherapy was associated with poor sPSA response and could act as an independent predictor of poor OS [29]. A major caveat in prognostic cfDNA quantification is the influence of cytotoxic therapies on cfDNA levels. Cytotoxic agents can increase cfDNA levels by inducing apoptosis or decrease them by inducing cell senescence [30]. This could limit its potential for baseline evaluations.

Profiling Somatic Alterations in Circulating DNA A number of studies have shown that ctDNA sequencing can be used to identify druggable somatic alterations and stratify the response to therapy in PCa. Somatic alterations in ctDNA and metastatic tissue biopsies are highly concordant in mCRPC [31]. Due to the short half-life of ctDNA, accurate real-time tumor profiling is possible [30]. Several pathways are involved in the development and progression of mCRPC, including *AR* alterations, DNA repair gene alterations, *TP53* alterations, and *PTEN* loss. However, the genomic landscape of mCRPC changes radically after exposure to systemic therapy [32]. Therefore, the detection of specific gene alterations in ctDNA before therapy could guide treatment strategies to target the underlying molecular pathology and improve response to therapy.

AR Gene Alterations Abnormal AR pathway activity is one of the main drivers of PCa progression. Genomic alterations in *AR* can lead to increased activity of the AR pathway and promote resistance to therapy [33]. These

alterations are rarely detected in hormone therapy-naive patients but are present in up to 60% of mCRPC patients [34]. *AR* gene alterations include *AR* gain, *AR* mutations and *AR* genomic structural variants (GSV). *AR* GSV have not been widely studied but are associated with the expression of splice variants. A correlation of *AR* GSV in ctDNA and splice variants in circulating tumor cells (CTCs) has been found [35]. The presence of two *AR* point mutations (*L702H* and *T878A*) in ctDNA were found to be predictive for resistance to abiraterone treatment [36–40].

Resistance to enzalutamide has been associated with another *AR* point mutation: *c.2629T>C* (*F877L*), although this mutation is very rare [41, 42]. Multiple studies have revealed that detection of *AR* gain in ctDNA is related to poor outcomes in CRPC patients treated with abiraterone or enzalutamide [33, 36, 37, 42, 43]. Annala et al. demonstrated that copy number gain of *AR* was not independently prognostic. In combination with established biomarkers and ctDNA levels, AR gain was not prognostic [44]. Only high *AR* copy number gain ($\geq$ 8 copies) was associated with poor response rates in first-line mCRPC patients [44]. It is reasonable to suggest that *AR* copy number gain evolves as a response to exposure to hormone therapy, leading to cross-resistance to next-generation ARSIs such as abiraterone and enzalutamide. Sumiyoshi et al. reported that *AR* genomic alterations were associated with poor abiraterone response but did not affect enzalutamide response [45]. Recent data suggest that docetaxel (chemotherapy) treatment is preferred for patients with *AR* copy number gain [46]. However, these studies were done using relatively small patient cohorts, and the methods used to profile *AR* copy numbers were not standardized (i.e., making meta-analysis difficult). In conclusion, evaluation of *AR* status at baseline (i.e., before starting therapy) might be useful in predicting therapy response and, therefore, stratifying patients with specific treatment modalities. Technical validation and standardization of copy number profiling methods are needed before such tests can be used in clinical practice.

DNA damage repair gene alterations Almost a quarter of mCRPC tumors have mutations in the DNA damage repair (DDR) genes such as, *BRCA1*, *BRCA2*, and *ATM* [47]. Genomic alterations in DDR genes are strongly associated with poor clinical response to next generation ARSIs. Alterations in *BRCA2* or *ATM* were independently and significantly associated with shorter time to progression [44]. Loss of function of homologous recombination repair genes (HRR) is predictive of response to poly ADP ribose polymerase (PARP) inhibitors and platinum-based chemotherapies [48]. Tumors with mutated *BRCA* or associated DNA repair deficiencies are highly susceptible to PARP inhibitors (PARPi). In 2015, the TOPARP-A trial demonstrated the therapeutic value of PARP inhibition in mCRPC patients with *BRCA2* loss or *ATM* alterations [48].

DNA repair mutations have since been detected in ctDNA of mCRPC patients before and after starting PARPi therapy. Goodall et al. demonstrated that all somatic (solid tumor) DNA repair mutations were detectable in ctDNA prior to disease progression. Interestingly, novel DNA repair mutations were detected at time of disease progression. The allele frequency of somatic mutations decreased selectively in responding patients [49]. This was validated in an independent study where ctDNA *BRCA2* reversion mutations were detected at the time of disease progression in patients receiving olaparib or talazoparib both effective PARP inhibitors [50]. Combined, detection of DNA repair mutations in ctDNA can help stratify patients for PARPi response and may be effective for monitoring therapy resistance in mCRPC.

TP53 alterations Genomic alterations in tumor protein 53 (*TP53*) have been associated with poor prognosis in several studies [44, 51, 52]. *TP53* is a tumor suppressor gene with a high alteration frequency in mCRPC patients (up to 50%) [47]. Loss of *TP53* has also been detected in ctDNA, and is predictive of poor ARSI response [44]. In fact, *TP53* loss/inactivation was found to be a stronger negative prognosticator for ARSI resistance than biomarkers associated with AR signaling in a large multicenter randomized

controlled trial [53]. In this trial, ctDNA and CTC samples were collected to detect *AR*, *AR* splice variant, and *TP53* alterations in 168 mCRPC patients prior to starting ARSI therapy. Stratifying patients on *TP53* alteration status identified two clinically significant groups: a poor prognostic group (median PFS $\leq$ 2.5 months), and favorable prognostic group (median PFS $\geq$ 14.0 months) [53]. These data suggest that *TP53* loss/inactivation status is an important biomarker for predicting ARSI response. However, as the authors point out, the study population was heterogeneous and the effect of confounding factors such as, hidden genomic subtypes, could not be assessed. At present, *TP53* loss/inactivation should not be used as a negative indicator for ARSI therapy. Instead, this cohort requires extra due diligence when monitoring for possible early ARSI resistance and disease progression.

PI3K signaling defects The phosphatidylinositol 3-kinase (PI3K) pathway is a highly active signaling pathway in PCa. Approximately half of all mCRPC patients have alterations in PI3K-associated genes such as *PIK3CA*, *PIK3CB*, *PTEN*, or *AKT* [47]. *PI3K* alterations have been detected in ctDNA and are associated with poor PFS and ARSI response [44]. A 2011 study found a reciprocal negative feedback loop between PI3K and AR activity providing a molecular basis for the prognostic utility of PI3K genomic alterations on ARSI response [54]. Suggesting that PCa cells may be able to switch between PI3K and AR signaling to ensure survival when challenged with pharmacological inhibition of either pathway. In a 2016 clinical trial, combined AKT and AR inhibition (ipatasertib and abiraterone) was found to be superior to AR inhibition alone, particularly in mCRPC patients with *PTEN* loss [55, 56]. In summary, *PIK3CA*, *PIK3CB*, *PTEN* or *AKT* alterations in ctDNA are promising biomarkers for the detection of early ARSI resistance (i.e., before radiographic or biochemical progression) and may be useful in for guiding treatment strategy (e.g., AKT inhibitors combined with ARSIs).

Circulating RNAs

Circulating messenger RNA Messenger RNA (mRNA) encompasses a large family of RNA molecules that transfer genetic information from genes to ribosomes for translation into protein products. Dysregulation of oncogenic and tumor-suppressive mRNAs is central to the progression of all cancers. Detecting cancer-specific mRNA transcripts in body fluids is a direct and relatively simple method to characterize tumors. The established mRNA markers *KLK3* and *TMPRSS2-ERG* are important for many urine-based diagnostic tests (SelectMDx, MPS, IntelliScore). Recent studies have explored the prognostic value of these markers in the blood of mCRPC patients. In a 2011 study, mCRPC patients with previous exposure to chemotherapy, were positive for *TMPRSS2-ERG* in peripheral blood mononuclear cell (PBMC) fractions in 37% of cases [57]. In patients receiving abiraterone, *TMPRSS2-ERG* was not predictive of therapy response. Conversely, levels of *TMPRSS2-ERG* and *KLK3* decreased with exposure to first-line chemotherapy (docetaxel) [58]. In an independent study, mCRPC patients who received docetaxel were negative for *TMPRSS2-ERG* at baseline but positive at the time of progression (41%) [59]. These findings hint at a possible role of *TMPRSS2-ERG* in chemotherapy resistance. However, circulating *TMPRSS2-ERG* may also simply reflect tumor-burden. Large prospective studies are needed to explore these findings prior to effective clinical implementation.

Circulating micro RNAs Transcriptional regulation is crucial for the survival of all cells. Micro RNAs (miRNAs) are short (approximately 21 nucleotides) single-stranded RNAs that regulate gene expression at the post-transcriptional level by attaching to specific motifs in RNA transcripts [60]. MiRNAs may initiate and drive tumor progression by modulating the expression of tumor suppressor genes and oncogenes. In contrast to cfDNA, miRNAs exhibit stability in biofluids, typically being encapsulated in exosomes or integrated into ribonucleoprotein complexes, thereby being protected from

enzymatic degradation [61, 62]. Enrichment of liquid biopsies with exosomes increases miRNA concentrations and enhances the sensitivity of molecular assays to detect tumor-associated miRNAs [61]. Circulating miRNAs have been thoroughly investigated for prognostic implications in mCRPC, though the data remain inconsistent with no consensus on the most valuable miRNA prognostic marker. To date, the mir-200 family (including *miRNA-141-3p*) and *miR-375* appear promising. In two clinical studies, levels of *miR-21*, *miR-200a*, *miR-200c*, and *miR-375* correlated with survival in mCRPC [35, 63]. When combined with established biomarkers like sPSA, these miRNAs have demonstrated sensitivity and specificity in both diagnostic and prognostic contexts [64, 65]. Although promising, the evidence is largely pre-clinical or gathered in small, underpowered studies. Thus, miRNA tests are currently used for research purposes and are not commercially available for PCa. The utility of several miRNAs for the clinical management of PCa is extensively reviewed below [boerrigter_clinical_2020].

MiR-141-3p Expression of *miR-141-3p* has been studied extensively in PCa liquid biomarker research. The biological effects of *miR-141-3p* are context-specific and may be oncogenic or tumor suppressive [66]. Increased *miR-141-3p* levels in urine can distinguish benign from malignant PCa, while elevated levels in circulation have been associated with disease progression and metastasis [67–70]. Exosomal *miR-141-3p* likely primes bone tissue to produce a tumor-favorable microenvironment while its expression in CTCs induces MET and promotes PCa cells to settle new metastatic sites [68, 69]. Two independent studies have demonstrated that increased *miR141-3p* levels are predictive for metastatic PCa [65, 71]. Monitoring plasma *miR-141-3p* levels in PCa patients could be predictive of metastatic risk.

MiRNA-375 *MiRNA-375* (*miR-375*) was first described as a tumor suppressor, but recent evidence suggests its biological effects are context and tissue-specific [71]. When measured in serum, *miR-375* levels were found to be significantly increased in PCa when compared to healthy controls [70, 72]. Moreover, expression levels of *miR-375* have been correlated with PCa progression, metastasis, and docetaxel resistance in CRPC [64, 67, 73]. Like *miR-141-3p*, *miR-375* also induces MET in CTCs to promote the formation of distant metastasis [74]. These findings are in line with the findings of Bryant *et al.,* who showed that serum-derived exosomes from metastatic PCa patients (n = 47) contained significantly higher miR-375 copy numbers than exosomes from a control cohort (n = 72) [75]. In summary, increased circulating *miR-375* levels could be predictive for the presence of metastasis and chemotherapy resistance in PCa.

Long Non-Coding RNAs Long non-coding RNAs (lncRNAs) are non-coding RNA transcripts consisting of $\geq$ 200 nucleotides. Current estimates suggest there are more than $6{\times}10^4$ lncRNAs in the human genome. Aberrant expression of many lncRNAs has been associated with many diseases, including PCa. However, the Progensa PCA3 urine test is the only clinically available lncRNA-based diagnostic test for PCa (Table 2.1). Yet, many novel PCa-related lncRNAs have been detected in both solid and liquid biopsies since the clinical implementation of the Progensa PCA3 test in 2012 [76–79].

SCHLAP1 The expression levels of the lncRNA known as *SWI/SNF Complex Antagonist Associated with Prostate Cancer 1* (*SCHLAP1*) have been associated with metastasis and biochemical recurrence when measured in solid tissue biopsies [80]. However, upon measuring expression in post-DRE urine sediments, *SCHLAP1* could only be detected in a subset of PCa patients. This could be attributed to the specific patient cohort (localized castration-sensitive disease) or the need for increased sensitivity when measuring *SCHLAP1* in liquid biopsies. Nevertheless, urine *SCHLAP1* levels were able to identify high-stage patients (T2 or higher). If *SCHLAP1* were reliably

detectable in blood, it could be a promising screening tool for monitoring metastatic risk in mCRPC. However, we were unable to detect *SCHLAP1* in the whole blood RNA of mCRPC patients starting enzalutamide therapy [78]. Interestingly, *SCHLAP1* was detectable in the circulating tumor-derived exosomes of primary PCa patients [81]. The clinical utility of circulating exosomes is discussed in this Chapter.

MALAT1 *Metastasis Associated Lung Adenocarcinoma Transcript 1* (*MALAT1*) is a lncRNA that is overexpressed in 82.5% of PCa tissue specimens compared with normal adjacent tissue [82]. *MALAT1* is highly stable in plasma and detectable even after 24h storage at room temperature, repeated freeze-thaw cycles, and acid-base treatment making it a promising biomarker for liquid biopsies [83]. In a PCa screening study, plasma *MALAT1* levels were found to be better predictors of malignancy than sPSA. However, diagnostic accuracy improved when both *MALAT1* and sPSA scores were combined [84]. With regards to the development of liquid biopsy tests for prognostic utility and patient stratification, *MALAT1* could be equally promising due to its ability to induce enzalutamide resistance via direct involvement with *ARv7* production [85]. Preclinical evidence demonstrates targeting *MALAT1* to increase susceptibility to PARP inhibition due to its ability to reprogram the homologous recombination pathway [86]. *MALAT1* is stable in plasma, detectable via accessible assays, a strong prognosticator for localized PCa, and may induce first-line mCRPC therapy resistance. Taken together, plasma *MALAT1* levels could be a promising biomarker for monitoring therapy response in mCRPC.

NAALADL2-AS2 *N-Acetylated Alpha-Linked Acidic Dipeptidase Like 2 Antisense Transcript 2* (*NAALADL2-AS2*) was until recently an obscure lncRNA with no known functions. In 2022 I published a paper showing *NAALADL2-AS2* to be highly expressed in PCa and specifically CRPC. From survival analyses using The Cancer Genome Atlas (TCGA) PCa data, we demonstrated high *NAALADL2-AS2* expression to be unfavorable

for progression-free survival (PFS) in localized PCa. Interestingly, whilst exploring the clinical utility of several circulating RNAs in mCRPC, we found serum high *NAALADL2-AS2* levels to be favorable for survival in patients receiving enzalutamide [78]. In a larger follow-up study including patients treated with either enzalutamide or abiraterone, there was a similar trend but the survival difference between high versus low *NAALADL2-AS2* expressors was not statistically significant [79]. The prognostic utility of circulating *NAALADL2-AS2* for mCRPC remains unclear as the data are conflicting. This could be an artifact related to the limit of detection (LoD) of molecular assays such as qPCR which makes quantitation of lncRNAs in liquid biopsies particularly difficult because of their relatively low expression levels compared to those of mRNAs. As demonstrated with *SCHLAP1*, enriching the *NAALADL2-AS2* signal by isolating tumor-derived exosomes could reduce background (leukocyte/platelet) RNA and make prognostic quantitation of circulating *NAALADL2-AS2* clinically viable [78, 81]. In Chapter 3, the role of *NAALADL2-AS2* in PCa and CRPC is described in detail.

Exosomes

Exosomes are small (30 to 150 nm) extracellular vesicles that are produced in the endosomal compartment of most eukaryotic cells. Exosomes are enriched with DNA, RNA, or protein and are highly representative of their cellular origin. Exosomes are present in solid tissues and biological fluids, including blood and urine. Characterizing tumor-derived exosomes could be informative on tumor biology. Tumor-derived exosomes protect biomarkers from degradation by nucleases, proteases, or other environmental stressors present. Liquid biopsies provide a platform for isolating tumor-derived exosomes that offer potential insight into biological processes in solid tumors along treatment regimes. Capture of tumor-derived exosomes is challenging and is a critical step toward developing exosome-based diagnostic tests. Isolation of tumor-derived exosomes shares many similarities with the enrichment

and isolation of CTCs. Exosome biogenesis, isolation, and characterization methods have been extensively reviewed by Gurunathan et al. and are outside the scope of this thesis [87].

Tumor Educated Platelets

Platelets, which are nonnucleated cells, aggregate to cease bleeding, a process known as hemostasis. When tumor cells enter the circulatory system, they can trigger platelet aggregation through similar hemostatic pathways. Interactions between tumors and platelets shield CTCs from immune and environmental dangers, consequently facilitating metastasis. Platelets are abundantly present in blood, ranging from 150,000 to 350,000 platelets per microliter, and may serve as an accessible source of tumor-related molecules. Various studies have detected tumor-associated RNA transcripts in platelets from cancer patients [88], including research evaluating the prognostic relevance of tumor-educated platelets in PCa [89]. This study found PCa-associated RNA transcripts in platelets from patients with CRPC but not in healthy controls. CRPC patients without prior therapy, exhibiting detectable levels of *KLK2*, *KLK3*, *FOLH1*, and *NPY* in platelet isolates, were linked with unfavorable PFS. Further research is essential to confirm the prognostic relevance of tumor-educated platelets in PCa.

Circulating Tumor Cells

The concept of characterizing cancer through blood originated with the 1869 discovery of CTCs [90]. The discovery of cfDNA in 1948 and later publications in the 1960s and 1970s, which reported elevated cfDNA levels in leukemia patients, renewed interest in liquid biopsy research. The introduction of PSA testing for the diagnosis and monitoring of PCa in the 1990s proves the clinical relevance of circulating biomarkers and liquid biopsies. Although useful, circulating PSA is a single prostate biomarker and is highly susceptible to false positives and overtreatment. Urine biopsy tests have been shown to be more specific and sensitive for the detection of PCa. Compared to

PSA, urine PCa tests use multiple biomarkers enabling risk assessment. In this light, molecular analysis of CTCs could significantly improve clinical management of PCa. Yet, the application of CTCs for active surveillance and disease management has been limited to clinical trials. The clinical relevance and potential of CTCs in advanced PCa are discussed below.

CTCs are the cellular units that enable cancer to disseminate and colonize distant sites i.e., metastasis. CTCs require motility to spread to distant metastatic sites, while being resilient against stressors of the bloodstream such as immune-induced cell death and shear stress of the vasculature [91]. The epithelial-to-mesenchymal transition (EMT) and mesenchymal-to-epithelial transition (MET) allow CTCs to be plastic, motile, or resilient when required [92]. Aggregates of CTC, referred to as a CTC cluster, comprise another survival strategy, as they are resilient to vascular stressors and their increased numbers promote survival increasing metastatic potential. CTC clusters are considered to be 50 times more metastatic than their single counterparts [93]. CTC levels reflect tumor burden providing a unique opportunity to characterize tumor material from a relatively non-invasive source (biopsied blood vs. solid tissue) [94]. CTCs can be identified for almost all solid malignancies, especially in the advanced stages of cancer [93]. However, the isolation of CTCs has remained a key challenge due to their low abundance compared to erythrocytes and leukocytes [93]. Most CTC systems use either positive selection and/or negative selection strategies to enrich CTCs for enumeration and characterization. Positive selection targets CTCs using tumor-specific antibodies bound to ferrofluids. Negative selection aims to deplete nonmalignant/blood cells [94]. Label-free CTC enrichment is a relatively new approach but may offer key strategic advantages over positive and negative selection systems.

CTC Enrichment Many molecular assays are constrained by their LoD, necessitating a specific tumor-to-background ratio to enable accurate characterization of CTC samples. CTC enrichment via positive selection forms

the basis of the FDA-approved CellSearch platform, which isolates cells expressing the epithelial antigen EpCAM. Given that most solid tumors exhibit epithelial characteristics, this method is straightforward and effective. Nonetheless, CTCs undergoing EMT lose their epithelial markers and are consequently missed by CellSearch and similar platforms. As highlighted previously, EMT plays a critical role in enhancing the metastatic potential of CTCs. Negative selection-based platforms, such as EasySep™ and RosetteSep™, remove erythrocytes, leukocytes, and/or platelets from samples, thereby mitigating the bias associated with positive selection; however, they often display low specificity due to CTCs binding with leukocytes and platelets [95]. Label-free CTC enrichment methods integrate both positive and negative selection by leveraging common properties of CTCs and blood cells. Microfluidic technologies, including Parsortix® and Labyrinth, exemplify label-free CTC enrichment platforms [96, 97]. These approaches reduce selection bias, maintain CTC viability, and facilitate a wide range of subsequent cellular and molecular analyses.

Parsortix utilizes a patented microfluidic chip with a gradually narrowing stepped separation structure to trap CTCs while allowing the passage of smaller deformable blood cells. By leveraging cell size and deformability, Parsortix facilitates the capture of epithelial and mesenchymal CTCs in single and aggregate forms (also known as CTC clusters) [95]. EMT and CTC clusters are key drivers of metastasis [93]. Parsortix enriched CTC samples are suitable for high-throughput multiplex molecular analysis as detailed in Chapter 5. The FDA recognized the prognostic utility of Parsortix and approved its use for monitoring progression in metastatic breast cancer in 2022 [98].

CTC Enumeration Enumeration was the first methodology to demonstrate the prognostic utility of CTCs. Unlike traditional PCa biomarkers, such as sPSA, which are directly regulated by androgens, CTC counts are not significantly affected by fluctuations in hormone levels. Therefore, CTC count

may serve as a more reliable indicator for evaluating treatment response in men with PCa undergoing antiandrogen therapy, compared to sPSA. Multiple large phase II and phase III clinical trials have shown that CTC count is a strong prognosticator of clinical outcomes in PCa [99–102]. A baseline level of ≥ 5 CTCs detected per 7.5 mL of blood is associated with significantly shorter OS ($\approx$50%) [99–102]. While prognostic in a metastatic setting, there are some clear limitations regarding the clinical implementation of CTC count in routine clinical protocols for managing PCa.

Men with localized PCa usually have a lower CTC count compared to metastatic patients, which limits their inclusion in early-disease CTC studies. In addition, as the primary vehicle for metastasis, CTCs must gain cellular plasticity and motility to invade and form distant metastases in a foreign microenvironment. These processes involve a transition between epithelial and mesenchymal phenotypes, which influences the expression of EpCAM [92, 103]. Thus, CellSearch and adjacent CTC enrichment systems can underestimate the CTC count. Label-free CTC enrichment, which selects tumor cells according to cell size and deformability, may provide a solution by capturing CTCs with any phenotype (including mesenchymal). Another challenge in incorporating CTC enumeration into clinical practice is their tendency to perish during sample collection and molecular analyses. As a result and in combination with the relatively high costs of sample collection and processing, CTC enumeration is not used in routine clinical management and monitoring of men diagnosed with PCa.

CTC Characterization Beyond CTC enumeration, molecular characterization of CTCs (both as pooled and single-cell samples) has been proposed to produce valuable predictive biomarkers. AR signaling is central to PCa progression, as such elevated *AR* expression, enhanced AR pathway activity, and *AR* mutations are frequent in mCRPC. These findings have given impetus for the development of next-generation ARSI (e.g. abiraterone,

enzalutamide, apalutamide, darolutamide). Since their implementation, patient outcomes have improved significantly. However, primary and acquired resistance to ARSIs is common. Non-canonical AR signaling, as well as the expression of *AR* splice variants, have been found to drive ARSI resistance in mCRPC. AR splice variant 7 (ARv7) lacks the ligand-binding domain, leading to ligand-independent AR signaling and insensitivity to ARSI [104]. In a 2014 study, the quantification of ARv7 mRNA in CTCs was associated with lower sPSA response rates and shorter PFS in patients with mCRPC receiving enzalutamide or abiraterone [105]. These findings were striking, as all patients with detectable *ARv7* RNA did not show sPSA responses. *ARv7* has been associated with resistance to abiraterone and enzalutamide but not to taxane-based chemotherapy in several studies of mCRPC [14, 106, 107].

Combining CTC enumeration with CTC ARv7 status improves prognostic performance beyond either biomarker alone. Patients with a negative CTC status have the most favorable prognosis, followed by CTC-positive/ARv7-negative patients, whereas CTC-positive/ARv7-positive patients have the poorest prognosis [108]. Accordingly, CTC ARv7 status has been proposed as a predictive biomarker of resistance to abiraterone and enzalutamide. Evidence across studies, however, has been inconsistent. The initial 2014 report linked detectable *ARv7* gene expression in CTCs with poor responses to ARSIs in a heavily pretreated cohort with substantial prior ARSI exposure [105]. In contrast, a 2017 study observed that some patients with ARv7-positive CTCs still responded to ARSIs [109]. A likely explanation is the difference in treatment history between cohorts: in patients who have already received multiple lines of ARSIs, resistance biology is more heterogeneous and ARv7 status alone may be a less definitive predictor, whereas in earlier-line or ARSI-naive settings it may better reflect intrinsic ARSI resistance. The prognostic value of CTC ARv7 status is therefore likely greatest after first-line ARSI therapy, given that genomic AR alterations (mutations/copy-number alterations [CNAs]), intracellular androgen biosynthesis, and non-canonical AR signaling also contribute to ARSI resistance [110–112]. Moreover, two

commercially available assays (AdnaTest and Oncotype DX) have produced conflicting results when applied to the same patient cohort [113, 114]. In Chapter 5, baseline *ARv7* gene expression levels were a weak prognostic marker relative to AR pathway activity in patients with mCRPC [115]. Similarly, Sperger et al. (2021) reported that AR signaling is prognostic for survival in PCa irrespective of ARv7 status [116]. Collectively, these findings support a multifaceted approach that integrates multiple antiandrogen-resistance mechanisms rather than reliance on a single biomarker [115].

References

1. Matuszczak, M., Schalken, J. A. & Salagierski, M. Prostate cancer liquid biopsy biomarkers' clinical utility in diagnosis and prognosis. *Cancers* 13 (July 1, 2021).
2. Hendriks, R. J., Van Oort, I. M. & Schalken, J. A. Blood-based and urinary prostate cancer biomarkers: a review and comparison of novel biomarkers for detection and treatment decisions. *Prostate Cancer and Prostatic Diseases* 20, 12–19 (Mar. 2017).
3. Marks, L. S. *et al.* PCA3 Molecular Urine Assay for Prostate Cancer in Men Undergoing Repeat Biopsy. *Urology* 69, 532–535 (Mar. 1, 2007).
4. Groskopf, J. *et al.* APTIMA PCA3 Molecular Urine Test: Development of a Method to Aid in the Diagnosis of Prostate Cancer. *Clinical Chemistry* 52, 1089–1095 (June 1, 2006).
5. Gittelman Marc C. *et al.* PCA3 Molecular Urine Test as a Predictor of Repeat Prostate Biopsy Outcome in Men with Previous Negative Biopsies: A Prospective Multicenter Clinical Study. *Journal of Urology* 190, 64–69 (July 1, 2013).
6. Van Neste, L. *et al.* Detection of High-grade Prostate Cancer Using a Urinary Molecular Biomarker–Based Risk Score. *European Urology* 70, 740–748 (2016).
7. Haese Alexander *et al.* Multicenter Optimization and Validation of a 2-Gene mRNA Urine Test for Detection of Clinically Significant Prostate Cancer before Initial Prostate Biopsy. *Journal of Urology* 202, 256–263 (Aug. 1, 2019).
8. Leyten, G. H. *et al.* Identification of a candidate gene panel for the early diagnosis of prostate cancer. *Clinical Cancer Research* 21, 3061–3070 (July 1, 2015).
9. Tomlins, S. A. *et al.* Urine TMPRSS2:ERG Plus PCA3 for Individualized Prostate Cancer Risk Assessment. *European Urology* 70, 45–53 (July 1, 2016).

10. Salami, S. S. *et al.* Combining urinary detection of TMPRSS2:ERG and PCA3 with serum PSA to predict diagnosis of prostate cancer. *Urologic Oncology: Seminars and Original Investigations* 31, 566–571 (July 1, 2013).
11. McKiernan, J. *et al.* A Novel Urine Exosome Gene Expression Assay to Predict High-grade Prostate Cancer at Initial Biopsy. *JAMA Oncology* 2, 882–889 (July 1, 2016).
12. Jacob, A., Raj, R., Allison, D. B. & Myint, Z. W. Androgen Receptor Signaling in Prostate Cancer and Therapeutic Strategies. *Cancers* 13, 5417 (Oct. 28, 2021).
13. Peyraud, F. & Italiano, A. Combined parp inhibition and immune checkpoint therapy in solid tumors. *Cancers* 12, 1–28 (June 1, 2020).
14. Onstenk, W. *et al.* Efficacy of Cabazitaxel in Castration-resistant Prostate Cancer Is Independent of the Presence of AR-V7 in Circulating Tumor Cells. *European Urology* 68, 939–945 (Dec. 1, 2015).
15. Fleming, T. R. & Powers, J. H. Biomarkers and surrogate endpoints in clinical trials. *Statistics in Medicine* 31, 2973–2984 (Nov. 10, 2012).
16. Latosinska, A., Frantzi, M., Merseburger, A. S. & Mischak, H. Promise and Implementation of Proteomic Prostate Cancer Biomarkers. *Diagnostics* 8, 57 (Aug. 29, 2018).
17. Mader, S. & Pantel, K. Liquid Biopsy: Current Status and Future Perspectives. *Oncology Research and Treatment* 40, 404–408 (July 13, 2017).
18. Stroun, M., Lyautey, J., Lederrey, C., Olson-Sand, A. & Anker, P. About the possible origin and mechanism of circulating DNA: Apoptosis and active DNA release. *Clinica Chimica Acta. Proceedings of the Chinese Congress of Clinical Chemistry and Laboratory Medicine 2000* 313, 139–142 (Nov. 1, 2001).
19. Huang, C.-C., Du, M. & Wang, L. Bioinformatics Analysis for Circulating Cell-Free DNA in Cancer. *Cancers* 11, 805 (June 11, 2019).

20. Barbany, G. *et al.* Cell-free tumour DNA testing for early detection of cancer - a potential future tool. *Journal of Internal Medicine* 286, 118–136 (Aug. 2019).
21. Siravegna, G., Marsoni, S., Siena, S. & Bardelli, A. Integrating liquid biopsies into the management of cancer. *Nature Reviews Clinical Oncology* 14. Number: 9, 531–548 (Sept. 2017).
22. Vandekerkhove, G. *et al.* Plasma ctDNA is a tumor tissue surrogate and enables clinical-genomic stratification of metastatic bladder cancer. *Nature Communications* 12, 184 (Jan. 8, 2021).
23. Casanova-Salas, I. *et al.* Quantitative and Qualitative Analysis of Blood-based Liquid Biopsies to Inform Clinical Decision-making in Prostate Cancer. *European Urology* 79, 762–771 (June 1, 2021).
24. Van Dessel, L. F. *et al.* Application of circulating tumor DNA in prospective clinical oncology trials – standardization of preanalytical conditions. *Molecular Oncology* 11, 295–304 (Mar. 2017).
25. Temilola, D. O. *et al.* The Prospect and Challenges to the Flow of Liquid Biopsy in Africa. *Cells* 8, 862 (Aug. 9, 2019).
26. Kwan, E. M., Wyatt, A. W. & Chi, K. N. Towards clinical implementation of circulating tumor DNA in metastatic prostate cancer: Opportunities for integration and pitfalls to interpretation. *Frontiers in Oncology* 12, 1054497 (Nov. 10, 2022).
27. Leon, S. A., Shapiro, B., Sklaroff, D. M. & Yaros, M. J. Free DNA in the serum of cancer patients and the effect of therapy. *Cancer Research* 37, 646–650 (Mar. 1977).
28. Mehra, N. *et al.* Plasma Cell-free DNA Concentration and Outcomes from Taxane Therapy in Metastatic Castration-resistant Prostate Cancer from Two Phase III Trials (FIRSTANA and PROSELICA). *European Urology* 74, 283–291 (Sept. 2018).
29. Kienel, A., Porres, D., Heidenreich, A. & Pfister, D. cfDNA as a Prognostic Marker of Response to Taxane Based Chemotherapy in Patients with Prostate Cancer. *The Journal of Urology* 194, 966–971 (Oct. 2015).

30. Stejskal, P. *et al.* Circulating tumor nucleic acids: biology, release mechanisms, and clinical relevance. *Molecular Cancer* 22, 15 (Jan. 21, 2023).
31. Wyatt, A. W. *et al.* Concordance of Circulating Tumor DNA and Matched Metastatic Tissue Biopsy in Prostate Cancer. *JNCI: Journal of the National Cancer Institute* 109, djx118 (Dec. 1, 2017).
32. Aw, H. *et al.* Evolution of the genomic landscape of circulating tumor DNA (ctDNA) in metastatic prostate cancer over treatment and time. *Cancer treatment and research communications* 19 (2019).
33. Azad, A. A. *et al.* Androgen Receptor Gene Aberrations in Circulating Cell-Free DNA: Biomarkers of Therapeutic Resistance in Castration-Resistant Prostate Cancer. *Clinical Cancer Research: An Official Journal of the American Association for Cancer Research* 21, 2315–2324 (May 15, 2015).
34. Kumar, A. *et al.* Substantial interindividual and limited intraindividual genomic diversity among tumors from men with metastatic prostate cancer. *Nature Medicine* 22, 369–378 (Apr. 2016).
35. De Laere, B. *et al.* Comprehensive Profiling of the Androgen Receptor in Liquid Biopsies from Castration-resistant Prostate Cancer Reveals Novel Intra-AR Structural Variation and Splice Variant Expression Patterns. *European Urology* 72, 192–200 (Aug. 2017).
36. Conteduca, V. *et al.* Androgen receptor gene status in plasma DNA associates with worse outcome on enzalutamide or abiraterone for castration-resistant prostate cancer: a multi-institution correlative biomarker study. *Annals of Oncology. Response evaluation criteria in lymphoma (RECIL 2017)* 28, 1508–1516 (July 1, 2017).
37. Romanel, A. *et al.* Plasma AR and abiraterone-resistant prostate cancer. *Science Translational Medicine* 7, 312re10 (Nov. 4, 2015).
38. Carreira, S. *et al.* Tumor clone dynamics in lethal prostate cancer. *Science Translational Medicine* 6, 254ra125 (Sept. 17, 2014).

39. Taplin, M.-E. & Balk, S. P. Has the Time Arrived for Biomarker-Directed Therapy in Castration-Resistant Prostate Cancer? *JAMA oncology* 1, 577–579 (Aug. 2015).
40. Chen, E. J. *et al.* Abiraterone treatment in castration-resistant prostate cancer selects for progesterone responsive mutant androgen receptors. *Clinical Cancer Research: An Official Journal of the American Association for Cancer Research* 21, 1273–1280 (Mar. 15, 2015).
41. Joseph, J. D. *et al.* A clinically relevant androgen receptor mutation confers resistance to second-generation antiandrogens enzalutamide and ARN-509. *Cancer Discovery* 3, 1020–1029 (Sept. 2013).
42. Wyatt, A. W. *et al.* Genomic Alterations in Cell-Free DNA and Enzalutamide Resistance in Castration-Resistant Prostate Cancer. *JAMA oncology* 2, 1598–1606 (Dec. 1, 2016).
43. Salvi, S. *et al.* Circulating cell-free AR and CYP17A1 copy number variations may associate with outcome of metastatic castration-resistant prostate cancer patients treated with abiraterone. *British Journal of Cancer* 112, 1717–1724 (May 12, 2015).
44. Annala, M. *et al.* Circulating Tumor DNA Genomics Correlate with Resistance to Abiraterone and Enzalutamide in Prostate Cancer. *Cancer Discovery* 8, 444–457 (Apr. 1, 2018).
45. Sumiyoshi, T. *et al.* Clinical utility of androgen receptor gene aberrations in circulating cell-free DNA as a biomarker for treatment of castration-resistant prostate cancer. *Scientific Reports* 9, 4030 (Mar. 11, 2019).
46. Conteduca, V. *et al.* Plasma Androgen Receptor and Docetaxel for Metastatic Castration-resistant Prostate Cancer. *European Urology* 75, 368–373 (Mar. 2019).
47. Robinson, D. *et al.* Integrative clinical genomics of advanced prostate cancer. *Cell* 161, 1215–1228 (May 21, 2015).
48. Mateo, J. *et al.* DNA-Repair Defects and Olaparib in Metastatic Prostate Cancer. *New England Journal of Medicine* 373, 1697–1708 (Oct. 29, 2015).

49. Goodall, J. *et al.* Circulating Cell-Free DNA to Guide Prostate Cancer Treatment with PARP Inhibition. *Cancer Discovery* 7, 1006–1017 (Sept. 2017).
50. Quigley, D. *et al.* Analysis of Circulating Cell-Free DNA Identifies Multiclonal Heterogeneity of BRCA2 Reversion Mutations Associated with Resistance to PARP Inhibitors. *Cancer Discovery* 7, 999–1005 (Sept. 2017).
51. Maughan, B. L. *et al.* p53 status in the primary tumor predicts efficacy of subsequent abiraterone and enzalutamide in castration-resistant prostate cancer. *Prostate Cancer and Prostatic Diseases* 21, 260–268 (June 2018).
52. Hussain, M. *et al.* Targeting Androgen Receptor and DNA Repair in Metastatic Castration-Resistant Prostate Cancer: Results From NCI 9012. *Journal of Clinical Oncology: Official Journal of the American Society of Clinical Oncology* 36, 991–999 (Apr. 1, 2018).
53. De Laere, B. *et al.* TP53 Outperforms Other Androgen Receptor Biomarkers to Predict Abiraterone or Enzalutamide Outcome in Metastatic Castration-Resistant Prostate Cancer. *Clinical Cancer Research: An Official Journal of the American Association for Cancer Research* 25, 1766–1773 (Mar. 15, 2019).
54. Carver, B. S. *et al.* Reciprocal feedback regulation of PI3K and androgen receptor signaling in PTEN-deficient prostate cancer. *Cancer Cell* 19, 575–586 (May 17, 2011).
55. De Bono, J. S. *et al.* Randomized Phase II Study Evaluating Akt Blockade with Ipatasertib, in Combination with Abiraterone, in Patients with Metastatic Prostate Cancer with and without PTEN Loss. *Clinical Cancer Research: An Official Journal of the American Association for Cancer Research* 25, 928–936 (Feb. 1, 2019).
56. Bono, J. S. d. *et al.* PTEN loss as a predictive biomarker for the Akt inhibitor ipatasertib combined with abiraterone acetate in patients with metastatic castration-resistant prostate cancer (mCRPC). *Annals of Oncology* 27, vi243 (Oct. 1, 2016).

57. Danila, D. C. *et al.* TMPRSS2-ERG Status in Circulating Tumor Cells as a Predictive Biomarker of Sensitivity in Castration-Resistant Prostate Cancer Patients Treated With Abiraterone Acetate. *European Urology* 60, 897–904 (Nov. 2011).
58. Dijkstra, S. *et al.* KLK3, PCA3, and TMPRSS2-ERG expression in the peripheral blood mononuclear cell fraction from castration-resistant prostate cancer patients and response to docetaxel treatment: Biomarker Expression in CRPC Patients. *The Prostate* 74, 1222–1230 (Sept. 2014).
59. Reig, Ò. *et al.* TMPRSS2-ERG in Blood and Docetaxel Resistance in Metastatic Castration-resistant Prostate Cancer. *European Urology* 70, 709–713 (Nov. 2016).
60. Pritchard, C. C., Cheng, H. H. & Tewari, M. MicroRNA profiling: approaches and considerations. *Nature Reviews Genetics* 13, 358–369 (May 2012).
61. Gallo, A., Tandon, M., Alevizos, I. & Illei, G. G. The Majority of MicroRNAs Detectable in Serum and Saliva Is Concentrated in Exosomes. *PLoS ONE* 7 (ed Afarinkia, K.) e30679 (Mar. 9, 2012).
62. Zhang, Z., Qin, Y.-W., Brewer, G. & Jing, Q. MicroRNA degradation and turnover: regulating the regulators: MicroRNA degradation and turnover. *Wiley Interdisciplinary Reviews: RNA* 3, 593–600 (July 2012).
63. Huang, X. *et al.* Exosomal miR-1290 and miR-375 as Prognostic Markers in Castration-resistant Prostate Cancer. *European Urology* 67, 33–41 (Jan. 1, 2015).
64. Bijnsdorp, I. V., van Royen, M. E., Verhaegh, G. W. & Martens-Uzunova, E. S. The Non-Coding Transcriptome of Prostate Cancer: Implications for Clinical Practice. *Molecular Diagnosis & Therapy* 21, 385–400 (Aug. 1, 2017).
65. Kelly, B. D. *et al.* A Circulating MicroRNA Signature as a Biomarker for Prostate Cancer in a High Risk Group. *Journal of Clinical Medicine* 4. Number: 7, 1369–1379 (July 2015).

66. Gao, Y. *et al.* The Roles of MicroRNA-141 in Human Cancers: From Diagnosis to Treatment. *Cellular Physiology and Biochemistry* 38, 427–448 (Feb. 1, 2016).
67. Brase, J. C. *et al.* Circulating miRNAs are correlated with tumor progression in prostate cancer. *International Journal of Cancer* 128. _eprint: https://onlinelibrary.wiley.com/doi/pdf/10.1002/ijc.25376, 608–616 (2011).
68. Zheng, Q. *et al.* Investigation of miR-21, miR-141, and miR-221 expression levels in prostate adenocarcinoma for associated risk of recurrence after radical prostatectomy. *The Prostate* 74, 1655–1662 (2014).
69. Ghorbanmehr, N. *et al.* miR-21-5p, miR-141-3p, and miR-205-5p levels in urine—promising biomarkers for the identification of prostate and bladder cancer. *The Prostate* 79, 88–95 (2019).
70. Porzycki, P., Ciszkowicz, E., Semik, M. & Tyrka, M. Combination of three miRNA (miR-141, miR-21, and miR-375) as potential diagnostic tool for prostate cancer recognition. *International Urology and Nephrology* 50, 1619–1626 (Sept. 1, 2018).
71. Mitchell, P. S. *et al.* Circulating microRNAs as stable blood-based markers for cancer detection. *Proceedings of the National Academy of Sciences* 105, 10513–10518 (July 29, 2008).
72. He, S. *et al.* The expression of miR-375 in prostate cancer: A study based on GEO, TCGA data and bioinformatics analysis. *Pathology - Research and Practice* 215, 152375 (June 1, 2019).
73. Wang, Y. *et al.* miR-375 induces docetaxel resistance in prostate cancer by targeting SEC23A and YAP1. *Molecular Cancer* 15, 70 (Nov. 10, 2016).
74. Selth, L. A. *et al.* A ZEB1-miR-375-YAP1 pathway regulates epithelial plasticity in prostate cancer. *Oncogene* 36. Number: 1, 24–34 (Jan. 2017).
75. Bryant, R. J. *et al.* Changes in circulating microRNA levels associated with prostate cancer. *British Journal of Cancer* 106, 768–774 (Feb. 14, 2012).

76. Helsmoortel, H., Everaert, C., Lumen, N., Ost, P. & Vandesompele, J. Detecting long non-coding RNA biomarkers in prostate cancer liquid biopsies: Hype or hope? *Non-coding RNA Research* 3, 64–74 (May 23, 2018).
77. Alshalalfa, M. *et al.* Low PCA3 expression is a marker of poor differentiation in localized prostate tumors: exploratory analysis from 12,076 patients. *Oncotarget* 8, 50804–50813 (Aug. 1, 2017).
78. Benoist, G. E. *et al.* Prognostic Value of Novel Liquid Biomarkers in Patients with Metastatic Castration-Resistant Prostate Cancer Treated with Enzalutamide: A Prospective Observational Study. *Clinical chemistry* 66, 842–851 (June 1, 2020).
79. Boerrigter, E. *et al.* RNA Biomarkers as a Response Measure for Survival in Patients with Metastatic Castration-Resistant Prostate Cancer. *Cancers* 13, 6279 (Dec. 14, 2021).
80. Prensner, J. R. *et al.* RNA biomarkers associated with metastatic progression in prostate cancer: a multi-institutional high-throughput analysis of SChLAP1. *The Lancet Oncology* 15, 1469–1480 (Dec. 1, 2014).
81. Wang, Y.-H. *et al.* Tumor-Derived Exosomal Long Noncoding RNAs as Promising Diagnostic Biomarkers for Prostate Cancer. *Cellular Physiology and Biochemistry* 46, 532–545 (2018).
82. Ren, S. *et al.* RNA-seq analysis of prostate cancer in the Chinese population identifies recurrent gene fusions, cancer-associated long noncoding RNAs and aberrant alternative splicings. *Cell Research* 22. Number: 5, 806–821 (May 2012).
83. Wang, W.-W. *et al.* Combination of long noncoding RNA MALAT1 and carcinoembryonic antigen for the diagnosis of malignant pleural effusion caused by lung cancer. *OncoTargets and therapy* 11, 2333–2344 (Apr. 24, 2018).
84. Ren, S. *et al.* Long non-coding RNA metastasis associated in lung adenocarcinoma transcript 1 derived miniRNA as a novel plasma-based

biomarker for diagnosing prostate cancer. *European Journal of Cancer* 49, 2949–2959 (Sept. 1, 2013).

85. Wang, R. *et al.* Preclinical Study using Malat1 Small Interfering RNA or Androgen Receptor Splicing Variant 7 Degradation Enhancer ASC-J9 to Suppress Enzalutamide-resistant Prostate Cancer Progression. *European Urology* 72, 835–844 (Nov. 1, 2017).
86. Yadav, A. *et al. Targeting MALAT1 Augments Sensitivity to PARP Inhibition by Impairing Homologous Recombination in Prostate Cancer* Pages: 2022.06.01.494272 Section: New Results. June 1, 2022.
87. Gurunathan, S., Kang, M.-H., Jeyaraj, M., Qasim, M. & Kim, J.-H. Review of the Isolation, Characterization, Biological Function, and Multifarious Therapeutic Approaches of Exosomes. *Cells* 8, 307 (Apr. 3, 2019).
88. Ding, S., Dong, X. & Song, X. Tumor educated platelet: the novel BioSource for cancer detection. *Cancer Cell International* 23, 91 (May 11, 2023).
89. Tjon-Kon-Fat, L.-A. *et al.* Platelets harbor prostate cancer biomarkers and the ability to predict therapeutic response to abiraterone in castration resistant patients. *The Prostate* 78, 48–53 (2018).
90. Ashworth, T. A case of cancer in which cells similar to those in the tumours were seen in the blood after death. *The Medical Journal of Australia* 14, 146–147 (1869).
91. Lin, D. *et al.* Circulating tumor cells: biology and clinical significance. *Signal Transduction and Targeted Therapy* 6, 1–24 (Nov. 22, 2021).
92. Kölbl, A. C., Jeschke, U. & Andergassen, U. The Significance of Epithelial-to-Mesenchymal Transition for Circulating Tumor Cells. *International Journal of Molecular Sciences* 17. Number: 8, 1308 (Aug. 2016).
93. Aceto, N. *et al.* Circulating Tumor Cell Clusters Are Oligoclonal Precursors of Breast Cancer Metastasis. *Cell* 158, 1110–1122 (Aug. 28, 2014).

94. Castro-Giner, F. & Aceto, N. Tracking cancer progression: From circulating tumor cells to metastasis. *Genome Medicine* 12 (Mar. 19, 2020).
95. Rushton, A. J., Nteliopoulos, G., Shaw, J. A. & Coombes, R. C. A review of circulating tumour cell enrichment technologies. *Cancers* 13, 1–33 (Mar. 1, 2021).
96. Miller, M. C., Robinson, P. S., Wagner, C. & O'Shannessy, D. J. The Parsortix™ Cell Separation System—A versatile liquid biopsy platform. *Cytometry Part A* 93, 1234–1239 (Dec. 1, 2018).
97. Lin, E. *et al.* High-Throughput Microfluidic Labyrinth for the Label-free Isolation of Circulating Tumor Cells. *Cell Systems* 5, 295–304.e4 (Sept. 27, 2017).
98. Templeman, A. *et al.* Analytical performance of the FDA-cleared Parsortix® PC1 system. *Journal of Circulating Biomarkers* 12, 26–33 (Aug. 7, 2023).
99. Scher, H. I. *et al.* Circulating tumour cells as prognostic markers in progressive, castration-resistant prostate cancer: a reanalysis of IMMC38 trial data. *The Lancet Oncology* 10, 233–239 (Mar. 1, 2009).
100. Okegawa, T., Itaya, N., Hara, H., Tambo, M. & Nutahara, K. Circulating Tumor Cells as a Biomarker Predictive of Sensitivity to Docetaxel Chemotherapy in Patients with Castration-resistant Prostate Cancer. *Anticancer Research* 34, 6705–6710 (Nov. 1, 2014).
101. Goldkorn, A. *et al.* Circulating Tumor Cell Counts Are Prognostic of Overall Survival in SWOG S0421: A Phase III Trial of Docetaxel With or Without Atrasentan for Metastatic Castration-Resistant Prostate Cancer. *Journal of Clinical Oncology* 32, 1136–1142 (Apr. 10, 2014).
102. Amato, R. J. *et al.* Epithelial Cell Adhesion Molecule-positive Circulating Tumor Cells as Predictive Biomarker in Patients With Prostate Cancer. *Urology* 81, 1303–1307 (June 1, 2013).
103. Markou, A. *et al.* Multiplex Gene Expression Profiling of In Vivo Isolated Circulating Tumor Cells in High-Risk Prostate Cancer Patients. *Clinical Chemistry* 64, 297–306 (Feb. 1, 2018).

104. Nakazawa, M., Antonarakis, E. S. & Luo, J. Androgen Receptor Splice Variants in the Era of Enzalutamide and Abiraterone. *Hormones and Cancer* 5, 265–273 (Oct. 1, 2014).
105. Antonarakis, E. S. *et al.* AR-V7 and Resistance to Enzalutamide and Abiraterone in Prostate Cancer. *New England Journal of Medicine* 371, 1028–1038 (Sept. 11, 2014).
106. Antonarakis, E. S. *et al.* Androgen Receptor Splice Variant 7 and Efficacy of Taxane Chemotherapy in Patients With Metastatic Castration-Resistant Prostate Cancer. *JAMA Oncology* 1, 582–591 (Aug. 1, 2015).
107. Scher, H. I. *et al.* Association of AR-V7 on Circulating Tumor Cells as a Treatment-Specific Biomarker With Outcomes and Survival in Castration-Resistant Prostate Cancer. *JAMA Oncology* 2, 1441–1449 (Nov. 1, 2016).
108. Antonarakis, E. S. *et al.* Clinical Significance of Androgen Receptor Splice Variant-7 mRNA Detection in Circulating Tumor Cells of Men With Metastatic Castration-Resistant Prostate Cancer Treated With First- and Second-Line Abiraterone and Enzalutamide. *Journal of Clinical Oncology* 35, 2149–2156 (July 1, 2017).
109. Bernemann, C. *et al.* Expression of AR-V7 in Circulating Tumour Cells Does Not Preclude Response to Next Generation Androgen Deprivation Therapy in Patients with Castration Resistant Prostate Cancer. *European Urology* 71, 1–3 (Jan. 1, 2017).
110. Dahiya, V. & Bagchi, G. Non-canonical androgen signaling pathways and implications in prostate cancer. *Biochimica et Biophysica Acta - Molecular Cell Research* 1869 (Dec. 1, 2022).
111. Hu, R., Denmeade, S. R. & Luo, J. Molecular processes leading to aberrant androgen receptor signaling and castration resistance in prostate cancer. *Expert review of endocrinology & metabolism* 5, 753–764 (Sept. 2010).
112. Heinlein, C. A. & Chang, C. Androgen Receptor in Prostate Cancer. *Endocrine Reviews* 25, 276–308 (Apr. 1, 2004).

113. Markowski, M. C. *et al.* Clinical Utility of CLIA-Grade AR-V7 Testing in Patients With Metastatic Castration-Resistant Prostate Cancer. *JCO Precision Oncology* 1, PO.17.00127 (Oct. 30, 2017).
114. Armstrong, A. J. *et al.* Prospective Multicenter Validation of Androgen Receptor Splice Variant 7 and Hormone Therapy Resistance in High-Risk Castration-Resistant Prostate Cancer: The PROPHECY Study. *Journal of Clinical Oncology* 37, 1120–1129 (May 2019).
115. Groen, L. *et al.* Transcriptome Profiling of Circulating Tumor Cells to Predict Clinical Outcomes in Metastatic Castration-Resistant Prostate Cancer. *International Journal of Molecular Sciences* 24, 9002 (May 19, 2023).
116. Sperger, J. M. *et al.* Prospective Evaluation of Clinical Outcomes Using a Multiplex Liquid Biopsy Targeting Diverse Resistance Mechanisms in Metastatic Prostate Cancer. *Journal of Clinical Oncology* 39, 2926–2937 (Sept. 10, 2021).

Chapter 3

The Androgen Regulated lncRNA NAALADL2-AS2 Promotes Prostate Cancer Survival

Adapted from:
Groen, L. et al. The Androgen Regulated lncRNA NAALADL2-AS2 Promotes Tumor Cell Survival in Prostate Cancer. ncRNA 8, 81 (2022).

3.1 Introduction

Prostate cancer (PCa) is a hormone-driven malignancy that depends on androgen receptor (AR) signaling for survival and progression. Accordingly, antagonizing the AR is an effective treatment in both early-stage and advanced disease. Globally, approximately 10–20% of patients progress to castration-resistant disease within five years of diagnosis, and longer follow-up indicates that the cumulative incidence continues to rise beyond five years [1]. Notably, most castration-resistant tumors remain dependent on AR signaling [2]. Multiple mechanisms can sustain AR activity in castration-resistant prostate cancer (CRPC), including amplification of AR pathway genes, AR splice variants, de novo steroidogenesis, and non-canonical AR signaling [3, 4].

Long non-coding RNAs (lncRNAs) can regulate transcription by interacting with transcription factors, modulating chromatin states, and scaffolding transcriptional complexes [5]. Through these functions, lncRNAs can activate and/or repress AR signaling, providing an additional route to castration resistance [6, 7]. Advances in next-generation sequencing have substantially expanded our understanding of cancer transcriptomes and the roles of non-coding RNAs. Consistent with this, preclinical studies have identified several lncRNAs that sustain AR signaling under androgen-deprived conditions [6, 8, 9]. The lncRNA *CCAT1* acts as a scaffold for the AR transcriptional complex and promotes AR target-gene expression under castrate conditions [8]. The expression of *ARv7*, a key driver of resistance to AR-targeted therapies, has been reported to depend on the lncRNA *MALAT1* [6, 10]. In addition, *PCA3* promotes PCa cell proliferation by suppressing the tumor-suppressor gene *p53* through regulation of chromatin organization [9]. Collectively, lncRNAs can support PCa progression under androgen deprivation therapy (ADT) via diverse molecular mechanisms. Characterizing highly expressed PCa-associated lncRNAs under castrate conditions may therefore reveal new prognostic biomarkers and therapeutic targets, strengthening links between

targeted therapy and precision diagnostics.

In this chapter, transcriptome analysis of an RNA-sequencing dataset comprising biopsy material from benign prostatic hyperplasia (BPH), low-grade hormone-sensitive PCa, high-grade hormone-sensitive PCa, and CRPC identified several previously unreported lncRNAs that are upregulated in CRPC. Following quantitative polymerase chain reaction (qPCR) validation of a subset of candidate lncRNAs in an expanded cohort, *NAALADL2-AS2* was selected for in-depth functional characterization. Tissue-specific expression was evaluated using The Cancer Genome Atlas (TCGA) and Genotype-Tissue Expression (GTEx) databases. Regulation of *NAALADL2-AS2* was examined using hormone modulation assays and RNA interference. Its role in tumor cell survival and apoptosis was assessed using RNA interference and cell viability assays. Subcellular localization was determined by quantifying nuclear and cytoplasmic transcripts and by RNA-fluorescent in situ hybridization (RNA-FISH). Finally, RNA interference followed by transcriptome and pathway analyses identified genes and pathways regulated by *NAALADL2-AS2* in androgen-sensitive PCa.

3.2 Results

3.2.1 NAALADL2-AS2 is Upregulated in CRPC

Differential gene expression analysis using RNA sequencing data from CRPC (n=4), high-grade hormone-sensitive PCa (n=4), and BPH/normal (n=7) tumor RNA specimens led to the identification of several CRPC-associated lncRNAs (Figure 3.1) (Table 3.1). *NAALADL2-AS2* was the most upregulated lncRNA in CRPC compared with localized PCa (Figure 3.1A). To further define its expression context, the Genotype-Tissue Expression (GTEx) and TCGA databases were interrogated [11]. Expression of *NAALADL2-AS2* is increased in esophageal carcinoma, diffuse large B-cell lymphoma, lung squamous cell carcinoma, stomach adenocarcinoma, ovarian serous cystadenocarcinoma, and prostate adenocarcinoma. In contrast, *NAALADL2-AS2*

is not expressed in their normal tissue counterparts (Figure 3.1B). In semi-quantitative PCR validation using tumor-derived RNA, *NAALADL2-AS2* was significantly upregulated in CRPC compared with normal tissue, BPH, low- and high-grade PCa (Figure 3.1C). Analysis of TCGA prostate adenocarcinoma (PRAD) transcriptomic data showed that patients with high tumoral *NAALADL2-AS2* expression have a shorter time to progression than those with low *NAALADL2-AS2* expression (Figure 3.1D).

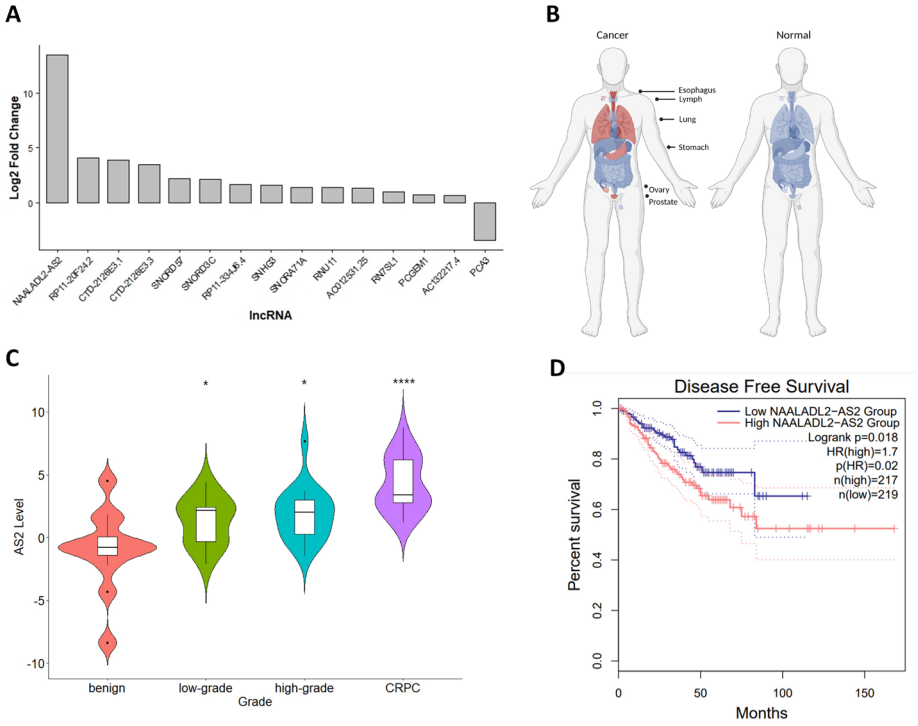

Figure 3.1: *NAALADL2-AS2* is upregulated in PCa.

The expression of *NAALADL2-AS2* CRPC versus localized PCa (A). Graphical representation of *NAALADL2-AS2* expression (red) in various malignant (left, TCGA data) and non-malignant (right, GTEx data) accessed via GEPIA2 [11], stylized with BioRender.com (B). *NAALADL2-AS2* expression as determined by qPCR in benign, hormone-sensitive low-grade PCa (Gleason score <7), high-grade PCa (Gleason score ≥ 7), and CRPC. Pairwise means comparison against the benign group was done using a T-test, $*p<0.05$, $****p<0.0001$ (C). Kaplan Meier survival analysis of localized PCa patients with high and low tumor *NAALADL2-AS2* expression (median cut off) (PRAD TCGA data) [11] (D).

Table 3.1: The expression of selected lncRNAs in Prostate Tissue Biopsies.

lncRNA	Normal	BPH	High-grade	mCRPC
NAALADL2-AS2	0,00	0,00	0,00	9,92
RP11-20F24.2	0,013	0,00	0,50	8,47
CTD-2126E3.1	0,14	0,20	0,11	1,64
CTD-2126E3.3	0,41	0,21	0,27	3,03
SNORD57	108,99	39,82	35,98	168,22
SNORD3C	94,61	3,19	4,78	21,06
RP11-334J6.4	29,23	1,29	4,49	14,63
SNHG3	113,47	25,03	65,36	197,05
SNORA71A	30,15	8,71	27,71	74,33
RNU11	112,55	20,8	10,74	28,28
AC012531.25	0,091	0,03	0,68	1,74
RN7SL1	39335,03	58220,24	31405,61	61942,52
PCGEM1	0,25	3,37	0,43	0,70
AC132217.4	4,94	12,49	2,61	4,22
PCA3	0,15	0,05	21,99	2,03

Expression is shown in normal prostate (Normal), BPH, High-grade PCa, and mCRPC. Normal (n=4); BPH (n=3); High-grade PCa (n=4); mCRPC (n=4). Average Fragments Per Kilobase Million (FPKM) expression values.

3.2.2 NAALADL2-AS2 is co-expressed with NAALADL2

NAALADL2-AS2 is located on the long arm of chromosome 3, in the antisense orientation of the oncogene *NAALADL2* (Figure 3.2A). To assess whether these two transcripts are co-expressed, we performed a correlation analysis using gene expression data from tumor-derived RNA samples from 44 PCa patients. There is a strong positive correlation between the expression of *NAALADL2-AS2* and *NAALADL2* (R=0.8, $p<2.2\times10^{-16}$) (Spearman) (Figure 3.2B). The outliers in this analysis correspond to benign

or metastatic samples. The low-grade, high-grade, and CRPC samples generally follow the regression line. Given that many antisense lncRNAs regulate their neighboring sense genes, we assessed *NAALADL2* expression following *NAALADL2-AS2* knockdown using GapmeR antisense oligonucleotides [12]. Notably, *NAALADL2-AS2* knockdown did not alter *NAALADL2* expression (Figure 3.2C, and Figure 3.2D).

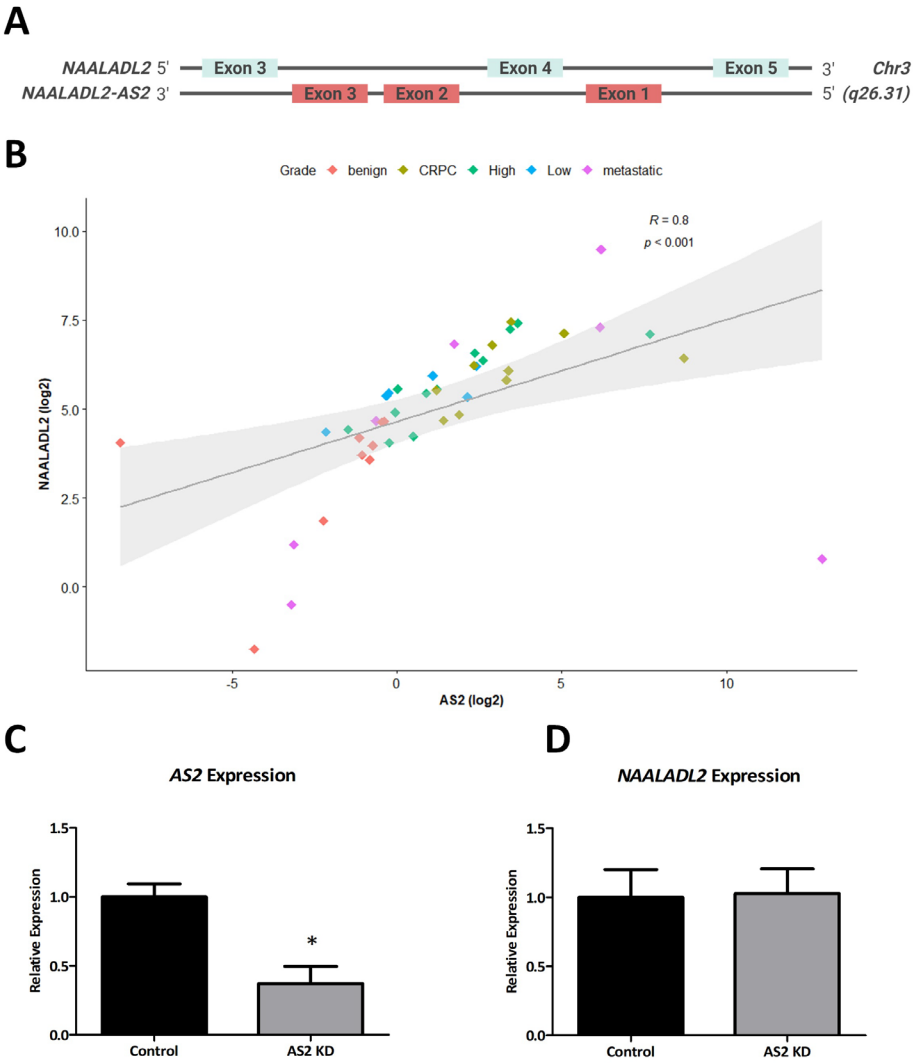

Figure 3.2: *NAALADL2-AS2* is co-expressed with *NAALADL2*.

The genomic structures of *NAALADL2* and *NAALADL2-AS2* as interpreted from the UCSC Genome Browser (GRCh38/hg38) (not to scale) (A). The expression of *NAALADL2-AS2* (AS2) and *NAALADL2* in tumor RNA samples measured by qPCR (n=44), Spearman correlation (B). The expression of *NAALADL2-AS2* (AS2) (C) and *NAALADL2* (D) measured by qPCR in LAPC-4 cells cultured with scrambled (Control) or *NAALADL2-AS2*-specific GapmeR antisense oligonucleotides (AS2 KD) for 72 hours. Pairwise means comparison was done using a T-test, *p<0.05 (n=3).

3.2.3 NAALADL2-AS2 Copy Number Alterations

Somatic alterations at the 3q26.31–32 locus, which harbors *NAALADL2-AS2*, occur in over 50% of PCa patients [13]. Copy-number gains encompassing this locus have been reported for *NAALADL2* and *TBL1XR1* in 20–30% of CRPC and neuroendocrine prostate cancer (NEPC) tumors (Figure 3.3A). Consistent with this, tumors harboring these gains show increased *NAALADL2* and *TBL1XR1* expression (Figure 3.3B). In contrast, copy-number gains at 3q26.31–32 do not appear to be associated with increased *NAALADL2-AS2* expression across PCa cell lines (PC3, DU145, LNCaP, 22Rv1, VCaP, and MDA-PCa 2B) (Figure 3.3C, and Figure 3.4).

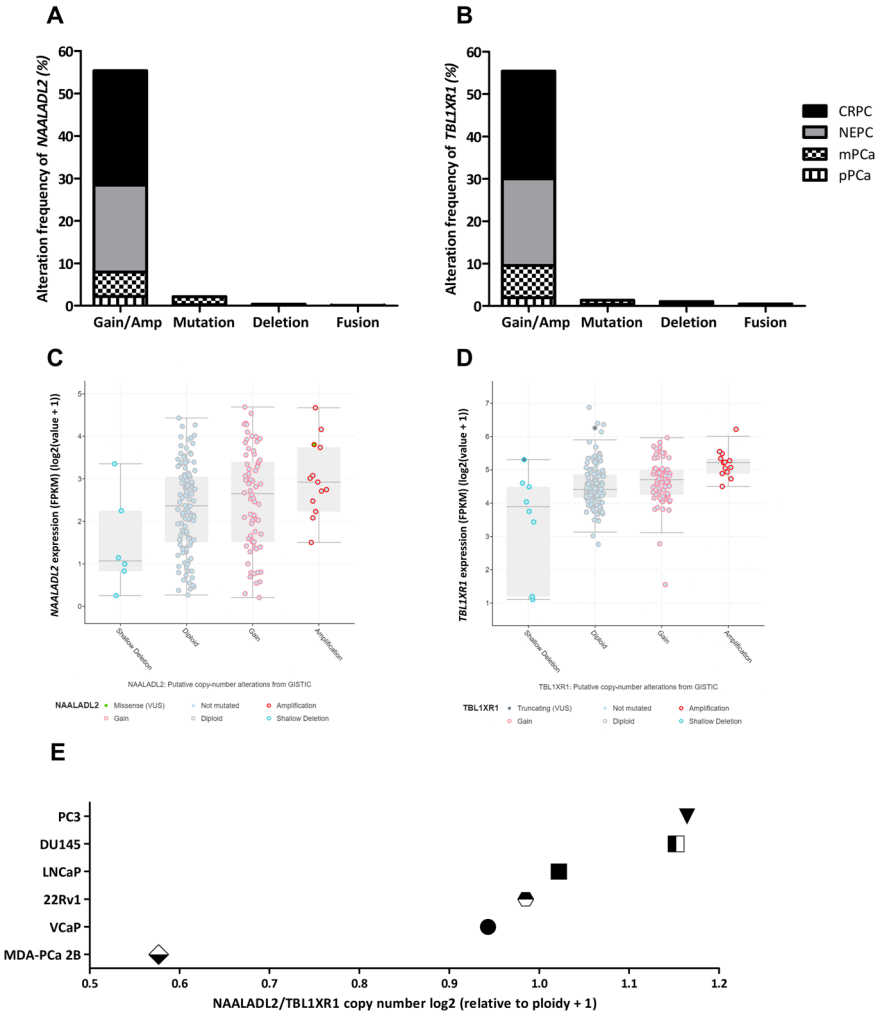

Figure 3.3: Copy number gain of the 3q26.31-32 locus.

Alteration frequency of *NAALADL2* (A) and *TBL1XR1* (B) in prostate cancer subtypes. Copy number alterations and relative mRNA expression levels of *NAALADL2* (C) and *TBL1XR1* (D) in PCa. Copy numbers of *NAALADL2* and *TBL1XR1* in six PCa cell lines (E). Publicly available data containing 3804 patients in 16 non-overlapping studies, of which eleven focused on primary PCa (pPCa), four on metastatic PCa (mPCa), one on NEPC, and one on CRPC (A/B) [13]. The copy number and mRNA plots were produced using cBioportal, including 2 studies (C/D) [14, 15]. Copy number alterations in cell lines were obtained from the Broad Institute's DepMap portal [16] (E).

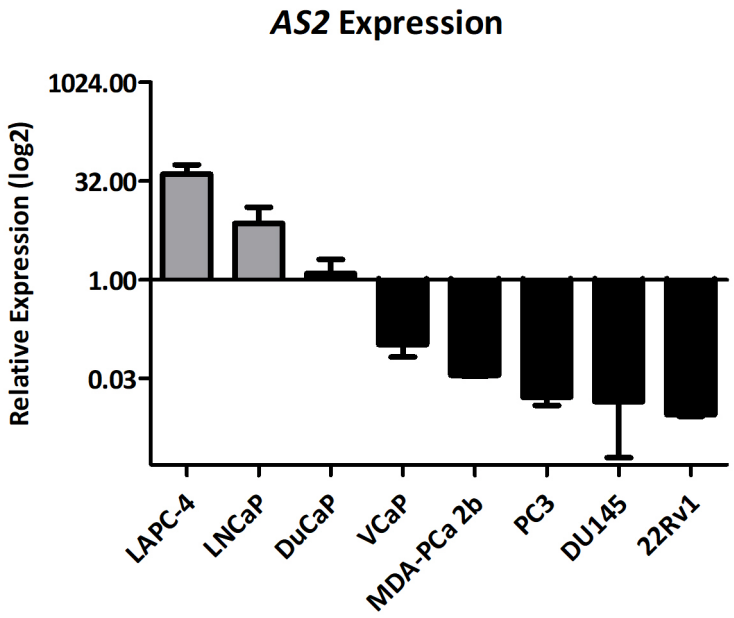

Figure 3.4: The expression of *NAALADL2-AS2* in PCa cell lines.

The expression of *NAALADL2-AS2* measured via qPCR in LAPC-4, LNCaP, DuCaP, VCaP, MDA-PCa 2b, PC3, DU145, and 22Rv1 PCa cell lines.

3.2.4 Androgens Regulate NAALADL2-AS2 Expression

To examine the regulation of *NAALADL2-AS2* expression, we established an in vitro androgen-deprivation model. Androgen-sensitive LNCaP cells were cultured under androgen-depleted conditions and subsequently stimulated with the synthetic AR ligand R1881. Androgen deprivation increased *AR* expression and markedly reduced *KLK3*, a canonical AR target gene (Figure 3.5A and Figure 3.5B). In contrast to *KLK3*, *NAALADL2-AS2* expression increased significantly following androgen depletion (Figure 3.5C). Consistent with this, LAPC-4 cells exposed to decreasing concentrations of R1881 showed

increased *NAALADL2-AS2* expression accompanied by reduced *KLK3* expression (Figure 3.5D). Together, these data indicate that acute androgen deprivation induces *NAALADL2-AS2* in androgen-sensitive PCa cells. To determine whether this effect persists under chronic castrate conditions, we compared *NAALADL2-AS2* expression in androgen-sensitive LAPC-4 and LNCaP cells with their castration-resistant counterparts (LAPC4-CR and LNCaP-CR). Contrary to our hypothesis, *NAALADL2-AS2* expression was reduced in LAPC4-CR and LNCaP-CR relative to the androgen-sensitive parental lines (Figure 3.6) [17].

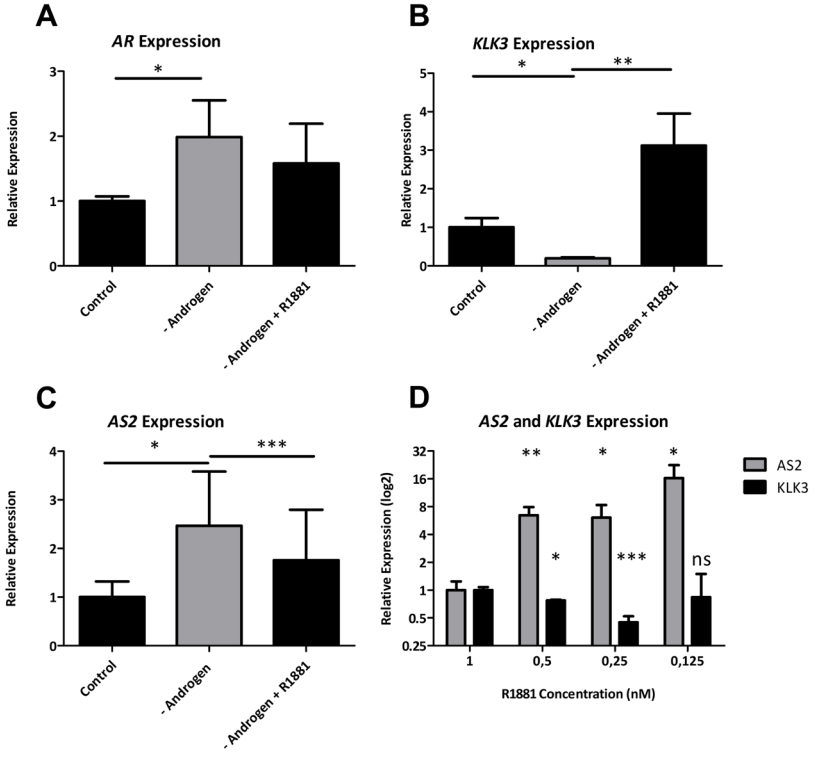

Figure 3.5: Androgen deprivation increases *NAALADL2-AS2* expression.

The expression of *AR* (A), *KLK3* (B), and *NAALADL2-AS2* (AS2) ()C measured via qPCR in LNCaP cells cultured with fetal bovine serum (Control), charcoal-stripped serum (CSS) (-Androgen) or CSS with synthetic androgen R1881 (-Androgen + R1881). *AS2* and *KLK3* expression measured via qPCR in LAPC-4 cells cultured in decreasing concentrations of R1881 (D). Pairwise means comparison was done using a T-test, $*p<0.05$, $**p<0.01$, $***p<0.001$.

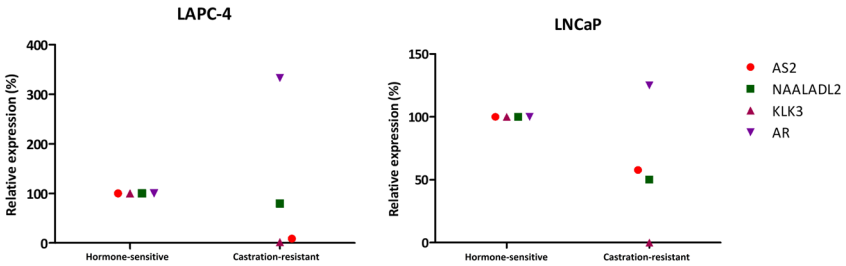

Figure 3.6: The expression of *NAALADL2-AS2* is reduced in castration-resistant LNCaP and LAPC-4.

Relative expression of *NAALADL2-AS2* (AS2), *NAALADL2*, *KLK3*, and *AR* in hormone-sensitive LAPC-4 and LNCaP cells, and castration-resistant LAPC-4 and LNCaP cells.

3.2.5 AR Does Not Directly Regulate NAALADL2-AS2 Expression

Following the observed androgen-dependent regulation of *NAALADL2-AS2*, we hypothesized that AR signaling might be involved. The AR transcriptional regulatory complex comprises multiple cofactors, and in silico analysis using the UCSC Genome Browser (GRCh37/hg19) identified putative binding sites for the AR cofactors GATA2 and FOXA1 near the *NAALADL2-AS2* transcription start site (TSS) [18] (Figure 3.7). To test whether AR, GATA2, or FOXA1 regulate *NAALADL2-AS2* expression, we performed small interfering RNA (siRNA)-mediated knockdown experiments in the androgen-sensitive cell lines LNCaP, LAPC-4, and DuCaP.

siRNAs targeting *AR* mRNA (AR knockdown (KD)) significantly reduced the expression of *AR* by approximately 70% in LNCaP and LAPC-4 cells (Figure 3.8A and Figure 3.8D). As expected, this decreased the expression of the canonical AR target gene *KLK3* (Figure 3.8B, and Figure 3.8E). In contrast, *NAALADL2-AS2* expression was unchanged following *AR* knockdown (Figure 3.8C, and Figure 3.8F). Similarly, knockdown of *GATA2* or *FOXA1* significantly reduced expression of each cofactor but did not affect

NAALADL2-AS2 levels in LAPC-4, LNCaP, or DuCaP cells (Figure 3.8G–I, and Figure 3.9).

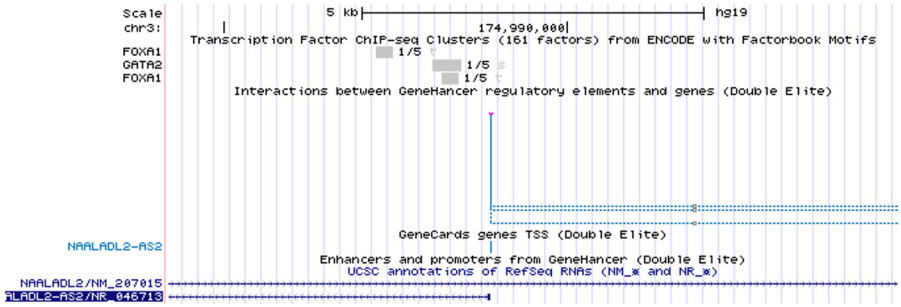

Figure 3.7: GATA2 and FOXA1 regulatory elements at the *NAALADL2-AS2* transcription start site (TSS).

UCSC Genome Browser on Human (GRCh37/hg19).

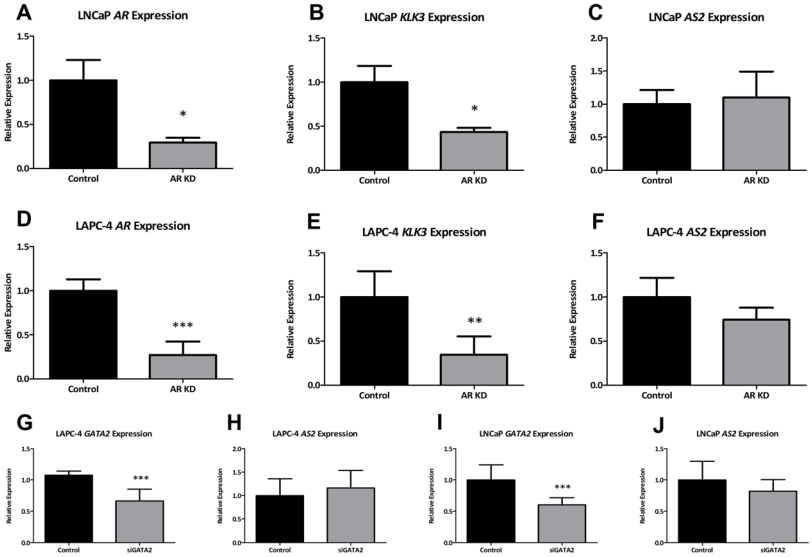

Figure 3.8: Knockdown of *AR* and *GATA2* does not affect *NAALADL2-AS2* expression.

The expression of *AR*, *KLK3*, and *NAALADL2-AS2* (AS2) measured via qPCR in LNCaP and LAPC-4 cells following knockdown of *AR* (A-F) and *GATA2* (G-J). All experiments were performed at $n \geq 3$. Pairwise means comparison was done using a T-test, $^{*}p<0.05$, $^{**}p<0.01$, $^{***}p<0.001$.

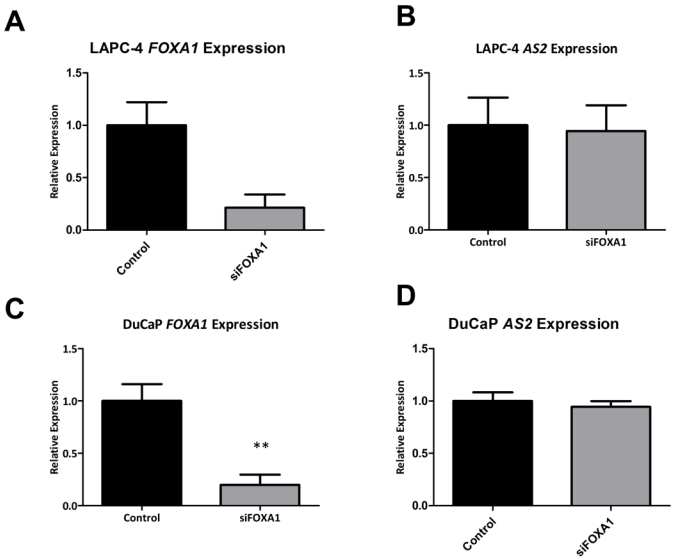

Figure 3.9: Knockdown of *FOXA1* does not affect *NAALADL2-AS2* expression.

The expression of *FOXA1*, and *NAALADL2-AS2* measured via qPCR in LAPC-4 (A/B), and DuCaP (C/D) cells following knockdown of *FOXA1*. All experiments were performed at $n \geq 3$. Pairwise means comparison was done using a T-test, $^{**}p<0.01$.

3.2.6 NAALADL2-AS2 Promotes PCa Survival by Inhibition of Apoptosis

To investigate the biological function of *NAALADL2-AS2* in localized PCa and CRPC, we used LAPC-4 cells as an androgen-sensitive model and DuCaP cells as a CRPC model. In LAPC-4 cells, transfection with chemically modified single-stranded antisense oligonucleotides (GapmeRs) achieved approximately 70% knockdown of *NAALADL2-AS2* (Figure 3.10A). We attempted to establish a comparable knockdown in DuCaP cells; however, GapmeR transfection consistently compromised cell viability, precluding reliable measurement of *NAALADL2-AS2* expression in this model.

An imbalance between cell proliferation and cell death is a central hallmark of cancer [19]. In this study, proliferative capacity was assessed via cell viability by quantifying cellular adenosine triphosphate (ATP) levels, whereas apoptosis was evaluated using caspase-3/7 activity and DNA fragmentation as surrogate readouts.

Cell viability decreased after *NAALADL2-AS2* knockdown, with a marked reduction by day 3 post-transfection and a significant reduction by day 6 compared with controls (Figure 3.10B). Caspase-3/7 activity increased from day 2 following *NAALADL2-AS2* knockdown in both LAPC-4 and DuCaP cells relative to controls (Figure 3.10C, and Figure 3.10D). Consistent with these findings, *NAALADL2-AS2* knockdown increased the proportion of cells with fragmented DNA, as indicated by an increased sub-G1 fraction in our cell cycle analysis (Figure 3.10E, and Supplementary Figure 1). In DuCaP cells, the sub-G1 fraction could not be quantified because extensive debris was present after *NAALADL2-AS2* knockdown.

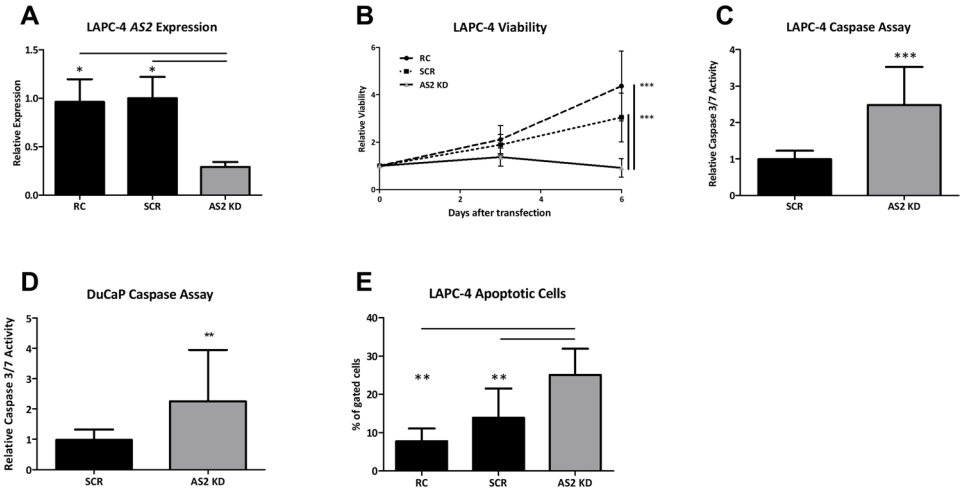

Figure 3.10: Knockdown of *NAALADL2-AS2* reduces cell viability and increases apoptosis.

The expression of *NAALADL2-AS2* (AS2) measured in LAPC-4 cells after transfection with transfection reagent (RC), scrambled GapmeR (SCR), and AS2-specific GapmeR (AS2 KD) for 72 hours (h) (A). LAPC-4 cell viability was assessed on days 0, 3, and 6 after transfection (B). Caspase activity was assessed two days after transfection in both LAPC-4 and DuCaP cells (C/D). DNA fragmentation was measured via flow cytometry five days following transfection in LAPC-4 cells (E). All experiments were performed at $n \geq 3$. Pairwise means comparison was done using a T-test, $*p<0.05$, $**p<0.01$, $***p<0.001$.

3.2.7 NAALADL2-AS2 Is a Nuclear RNA

To define the subcellular context of *NAALADL2-AS2*, which may act as a transcriptional regulator, we hypothesized that it localizes to the nucleus. We assessed *NAALADL2-AS2* in tumor cells using two approaches: qPCR of isolated cytoplasmic and nuclear RNA fractions, and RNA-FISH in formaldehyde-fixed cells. RNA was extracted from cytoplasmic and nuclear fractions of LNCaP and MDA-PCa 2b cells and analysed by qPCR. *RNU6* was used as a nuclear marker and *GAPDH* as a cytoplasmic marker. As expected, *RNU6* was enriched in nuclear fractions. *GAPDH* was largely

cytoplasmic in LNCaP cells; however, in MDA-PCa 2b cells it was detected in both fractions, consistent with potential nuclear-fraction contamination. Nevertheless, *NAALADL2-AS2* was detected almost exclusively in the nuclear fractions of both cell lines (Figure 3.11A and Figure 3.11B).

A combined RNA-FISH and immunofluorescence assay was devised to visualize *NAALADL2-AS2* RNA molecules, cytokeratin (CK) -8 -18 -19 proteins, and nuclear DNA in PCa cells. LAPC-4 cells were used due to their relatively high levels of *NAALADL2-AS2* expression. PC3 cells were used as a negative control, as this PCa line lacks *NAALADL2-AS2* expression effectively. Molecules of *NAALADL2-AS2* (green) were imaged by hybridizing fluorescent probes conjugated to LNA-GapmeR with complementary sequences, enabling accurate cellular localization. The nuclear environment was imaged using DAPI (4',6-diamidino-2-phenylindole), which targets the adenine-thymine DNA regions (blue). Cytoplasmic environments were visualized using fluorescent antibodies against CK -8 -18 -19 (red) (Figure 3.11C and Figure 3.11D). Figure 3.11C illustrates a fluorescent image of LAPC-4 cells, where distinct foci indicate *NAALADL2-AS2* concentrations in the nuclear environment but not the cytoplasmic environment. In contrast, no *NAALADL2-AS2* concentrations were detected in PC3 cells (Figure 3.11D).

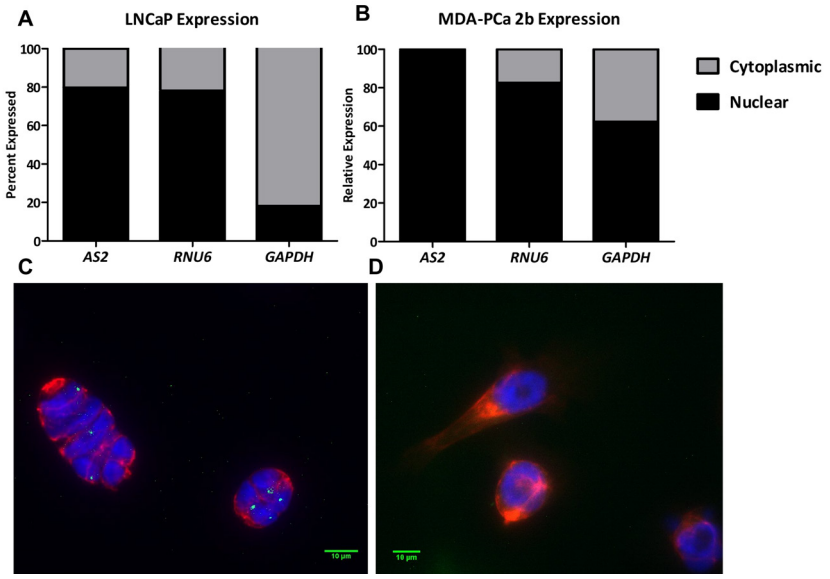

Figure 3.11: *NAALADL2-AS2* transcripts localize in the nucleus.

NAALADL2-AS2 (*AS2*), *RNU6*, and *GAPDH* transcripts levels were analyzed via qPCR in the cytoplasmic and nuclear fractions of LNCaP and MDA-PCa 2b cells (A/B). *AS2* RNA transcripts (green), cytokeratin protein (red), and nuclear DNA (blue) were visualized using RNA in situ hybridization and immunofluorescence in LAPC-4 (C) and PC3 (D), respectively.

3.2.8 NAALADL2-AS2 Modulates the Expression of Survival Genes

Nuclear lncRNAs are crucial in controlling gene expression by impacting transcriptional processes occurring before and after transcription, as well as directly at active transcription sites [5]. This chapter investigates the regulatory role of *NAALADL2-AS2* through transcriptome analysis of LAPC-4 cells following *NAALADL2-AS2* knockdown via GapmeR transfection. RNA was extracted from three independent experiments 72 hours after transfection. Knockdown efficacy was confirmed using qPCR. To mitigate potential off-target effects, cells transfected with scrambled control oligonucleotides (SCR) were omitted from the analysis. The DESeq2 package in RStudio was

used to assess differential gene expression, following the protocol described by Love et al. [20]. Changes were considered significant based on an adjusted p-value ($p < 0.001$). Significant differentially expressed genes (DEGs) were defined using an adjusted p-value threshold of $p<0.001$. A total of 333 genes were differentially expressed in *NAALADL2-AS2* knockdown group compared to controls (Figure 3.12A). A significant majority of DEGs showed increased expression in *NAALADL2-AS2* knockdown cells. Hence, the expression of these genes is likely suppressed by *NAALADL2-AS2*. Reactome Pathway Browser was used to visualize and interpret the biological function of *NAALADL2-AS2* in PCa. This revealed deregulated pathways associated with TP53, CDKN1A, and glycogen metabolism following *NAALADL2-AS2* knockdown (Figure 3.12B) [21]. DESeq2 results were validated by qPCR (Figure 3.13).

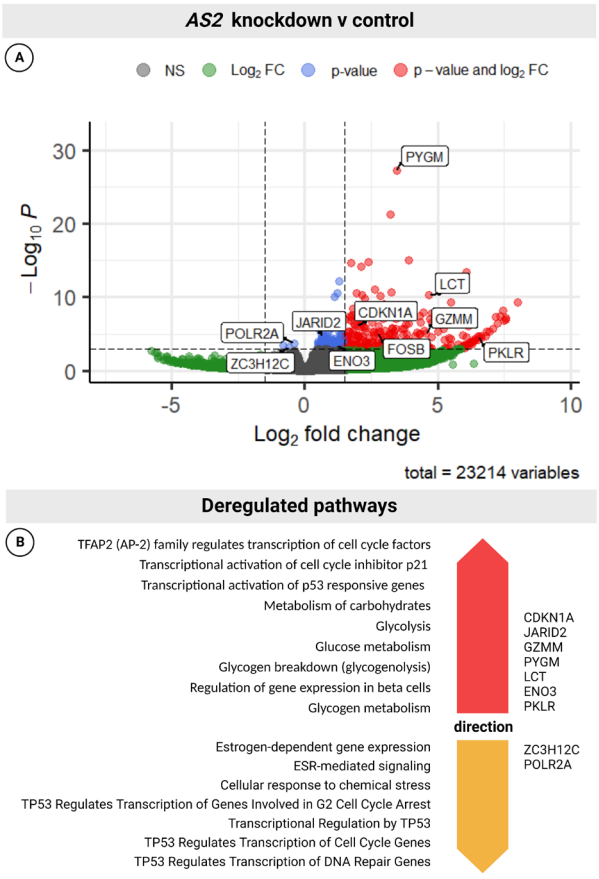

Figure 3.12: *NAALADL2-AS2* regulates the expression of genes related to cell cycle control, apoptosis, and glycogen metabolism.

Volcano plot showing the DEGs between *NAALADL2-AS2* knockdown (AS2 KD) and reagent control (A). Pathways that are deregulated upon *AS2* knockdown, upregulated pathways shown in orange, downregulated pathways shown in yellow (B). Statistical significance for the selection of DEGs was set to $padj<0.001$, $n=3$. The figure was stylized using BioRender.com.

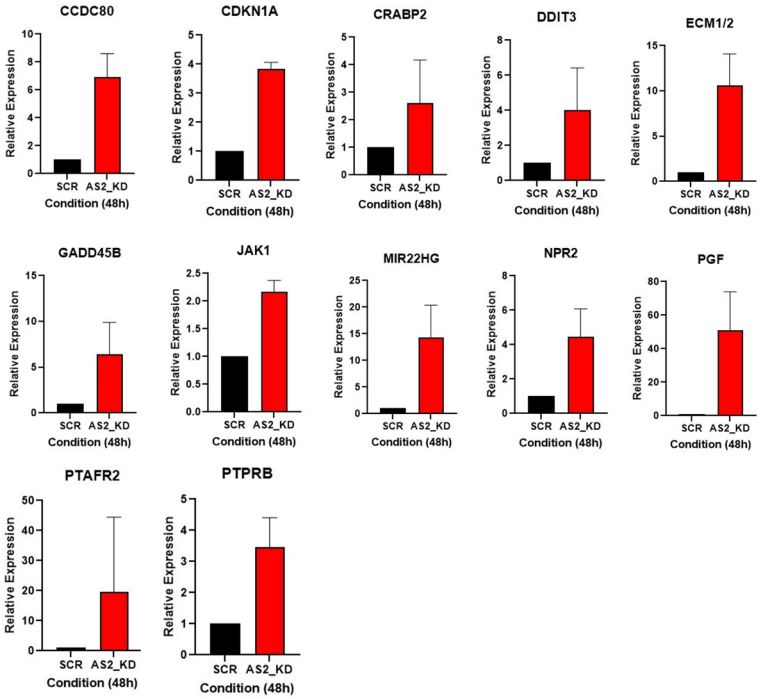

Figure 3.13: Quantitative validation of *NAALADL2-AS2* gene targets.

Quantitative PCR validation of *NAALADL2-AS2* regulated genes.

3.3 Discussion

Castration resistance is the leading cause of PCa-related death. Sustained androgen signaling under ADT is a hallmark in the progression from androgen-sensitive PCa to CRPC. Low levels of remaining androgens are likely the primary drivers of progression under ADT [22]. In fact, tumor dihydrotestosterone (DHT) levels have been shown to remain at 25% of pre-ADT levels 6 months into treatment [22]. In an effort to tackle this issue, ADT, in combination with CYP17A inhibitors or AR antagonists, is now the standard of care in most Western countries. Although modestly successful, there is room for improvement [23]. By directing research efforts toward unraveling the survival mechanisms employed by primary PCa cells under ADT, future lives may be spared. Clinical trials have largely mobilized around more potent AR antagonists, inhibitors of de novo steroidogenesis, and more recently targeting AR splice variants as novel AR targeted therapies (NCT03123978, NCT02807805, NCT02566772, NCT03888612). Unfortunately, less than 1% of primary PCa patients are ARv7 positive. This number increases marginally to 3% of first-line CRPC patients [24]. However, approximately 20% of all PCa patients will develop castration resistance within 5 years of their diagnosis [25].

As mentioned in Chapter 1, ncRNAs constitute a major part of a cell's transcriptional regulation. In the nucleus, ncRNAs can modulate transcription by scaffolding with other RNAs and proteins to guide or block access to chromatin, interact with active transcriptional sites, alter splicing, or stabilize mRNA [5]. For example, the lncRNA *PCGEM1* has been found to aid AR binding to the promoter regions of AR-regulated genes under ADT, while lncRNA *PCA3* suppresses the function of the tumor suppressor p53, of which the inactivation is central to PCa tumor progression [9, 26, 27]. Another example is *MALAT1*, which alters splicing to produce therapy-resistant splice variant ARv7 [6]. ncRNAs can form an integral part of a cancer cell's adaptive response when exposed to targeted therapies such as ADT.

In this study, the lncRNA *NAALADL2-AS2* was found to be upregulated in CRPC tumor biopsies when compared to low-and high-grade PCa and benign prostatic tissue. In silico analysis using TCGA data suggests that *NAALADL2-AS2* may be overexpressed in a number of other malignancies. In localized hormone-sensitive PCa, *NAALADL2-AS2* likely functions as a driver for progression, as patients with high expression of *NAALADL2-AS2* have reduced PFS when compared to patients with low *NAALADL2-AS2* expression (Figure 3D). A previous publication identified the *NAALADL2-AS2* overlapping protein-coding *NAALADL2* gene as an oncogene in PCa, although the function of *NAALADL2* remains elusive [28]. We found that *NAALADL2* and its antisense transcript, *NAALADL2-AS2*, are co-expressed. Being an antisense lncRNA, we hypothesized that *NAALADL2-AS2* functions as an mRNA stabilizer of NAALADL2 [12]. Yet, the knockdown of *NAALADL2-AS2* did not affect *NAALADL2* expression levels. Cell viability, however, was markedly decreased upon *NAALADL2-AS2* knockdown, which was accompanied by the increased induction of apoptosis. This suggests that *NAALADL2-AS2* functions to promote tumor cell survival. Transcriptome analysis of LAPC-4 cells with *NAALADL2-AS2* knockdown identified 333 DEGs, the majority of which were upregulated. Amongst those upregulated DEGs, *CDKN1A*, *GZMM*, and *FOSB* are known modulators of apoptosis. In cancer cell lines, overexpressed *CDKN1A* has been found to enhance cell death responses following DNA damage induced by cisplatin [29, 30]. Furthermore, *CDKN1A* is transcriptionally controlled by tumor suppressor TP53, which controls key biological pathways related to cell cycle control and apoptosis. As shown in our pathway analysis, TP53-related pathways were significantly deregulated. Interestingly, amongst the few downregulated DEGs, *ZC3H12C* mapped to several TP53-related pathways. By modulating the expression of TP53-signaling genes, *NAALADL2-AS2* could suppress apoptosis and promote the survival of PCa cells. Independent of TP53 signaling, *GZMM*, and *FOSB* are known to promote apoptosis by caspase activation and as part of the AP-1 transcription factor complex, respectively [31, 32]. Increased *FOSB* expression has been shown to be pro-apoptotic

in MCF7 cells [33]. By modulating glycogen metabolism, *NAALADL2-AS2* may also indirectly promote survival in PCa cells [34]. Amongst the *NAALADL2-AS2*-modulated genes, there were three enzymes involved with glycogen and carbohydrate metabolism, namely *PYGM*, *ENO*, and *LCT*. Glycogen is an important source of energy for cancer cells under stressful and hypoxic conditions [35]. In this light, ADT-induced *NAALADL2-AS2* expression could preserve glycogen stores by the downregulation of glycolytic enzymes such as PYGM. In turn, increased glycogen storage may promote the survival of ADT-stressed PCa cells. This hypothesis finds credence in a study from Schnier *et al.,* who found that androgen deprivation led to glycogen accumulation in hormone-sensitive LNCaP cells but not in hormone-insensitive PC3 cells [36]. As shown in Figure 7, *NAALADL2-AS2* expression increases in LNCaP cells exposed to ADT. Future studies could help elucidate the role of *NAALADL2-AS2* in the context of ADT, glycogen homeostasis, and PCa cell survival.

Over 50% of all PCa tumors bear an amplification in the 3q26.31-32 locus, a genetic region on chromosome 3 known for its high density of oncogenes including *NAALADL2* and *TBL1XR1.* CN gains of these genes are associated with their increased expression, consistent with the mechanism of self-regulating expression. *NAALADL2* is co-expressed with various AR-target genes while its genetic neighbor, *TBL1XR*, is a known AR co-activator [13]. This prevalent CN alteration (CNA) could also be a key driver of *NAALADL2-AS2* expression. Indeed, we found *NAALADL2-AS2* to be androgen-regulated, but not via direct control of the AR or two of its major co-factors, GATA2 and FOXA1. GATA2 remains a candidate of interest due to its association with *NAALADL2* expression and its binding motifs at the *NAALADL2* and *NAALADL2-AS2* promoters. With this in mind, one could expect a positive association between CNs of *NAALADL2* and *TBL1XR1* and *NAALADL2-AS2* expression. Yet, DU145 and PC3 cells do not express *AS* but have the highest CNs of *NAALADL2*/*TBL1XR* (Figures 5 & 6A). By focusing on transcription factors that are negatively regulated

by androgens with binding sites near the *NAALADL2-AS2* promoter, future studies may identify the drivers of *NAALADL2-AS2*, and accordingly *NAALADL2*, expression. To summarize, we found *NAALADL2-AS2* to be androgen-regulated, promote tumor cell survival, and modulate the expression of genes involved with apoptosis and glycogen metabolism. Together, *NAALADL2-AS2* could provide an adaptive response to ADT by preventing apoptosis and promoting survival in hormone-sensitive PCa cells.

Due to remaining androgens under primary ADT and sustained AR signaling, ARSIs are used to enhance castration in first-line CRPC therapy [37, 38]. Successive lines of AR-targeted therapy induce an evolutionary selection for androgen-insensitive cells. In fact, clonal expansion of these cells has been shown to drive resistance to enzalutamide and abiraterone, two commonly used ARSIs [14]. Under the pressure of ARSIs, castration-resistant cells gain an adaptive advantage. In this scenario, high *NAALADL2-AS2* levels may help to identify patients with largely androgen-driven tumors and sensitivity to ARSIs. Vice versa, patients with low *NAALADL2-AS2* levels might benefit from alternative treatments. In this light, castration-resistant LAPC-4-CR and LNCaP-CR show decreased expression of *NAALADL2-AS2* when compared to their parental lines, suggesting a redundant role for *NAALADL2-AS2* in a castration-resistant setting [17]. This could also explain the perceived discordance of *NAALADL2-AS2* levels in CRPC tissue and CRPC-like cell lines. In the context of CRPC tissue samples, *NAALADL2-AS2* expression is increased due to exposure to first-line ADT. In contrast, CRPC-like cell lines are continuously cultured under hormone-deprived conditions, akin to successive lines of AR-targeted therapy. Having adequately adapted to these conditions, *NAALADL2-AS2* expression is likely to become redundant. As such, increased *NAALADL2-AS2* expression constitutes part of an acute adaptive response for survival under ADT, a response that is not required for adequately adapted castration-resistant cells. This hypothesis is supported by two studies I published in collaboration with the Radboudumc Department of Pharmacology. Here we found high blood-*NAALADL2-AS2* levels in

CRPC patients treated with ARSIs to be favorable for survival, while low *NAALADL2-AS2* levels were unfavorable [39, 40]. These findings support the clinical utility of *NAALADL2-AS2* as a liquid biopsy-based ARSI response biomarker in CRPC. Future clinical trials should evaluate the potential of *NAALADL2-AS2* as a liquid biopsy-based ADT response biomarker in the hormone-sensitive setting.

3.4 Conclusion

The lncRNA *NAALADL2-AS2* is overexpressed in various cancers, including PCa. In PCa, the expression of *NAALADL2-AS2* is increased in high-grade and CRPC tumors when compared to low-grade and benign prostate specimens. In the androgen-sensitive setting, high *NAALADL2-AS2* expression is a poor prognosticator for PFS. In PCa cell lines, *NAALADL2-AS2* is expressed at the highest levels in androgen-sensitive cell lines, with hormone deprivation leading to a further increase in *NAALADL2-AS2* expression. RNA interference knockdown of *NAALADL2-AS2* resulted in reduced cell viability and increased apoptosis. *NAALADL2-AS2* is localized in the nucleus, where it is involved in the transcriptional regulation of various genes related to glycogen metabolism, cell cycle control, and apoptosis. *NAALADL2-AS2* likely promotes the survival of androgen-sensitive PCa cells by preventing caspase activation and cell death and, therefore, is a poor prognosticator for PCa patients. The molecular mechanisms driving *NAALADL2-AS2* expression remain elusive. By identifying androgen-responsive TFs with binding motifs near the *NAALADL2-AS2* TSS, future studies could further characterize the role of this lncRNA in PCa.

3.5 Methods

3.5.1 Clinical Samples

The present study used archival biomaterials collected between 1980 and 2000 under an opt-out regulation at Radboudumc, Nijmegen, The Netherlands. All materials were anonymized. The clinical samples comprised a panel of samples from various stages of prostate disease. The panel included four non-malignant samples, three BPH samples, four CSPC samples, four CRPC samples, and four metastatic lesions (meta) samples. Upon radical prostatectomy or transurethral resection of tumor tissue, specimens were snap-frozen in liquid nitrogen. Specimens were selected for purity of benign or cancer cells, respectively, and processed by step sectioning. Total RNA was isolated using Trizol reagent according to the manufacturer's protocol (Invitrogen, Waltham, MA, USA).

3.5.2 RNA Sequencing

Total RNA from clinical samples was subjected to DNase treatment with Turbo DNase to remove contaminating DNA. RNA was purified using an RNeasy MinElute Cleanup Kit (Qiagen, Hilden, Germany), and ribosomal RNA was removed using a Ribo-Zero Magnetic Gold kit (Westburg, Utrecht, The Netherlands). A 5× fragmentation buffer (200 mM Trisacetate (pH 8.2), 500 mM potassium acetate, and 150 mM magnesium acetate) was used to fragment RNA. First-strand cDNA synthesis was performed using random hexamers, Superscript III, and Actinomycin D, which was followed by sample clean-up and second-strand cDNA synthesis involving dUNPs. Next, an A-base was added to the 3′ end of the cDNA, and Illumina adapters were ligated to the cDNA. The second strand was degraded using the USER enzyme (Bioke, Leiden, The Netherlands), and a pre-PCR was performed to replace the second strand to ensure the strand-specificity of the data. Size selection using the EGel iBase Power System was performed to obtain fragments of approximately 200 to 400 bp, depending on the sequencing

protocol (Thermo Fisher Scientific, Waltham, MA, USA). Next, another PCR, using 10 to 12 cycles, depending on input quantity, was performed to enrich for fragments carrying adapters. Finally, the PCR product was purified using AMPure XP beads (Beckman-Coulter, Brea, CA, USA), and final concentrations were measured using Qubit fluorometric quantitation (Invitrogen, Waltham, MA, USA), while fragment lengths were determined by TapeStation (Agilent Genomics, Santa Clara, CA, USA). cDNA quality and rRNA depletion was ascertained via qPCR. If the samples passed this quality check, they were pooled at two samples per lane at a final concentration of 2 or 20 nM, depending on the sequencing protocol. Clinical samples were sequenced paired-end using 100 bp reads on the Illumina HiSeq 2000 at Maastricht UMC (Maastricht, The Netherlands).

3.5.3 RNA Sequencing Data Analysis

Clinical samples sequenced in Maastricht returned, on average, 200 million reads. Reads were paired–end mapped to human genome hg19 as provided by the UCSC genome browser using the Genomic Short-read Nucleotide Alignment Program (GSNAP) [41]. For downstream analysis, genes were annotated using a modified version of GENCODE V17, for which all known isoforms of a gene (defined by ENSTs corresponding to the same ENSG) were combined to generate the longest possible transcript. RPKMs (read per kb per million) were calculated using the rpkmforgenes.py tool for each (adjusted) ENSG [42].

3.5.4 Cell Culture

LNCaP (CRL-1740) and 22Rv1 (CRL-2505) cell lines were obtained from the American Type Culture Collection (ATCC) (Manassas, Virginia, USA). DuCaP cells were kindly provided by Dr. Ken Pienta (the University of Michigan, MI, USA), and LAPC-4 cells by Dr. Rob Reiter (University of California, CA, USA). All cells were cultured at 37 °C and 5% CO2 in a humidified atmosphere. Cell lines were authenticated using the PowerPlex 21

system (Promega) by Eurofins Genomics (Ebersberg, Germany). Cell lines were frequently tested for Mycoplasma infection using a Mycoplasma-specific PCR, and cells were propagated for no more than 6 months or 30 passages after resuscitation from stocks. Details regarding culture media composition can be found in Supplementary Table 3.1.

3.5.5 Androgen Modulation Assays

LNCaP and LAPC-4 cells were used for androgen modulation assays. Approximately 120,000 cells were plated per well in 12-well plates in 1 mL phenol red-free RPMI medium supplemented with androgen-containing (FCS) or androgen-depleted (CSS) serum and treated with synthetic AR ligand R1881 (Organon, Oss, The Netherlands) for 0 to 72 h.

3.5.6 Androgen Taper Assays

LAPC-4 cells were cultured in 25 cm2 flasks in a normal IMDM culture medium. With each subsequent passage, the concentration of R1881 in the culture medium was reduced from 1nM to 0nM of R1881.

3.5.7 RNA Extraction

Fresh frozen tissue sections were cut into 20-micron sections for RNA extraction. Cultured cells were lysed in TRIzol reagent. RNA was extracted using TRIzol reagent as described by the manufacturer (Invitrogen, Waltham, MA, USA). Pelleted RNA was resuspended in RNAse-free milliQ water. RNA concentration and purity were determined using a NanoDrop1000 spectrophotometer (Thermo Fisher Scientific, Waltham, MA, USA).

3.5.8 Reverse Transcription (RT) Reactions

Total RNA (0.5 to 2 μg) was first treated with DNaseI (Invitrogen) and then converted into single-stranded complementary DNA (cDNA) via random-primed reverse transcription, using Superscript II reverse transcriptase (Invitrogen). The produced cDNA was diluted 1:1 in RNAse-free MilliQ water and stored at negative 20 °C. RNA samples not treated with RT were used as a control to test for genomic DNA contamination.

3.5.9 Real–time qPCR

Real–time qPCR analysis was performed using LightCycler 480 SYBR Green I Master mix (Roche, Basel, Switzerland). Amplification and analysis were done on an LC480 LightCycler (Roche), using the following program: first 5 min at 95 °C, then 40 cycles of 10 s at 95 °C, 20 s at 60 °C, and 10 s at 72 °C. All lncRNA and AR-related primers used are listed in Supplementary Table 3.2. Expression levels of GAPDH were used for normalization. Relative gene expression levels were calculated according to the mathematical model for relative quantification in real–time PCR described by Pfaff [43].

3.5.10 Cytoplasmic and Nuclear RNA Isolation

Cytoplasm and nuclear RNAs were isolated as described elsewhere [44].

3.5.11 RNA Fluorescent In Situ Hybridization (RNA-FISH) and Immunofluorescence

Fluorescent labeled probes targeting *NAALADL2-AS2* were used for RNA-FISH (Biosearch Technologies, Hoddesdon, United Kingdom) (Supplementary Table 3.3). Samples were prepared as described by the manufacturer's protocol. Anti-cytokeratin (CK) -8 (ab192467), -18 (ab206091), and -19 (ab192643) antibodies were supplied by Abcam, and 0.66 μL was added directly to 100 μL of hybridization buffer. Each experiment included the following conditions: negative control (hybridization buffer), AS2, and CK8/18/19.

3.5.12 Transfection of GapmeR Antisense Oligonucleotides

Cell lines were transfected with 0.7 μM GapmeR antisense oligonucleotides (Eurogentec, Seraing, Belgium) using XtremeGene9 DNA Transfection Reagent (Roche, Basel, Switzerland) following the manufacturer's protocol. Sequence details can be found in Supplementary Table 3.4. Reagent control consisted of Opti-MEM and XtremeGene9 reagent.

3.5.13 Transfection of siRNAs

Cells were transfected with 10nM siRNAs (Ambion, Waltham, MA, USA) using Lipofectamine RNAiMAX reagent (Invitrogen, Waltham, MA, USA) according to the manufacturer's protocol. Sequence details can be found in Supplementary Table 3.4. Reagent control consisted of Opti-MEM and RNAiMAX reagent.

3.5.14 Cell Viability Assay

To assess cell viability, 10,000 cells were cultured in 96-well culture plates. Transfection with oligonucleotides was done 24 h after cell seeding. Cell viability was measured at regular intervals using a CellTiter-Glo assay according to the manufacturer's protocol (Promega, Madison, WI, USA). Luminescence was measured using a Victor3 multilabel reader (PerkinElmer, Waltham, MA, USA). Luminescence readouts from day 0 were used as a reference to calculate the relative cell viability over time. Each experiment was performed in triplicate and repeated at least three times.

3.5.15 Apoptosis Assay

In parallel to the cell viability assays, cells were seeded into 96-well plates for assessment of Caspase-3/7 activity using the Apo-ONE Homogenous Caspase-3/7 Assay (Promega, Madison, WI, USA), following the manufacturer's instructions. After 4 h of incubation, fluorescence was measured on a

Victor3 multilabel reader (PerkinElmer, Waltham, MA, USA). The luminescence signal from the medium alone was used for background normalization. Caspase-3/7 activity was normalized to values in scramble control-transfected cells. Each experiment was performed in triplicate and repeated at least three times.

3.5.16 Cell Cycle Analysis

One day before transfection, 300,000 cells were seeded per well of a 6-well plate. The next day, cells were transfected with oligonucleotides, as described above. Samples were harvested five days after transfection. Briefly, cells were washed with 0.9% NaCl and harvested using trypsinization. The medium was saved to keep apoptotic cells. Following centrifugation at 200× g for 5 min, cell pellets were resuspended in Hank's balanced salt solution (Invitrogen, Waltham, MA, USA), and cells were fixated with ice-cold ethanol (58%). Fixated cells were centrifuged and washed in 500 μL PBS with 1% BSA and 2 mM EDTA. Washed cells were centrifuged for 5 min at 200× g and resuspended in 500 μL PBS with 1% BSA and treated with RNase A (100 μg/mL, Sigma, St. Louis, MO, USA) for 40 min at 37 °C. Subsequently, cells were stained with propidium iodide (40 μg/mL, Sigma, St. Louis, MO, USA) for 15 min in the dark. The samples were analyzed on a CytoFlex (13-color) flow cytometer (Beckman-Coulter, Brea, CA, USA), and histograms were created and analyzed using Kaluza Flow Analysis software (version 2.1.3) (Beckman-Coulter, Brea, CA, USA). Results were reproduced in four independent experiments.

3.5.17 In Silico Analysis

Tissue-specific expression of *NAALADL2-AS2* was studied using The Cancer Genome Atlas (TCGA) and the Genotype-Tissue Expression project (GTEx) databases using the GEPIA2 portal [11]. The Kaplan-Meier plot was created using GEPIA2 [11]. The bodymap was stylized using BioRender. Copy number alterations in cell lines were downloaded from the Broad Institute's

depmap portal, accessed on 2 May 2022 (https://depmap.org/portal/ccle/). Significant DEGs identified via DESeq2 were used as input for the Reactome Pathway Browser to identify biological pathways regulated by *NAALADL2-AS2* [21]. Pathways were reported based on overlapping results between the up versus down analyses as well as the statistical significance and effect size of the DEGs. Figure 3.1, Figure 3.2, and 3.12 were stylized with BioRender.

3.5.18 Transcriptome Analysis

PolyA-enriched total RNA was used for RNA sequencing and differential gene expression analysis. Short-read data sets were obtained using Illumina NovaSeq 6000 next-generation sequencing and the RNA-Seq v4 pipeline, which was developed in-house by GenomeScan B.V. (Leiden, The Netherlands). Read counts were loaded into the DESeq2 package to find DEGs between two conditions: *NAALADL2-AS2* knockdown versus reagent control (n=3 independent samples).

3.5.19 Statistical Analysis and Data Visualization

Bar charts and scatterplots shown in Figures, 3.3E, 3.4, 3.5, 3.6, 3.8, 3.9, 3.10, 3.11A, 3.11B, and 3.13 were created in GraphPad Prism 9. The waterfall plot and violin plot in Figure 3.1A, and 3.1C was created in RStudio (version 2022.07.2 + 576). When not specified in the figure, statistical tests were done using a paired student's T-test in GraphPad Prism9. The violin plot and scatterplot were made using the ggpubr (version 0.4.0) package for RStudio. [45].

3.6 Supplementary Figures

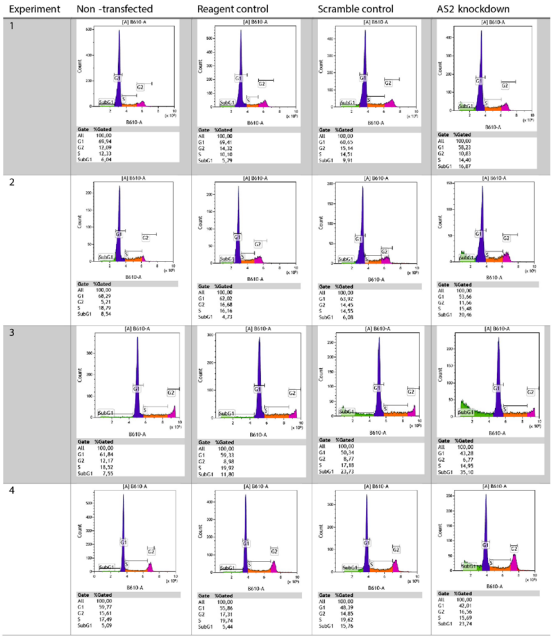

Supplementary Figure 3.1: Cell cycle histograms of LAPC-4 cells following transfection.

3.7 Supplementary Tables

Supplementary Table 3.1: Cell culture media.

Cell line	Media	Supplemented nutrients	
LNCaP	RPMI 1640*	2mM L-Glutamine*	Fetal Calf Serum (10%)**
22Rv1	RPMI 1640*	2mM L-Glutamine*	Fetal Calf Serum (10%)**
DuCaP	RPMI 1640*	2mM L-Glutamine*	Fetal Calf Serum (10%)**
LAPC-4	IMDM*	1nM R1881***	Fetal Calf Serum (7.5%)**

Supplementary Table 3.2: Primer list.

Gene	Forward primer	Reverse primer
NAALADL2-AS2	5'-ACACGGGAAATTGAAAGCAA-3'	5'-GCTCAGCTCATGTCTCTCCT-3'
RP11-20F24.2	5'-TTCCAGTGTTTTGCACGTGGT-3'	5'-TCTAGTTTCAGCACACCCGT-3'
CTD-2126E3.1	5'-TGGCCAAAGCCAAGACTTAT-3'	5'-AGACGCCGGAGCCTTAAACAG-3'
CTD-2126E3.3	5'-GCCTGACCCGAAGATTCTT-3'	5'-CAGGCAATTGTCTAGGCTC-3'
SNORD57	5'-GGAGGTGATGAAGTCTCT-3'	5'-GGATCAGGCTCATTAAATC-3'
SNORD3C	5'-CTTGGCATGTCGGCAGAAAG-3'	5'-AATAGGAGGTGCCACACAGC-3'
RP11-334J6.4	5'-CCAATAGATCCTTCGTACCC-3'	5'-TCTCTCAGTCACTGCTCCTTCA-3'
SNHG3	5'-TGCATCTGCCATTTCGGCAT-3'	5'-GCACCTCAACTCTTTGCTCCA-3'
SNORA71A	5'-GCCTGTCCTAGTGTCATTAT-3'	5'-TAGGGTGGACCCTCAAAAC-3'
RNU11	5'-AAGGGCTCTCTGCTGAGTG-3'	5'-CGGGACCAACAGTACACACG-3'
AC012531.25	5'-CCCTGTGGTGCAGACACTC-3'	5'-GGGTGGGCTCAACTTTCTCA-3'
RN7SL1	5'-TCCGCACATAAGTTCGGCATC-3'	5'-TCAGCACCGGAGGTTTGACC-3'
PCGEM1	5'-AGATGCACGTGGCACTCAACG-3'	5'-CCCTAGGAGTAGGCCCTGTG-3'
AC132217.4	5'-CTGCCCATCGACCAGGTTTG-3'	5'-CACGGGGAGGAGACAAGATG-3'
PCA3	5'-AGGGGAGATTGTGTGGCTG-3'	5'-ATGTCCTTCCCTCCACAGCG-3'
AR	5'-AAGGAATCTGCATGTCTATCATGG-3'	5'-TTGGGCACCTGGCACAGAGT-3'
NAALADL2	5'-CTTAACACGTCTTTGCAAGGTAA-3'	5'-CTAAGTCAAGGGCCAGTGGCT-3'
KLK3	5'-CGGTGTCTCTCCACCCCTG-3'	5'-CTCCCACACATCCGAGACAG-3'
GATA2	5'-AAGAGTCCCGTGCTGTAGTC-3'	5'-AGGCCTAGCTACTATGGGCA-3'
FOXA1	5'-AGGGCATGAAACACGCAGC-3'	5'-GAGTTCATGTTGCTGACCGG-3'
GAPDH	5'-TCAACGGGTGAGAAGCGGAAG-3'	5'-TGGCATCCACGAGCTACTA-3'

Supplementary Table 3.3: Probe set used to image NAALADL2-AS2.

Probe #	Probe (5'-3')	Probe position	Percent GC
1	gaagttgctttgatgtctca	26	40.0%
2	attcagctttccgaagacta	48	35.0%
3	ctcatttcagcagatgtcgc	70	50.0%
4	ccgctggtgaacattgatta	93	45.0%
5	ccacttcttgcttttcaat	115	35.0%
6	cttgagtggaatcttggatt	140	45.0%
7	agctcatgtcttctctaa	205	40.0%
8	tttcaaccttcttttattcc	235	35.0%
9	tactctgctaacgcatcag	258	45.0%
10	aagactctaaaagttaaccc	299	40.0%
11	tcagagctttggccttaag	321	45.0%
12	gaaggcaactgtcactttt	348	45.0%
13	tattatgtcttttctggcag	408	40.0%
14	atttctactgtgagactcat	446	35.0%
15	cacctgaaatgtcttacca	503	40.0%
16	ttttagccaaaagagtcgat	534	40.0%
17	cagcatgtttctattctgt	571	40.0%
18	tgctgcttctaataagtct	629	40.0%
19	cctttatgagctagttttt	878	35.0%
20	acgtgtaattgtgcaacgt	900	40.0%

Supplementary Table 3.4: GapmeR and siRNA oligos.

Name	siRNA/LNA	Sequence	Supplier
SCR (Control)	LNA	[C*C*U*U*C*C*T*G*A*G*G*T*T*F*C*C*U*C*C]	Eurogentec
AS2_IDT	LNA	A*U*A*-{A*C*5*-7*8*-5*5*8*-7*6*8*-C*G*U*-U*C	Eurogentec
siFOXA1	siRNA	ACUAGCACCAUGAACCACAUtt	Ambion, Silencer Select
siGATA2	siRNA	GGCGCACAAUCACUUGGAAtt	Ambion, Silencer Select
SCR (Control)	siRNA	Ambion Silencer Select® Negative Control #2 (P/N AM4613)	Ambion, Silencer Select

References

1. Vidal, N., Rivas, J. G., Fernández, L., Moreno, J. & Puente, J. The past, present, and future of non-metastatic castration-resistant prostate cancer (nmCRPC): a narrative review. *Precision Cancer Medicine* 5. Number: 0 (June 30, 2022).
2. Coutinho, I., Day, T. K., Tilley, W. D. & Selth, L. A. Androgen receptor signaling in castration-resistant prostate cancer: A lesson in persistence. *Endocrine-Related Cancer* 23, T179–T197 (Dec. 1, 2016).
3. Wen, S., Niu, Y., Lee, S. O. & Chang, C. Androgen receptor (AR) positive vs negative roles in prostate cancer cell deaths including apoptosis, anoikis, entosis, necrosis and autophagic cell death. *Cancer Treatment Reviews* 40, 31–40 (Feb. 2014).
4. Crona, D. J. & Whang, Y. E. Androgen receptor-dependent and -independent mechanisms involved in prostate cancer therapy resistance. *Cancers* 9 (June 12, 2017).
5. Villegas, V. E. & Zaphiropoulos, P. G. Neighboring gene regulation by antisense long Non-Coding RNAs. *International Journal of Molecular Sciences* 16, 3251–3266 (Feb. 3, 2015).
6. Wang, R. *et al.* Preclinical Study using Malat1 Small Interfering RNA or Androgen Receptor Splicing Variant 7 Degradation Enhancer ASC-J9 to Suppress Enzalutamide-resistant Prostate Cancer Progression. *European Urology* 72, 835–844 (Nov. 1, 2017).
7. Yang, Y., Liu, K. Y., Liu, Q. & Cao, Q. Androgen Receptor-Related Non-coding RNAs in Prostate Cancer. *Frontiers in Cell and Developmental Biology* 9 (Apr. 1, 2021).
8. You, Z. *et al.* LncRNA CCAT1 Promotes Prostate Cancer Cell Proliferation by Interacting with DDX5 and MIR-28-5P. *Molecular cancer therapeutics* 18, 2469–2479 (Dec. 1, 2019).
9. Ito, S. *et al.* PCA3 controls chromatin organization and p53 signal activation by regulating LAP2α-lamin A complexes. *Cancer Gene Therapy* (2021).

10. Li, H. *et al.* Androgen Receptor Splice Variant 7 Predicts Shorter Response in Patients with Metastatic Hormone-sensitive Prostate Cancer Receiving Androgen Deprivation Therapy. *European Urology* 79, 879–886 (June 1, 2021).
11. Tang, Z., Kang, B., Li, C., Chen, T. & Zhang, Z. GEPIA2: an enhanced web server for large-scale expression profiling and interactive analysis. *Nucleic Acids Research* 47, W556–W560 (W1 July 1, 2019).
12. Zhou, M., Guo, X., Wang, M. & Qin, R. The patterns of antisense long non-coding RNAs regulating corresponding sense genes in human cancers. *Journal of Cancer* 12, 1499–1506 (Jan. 1, 2021).
13. Simpson, B. S. *et al.* Genetic alterations in the 3q26.31-32 locus confer an aggressive prostate cancer phenotype. *Communications Biology* 3 (Dec. 1, 2020).
14. Beltran, H. *et al.* Divergent clonal evolution of castration-resistant neuroendocrine prostate cancer. *Nature Medicine* 22, 298–305 (Mar. 1, 2016).
15. Weinstein, J. N. *et al.* The cancer genome atlas pan-cancer analysis project. *Nature Genetics* 45, 1113–1120 (Oct. 1, 2013).
16. Ghandi, M. *et al.* Next-generation characterization of the Cancer Cell Line Encyclopedia. *Nature* 569, 503–508 (May 2019).
17. Haffner, M. C. *et al.* Phenotypic characterization of two novel cell line models of castration-resistant prostate cancer. *Prostate* 81, 1159–1171 (Nov. 1, 2021).
18. *UCSC Genome Browser Home* `https://genome.ucsc.edu/` (2023).
19. Ahmed Fouad, Y. & Aanei, C. Revisiting the hallmarks of cancer. *Am J Cancer Res* 7, 1016–1036 (2017).
20. Love, M. I., Huber, W. & Anders, S. Moderated estimation of fold change and dispersion for RNA-seq data with DESeq2. *Genome Biology* 15 (Dec. 5, 2014).
21. Fabregat, A. *et al.* Reactome pathway analysis: A high-performance in-memory approach. *BMC Bioinformatics* 18 (Mar. 2, 2017).

22. Wadosky, K. M. & Koochekpour, S. Molecular mechanisms underlying resistance to androgen deprivation therapy in prostate cancer. *Oncotarget* 7, 64447–64470 (July 28, 2016).
23. Attard, G. *et al.* Abiraterone acetate and prednisolone with or without enzalutamide for high-risk non-metastatic prostate cancer: a meta-analysis of primary results from two randomised controlled phase 3 trials of the STAMPEDE platform protocol. *The Lancet* 399, 447–460 (Jan. 29, 2022).
24. Zhang, T., Karsh, L. I., Nissenblatt, M. J. & Canfield, S. E. Androgen Receptor Splice Variant, AR-V7, as a Biomarker of Resistance to Androgen Axis-Targeted Therapies in Advanced Prostate Cancer. *Clinical Genitourinary Cancer* 18, 1–10 (Feb. 1, 2020).
25. Kirby, M., Hirst, C. & Crawford, E. D. Characterising the castration-resistant prostate cancer population: A systematic review. *International Journal of Clinical Practice* 65, 1180–1192 (Nov. 2011).
26. Jiang, G. *et al.* Long non-coding rnas in prostate tumorigenesis and therapy (Review). *Molecular and Clinical Oncology* 13, 1–7 (Dec. 1, 2020).
27. Osman, I. *et al. Inactivation of the p53 Pathway in Prostate Cancer: Impact on Tumor Progression 1* (1999).
28. Whitaker, H. C. *et al.* N-acetyl-L-aspartyl-L-glutamate peptidase-like 2 is overexpressed in cancer and promotes a pro-migratory and pro-metastatic phenotype. *Oncogene* 33, 5274–5287 (Nov. 6, 2014).
29. Kreis, N. N., Louwen, F. & Yuan, J. The multifaceted p21 (Cip1/Waf1/CDKN1A) in cell differentiation, migration and cancer therapy. *Cancers* 11 (Sept. 1, 2019).
30. Gartel, A. L. The conflicting roles of the cdk inhibitor p21(CIP1/WAF1) in apoptosis. *Leukemia Research* 29, 1237–1238 (Nov. 2005).
31. Pardo, J. *et al.* Apoptotic pathways are selectively activated by granzyme A and/or granzyme B in CTL-mediated target cell lysis. *Journal of Cell Biology* 167, 457–468 (Nov. 8, 2004).

32. Gazon, H., Barbeau, B., Mesnard, J. M. & Peloponese, J. M. Hijacking of the AP-1 signaling pathway during development of ATL. *Frontiers in Microbiology* 8 (JAN Jan. 15, 2018).
33. Park, J. A., Na, H. H., Jin, H. O. & Kim, K. C. Increased expression of fosb through reactive oxygen species accumulation functions as pro-apoptotic protein in piperlongumine treated MCF7 breast cancer cells. *Molecules and Cells* 42, 884–892 (Dec. 31, 2019).
34. Migocka-Patrzałek, M. & Elias, M. Muscle glycogen phosphorylase and its functional partners in health and disease. *Cells* 10 (Apr. 1, 2021).
35. Zois, C. E. & Harris, A. L. Glycogen metabolism has a key role in the cancer microenvironment and provides new targets for cancer therapy. *Journal of Molecular Medicine* 94, 137–154 (Feb. 1, 2016).
36. Schnier, J. B., Nishi, K., Gumerlock, P. H., Gorin, F. A. & Bradbury, E. M. Glycogen synthesis correlates with androgen-dependent growth arrest in prostate cancer. *BMC Urology* 5, 6 (Mar. 24, 2005).
37. Liu, C. *et al.* Niclosamide inhibits androgen receptor variants expression and overcomes enzalutamide resistance in castration-resistant prostate cancer. *Clinical Cancer Research* 20, 3198–3210 (June 15, 2014).
38. Rehman, Y. & Rosenberg, J. E. Abiraterone acetate: Oral androgen biosynthesis inhibitor for treatment of castration-resistant prostate cancer. *Drug Design, Development and Therapy* 6, 13–18 (2012).
39. Benoist, G. E. *et al.* Prognostic Value of Novel Liquid Biomarkers in Patients with Metastatic Castration-Resistant Prostate Cancer Treated with Enzalutamide: A Prospective Observational Study. *Clinical chemistry* 66, 842–851 (June 1, 2020).
40. Boerrigter, E. *et al.* RNA Biomarkers as a Response Measure for Survival in Patients with Metastatic Castration-Resistant Prostate Cancer. *Cancers* 13, 6279 (Dec. 14, 2021).
41. Wu, T. D., Reeder, J., Lawrence, M., Becker, G. & Brauer, M. J. in *Methods in Molecular Biology* 283–334 (Humana Press Inc., 2016).

42. Ramsköld, D., Wang, E. T., Burge, C. B. & Sandberg, R. An abundance of ubiquitously expressed genes revealed by tissue transcriptome sequence data. *PLoS Computational Biology* 5 (Dec. 2009).
43. Pfaffl, M. W. *Quantification strategies in real-time PCR* (2004).
44. Bishop, E. *et al.* Evolution of sex in RNA viruses. *Journal of Theoretical Biology* 86. Place: College Park, 99–112 (Feb. 25, 1989).
45. Blighe K, Rana S & Lewis M. Publication-ready volcano plots with enhanced colouring and labeling. *Bioconductor* (2022).

Chapter 4

The Prognostic Value of lncRNA NAALADL2-AS2 in Epithelial Prostate Cancer

Adapted from:
Groen, L., et al. The Expression of NAALADL2-AS2 Associates with a Luminal PCa Subtype. Submitted for publication in the International Journal of Molecular Sciences (2025).

4.1 Introduction

The Gleason grading system, introduced in the mid-twentieth century, profoundly influenced the development of prostate cancer (PCa) diagnostics and continues to be essential in contemporary clinical practice. Although beneficial, this system requires subjective evaluation by highly skilled professionals to categorize clinically relevant PCa subtypes. As healthcare progresses into the molecular era, subjective histological assessment of tumor tissue does not meet the sensitivity and specificity standards necessary for precision medicine [1].

Molecular subtyping provides an objective alternative to current tumor classification standards in PCa. This approach employs genomic, transcriptomic, and proteomic profiling to categorize tumors, thereby facilitating a deeper understanding of the underlying pathology. The implementation of this strategy has significantly improved clinical outcomes across various cancers, including breast cancer subtyping (basal/luminal/HER2; human epidermal growth factor receptor 2) [2], colorectal cancer subtyping (microsatellite instability (MSI)) [3], and lung cancer subtyping (epidermal growth factor receptor (EGFR)/anaplastic lymphoma kinase (ALK)/programmed death-ligand 1 (PD-L1)) [4]. In recent years, there has been a considerable increase in both the quantity and quality of studies focused on the molecular classification of PCa subtypes [5, 6]. In 2023, a study conducted by leading urologist Dr. Edward Schaeffer established a novel PCa classifier based on luminal and basal transcriptome profiles using an extensive dataset of 100,000 tumor samples [6]. Numerous studies have introduced classification systems, with at least eight distinct models based on genomic, transcriptomic, and/or multi-omic alterations [5]. Despite methodological differences and varying classifiers, the molecular and clinical characteristics of epithelial subtypes in PCa remain remarkably consistent [6–9]. Generally, luminal subtypes exhibit androgen sensitivity, demonstrate responsiveness to hormone therapy, and represent the most prevalent form of PCa in therapy-naive patients. Conversely, basal

subtypes tend to be less responsive to hormone therapy, are associated with neuroendocrine phenotypes, and dominate in castration-resistant cases [6, 9–12].

Chapter 3 of this thesis highlights *NAALADL2-AS2* as a novel lncRNA significantly present in androgen-sensitive PCa and identified as a poor prognostic indicator in therapy-naive individuals [13]. However, data from two exploratory clinical trials evaluating the prognostic efficacy of circulating RNA biomarkers showed that plasma *NAALADL2-AS2* levels do not serve as indicators of poor prognosis and may potentially function as favorable prognostic markers for patients with castration-resistant disease [14, 15]. This discrepancy raises a key question: why would a CRPC-associated lncRNA predict outcomes in castration-sensitive disease, but not in established castration-resistant disease? In addition to being androgen-sensitive, PCa can be further classified based on the tumor's epithelial origins, namely luminal or basal. A pilot differential gene expression analysis of luminal and basal PCa subtypes supports the hypothesis that *NAALADL2-AS2* expression correlates with luminal PCa [16]. This chapter explores this hypothesis, examines the role of *NAALADL2-AS2* in PCa subtypes, and evaluates its clinical implications.

4.2 Results

4.2.1 Stratifying TCGA Molecular Subtypes with Clinical Outcomes

In 2015, The Cancer Genome Atlas (TCGA) characterized the molecular landscape of 333 primary prostate tumors and defined seven molecular subtypes in 74% of cases, based on fusions involving *ERG*, *ETV1*, *ETV4*, and *FLI1* or mutations in *SPOP*, *FOXA1*, and *IDH1* [17]. The remaining 26% of tumors did not meet these fusion/mutation criteria and were classified as "other." An integrated, unsupervised analysis of genomic and transcriptomic features further resolved three transcriptomic subtypes with complete coverage: TCGA-iCluster 1 (n = 85, 26%), TCGA-iCluster 2 (n = 109,

33%), and TCGA-iCluster 3 (n = 139, 42%). The clinical relevance of TCGA-iClusters remains underexplored, and their implications for patient outcomes, treatment response, and decision-making are still poorly defined. To evaluate their association with outcome, TCGA prostate adenocarcinoma (PRAD) survival data were retrieved from cBioPortal and patient IDs were grouped into iCluster 1 (n = 67), iCluster 2 (n = 93), and iCluster 3 (n = 123) [18]. Five-year Kaplan–Meier analyses were generated in RStudio using the survivalAnalysis package. iCluster 3 showed the most favorable progression-free survival (PFS) and was used as the reference (hazard ratio (HR) = 1); relative to iCluster 3, the risk of progression was higher in iCluster 2 (HR = 2.33) and iCluster 1 (HR = 2.46) (p = 0.015; Figure 4.1).

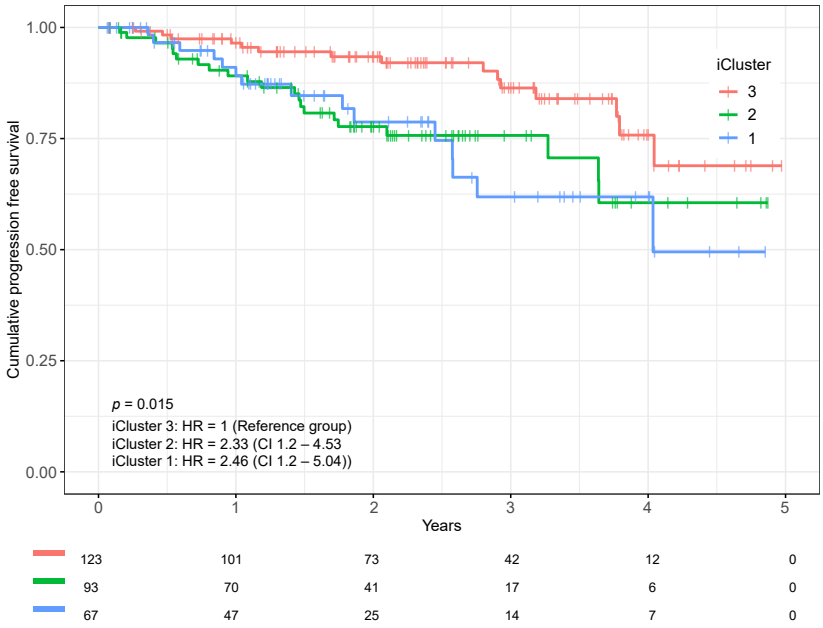

Figure 4.1: Survival analysis of TCGA-iClusters.

Kaplan-Meier curves depicting the cumulative PFS of patients stratified into TCGA-iClusters over a five-year period. iCluster 1 (blue line) represents 67 patients, iCluster 2 (green line) represents 93 patients, and iCluster 3 (red line) represents 123 patients. iCluster 3 was used as a reference group (HR = 1). Patients in iCluster 1 (HR = 2.46 (95% confidence interval (CI) 1.2–5.04)) and iCluster 2 (HR = 2.33 (95% CI 1.2–4.53)) show increased risk for early progression compared to iCluster 3. The number at risk for each group selected time intervals is indicated in the risk tables below each Kaplan-Meier plot. The global p-value = 0.015, indicating survival probabilities are statistically significant.

4.2.2 TCGA-iClusters Align with Epithelial PCa Subtypes

To assess whether TCGA-iClusters correspond to epithelial PCa subtypes, TCGA-PRAD transcriptome data were scored using published gene signatures for androgen receptor (AR) signaling, basal differentiation, and luminal differentiation [19]. Expression values were aggregated into signature scores for AR activity (*AR*, *FOLH1*, *DLX1*, *GATA2*, *CDK1*), basal (*TP63*,

IL6, *GSTP1*, *ACTA2*), luminal adipogenic (luminal A; *GNG13*, *UNC5A*, *MESP1*, *MESP2*), and luminal secretory (luminal S; *ERG*, *ALOX15*, *TOP2A*, *COL2A1*) subtypes [6–8, 19]. AR activity scores were high in iCluster 1 and iCluster 2, but low in iCluster 3. Basal scores were highest in iCluster 3 and low in iCluster 1 and iCluster 2. Luminal A scores were highest in iCluster 1 and low in iCluster 2 and iCluster 3, whereas luminal S scores were highest in iCluster 2 and low in iCluster 1 and iCluster 3. Collectively, these results indicate that TCGA-iClusters recapitulate epithelial PCa subtypes, with iCluster 1 resembling luminal A, iCluster 2 resembling luminal S, and iCluster 3 resembling basal PCa (Figure 4.2).

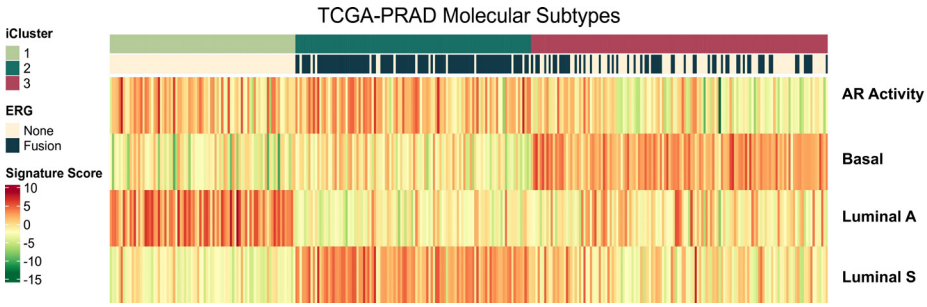

Figure 4.2: TCGA-iClusters align with PCa epithelial subtypes.

TCGA molecular subtypes (iClusters) align with PCa epithelial subtypes. AR activity gene signature is based on the aggregate expression of *AR*, *FOLH1*, *DLX1*, *GATA2*, and *CDK1*. Luminal A gene signature is based on the expression of *GNG13*, *UNC5A*, *MESP1* and *MESP2*. Luminal S gene signature is based on the expression of *ERG*, *ALOX15*, *TOP2A*, and *COL2A1*. Basal gene signature is based on the expression of *TP63*, *IL6*, *GSTP1*, and *ACTA2*. Signatures represent aggregate expression values of individual genes. Plot was created using the complexHeatmap package in R Studio.

4.2.3 Differential Expression of NAALADL2-AS2 in PCa Subtypes

Given the alignment of TCGA-iClusters with epithelial PCa subtypes, we next assessed whether *NAALADL2-AS2* expression differed across TCGA-iClusters. To test this, *NAALADL2-AS2* expression was quantified in TCGA-PRAD transcriptome data stratified by iCluster status [17]. Samples were assigned to iCluster 1 ($n = 85$), iCluster 2 ($n = 108$), and iCluster 3 (basal; $n = 136$); four samples were excluded due to missing data. Raw counts were variance-stabilized and log2-transformed using DESeq2 [20]. Subtype-specific expression was visualized using ggplot2 (Figure 4.3A) [21]. *NAALADL2-AS2* expression was significantly higher in iCluster 2 (median = 3.25) than in iCluster 1 (median = 2.38; $p = 0.012$) or iCluster 3 (median = 3.03; $p = 0.001$). These differences were supported by differential expression analysis comparing iCluster 2 ($n = 108$) with all other tumors ("Other"; $n = 221$, TCGA-iClusters 1 and 3 combined). Results were visualized with EnhancedVolcano (Figure 4.3B) [22]. *NAALADL2-AS2* was upregulated in iCluster 2 relative to "Other" (log2FC = 1.2, -log10p = 9.1), consistent with subtype-specific expression.

(a) *NAALADL2-AS2* expression levels in TCGA-iClusters.

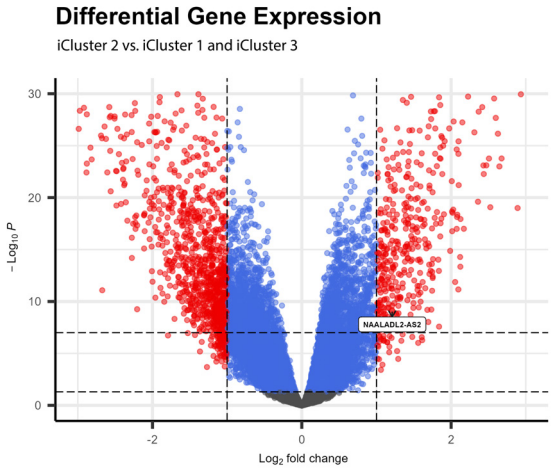

(b) Differential gene expression analysis shows *NAALADL2-AS2* upregulated in TCGA-iCluster 2 compared to TCGA-iCluster 1 and TCGA-iCluster 3 combined.

Figure 4.3: *NAALADL2-AS2* expression in TCGA-iClusters.

NAALADL2-AS2 is highly expressed in TCGA-iCluster 2 (A/B). Figures were created using transcriptome data from TCGA-PRAD. TCGA-iClusters subtypes were derived from TCGA-PRAD integrated molecular subtypes (iClusters).

4.2.4 NAALADL2-AS2 Expression Associates with Luminal S Genes

NAALADL2-AS2 expression is strongly associated with androgen sensitivity, suggesting a potential role in the development and progression of androgen-sensitive (and therefore likely luminal) PCa. To assess this, a Pearson correlation matrix was generated from TCGA-PRAD transcriptome data processed with DESeq2 [17, 20] (Figure 4.4). *NAALADL2-AS2* expression was positively correlated with *ALOX15*, *AR*, *CDK1*, *COL2A1*, *DLX1*, *ERG*, *FOLH1*, *GATA2*, *GNG13*, and *TOP2A*, consistent with AR signaling and a Luminal S transcriptional program. In contrast, *NAALADL2-AS2* was negatively correlated with the basal markers *ACTA2*, *GSTP1*, *IL6*, *TP63*, and *UNC5A*. No clear correlation was observed with luminal A-associated genes (*GNG13*, *MESP1*, *MESP2*, and *UNC5A*). Collectively, these results support *NAALADL2-AS2* as part of the Luminal S transcriptome.

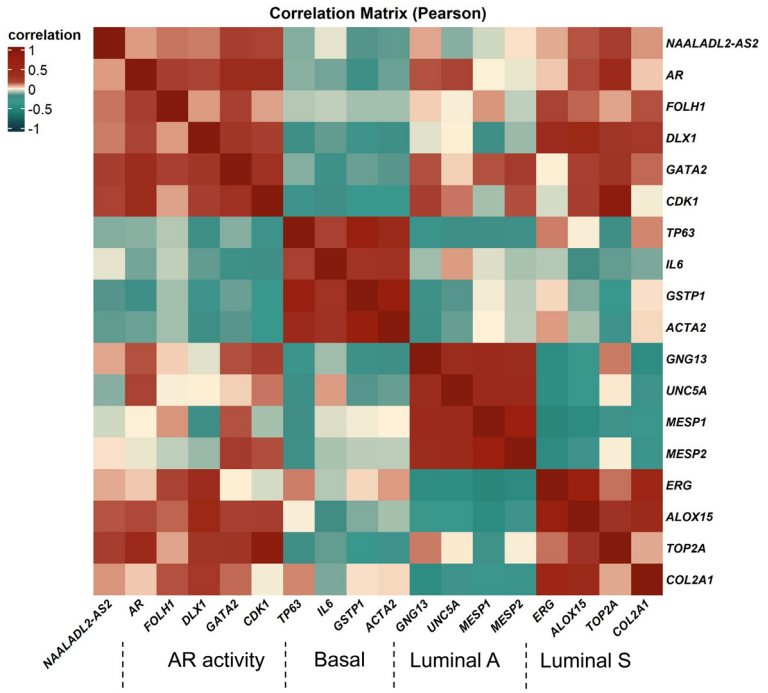

Figure 4.4: *NAALADL2-AS2* expression correlates with AR activity and Luminal S gene signatures.

NAALADL2-AS2 expression correlates with AR activity and Luminal S gene signatures. Gene expression data was sourced from TCGA-PRAD. Analysis was done using DESeq2 in R Studio [20].

4.2.5 NAALADL2-AS2: A Marker of Early Progression

Differential *NAALADL2-AS2* expression across TCGA-iClusters suggests that its molecular role may be subtype-specific. Given its proposed pro-survival function in PCa, we hypothesized that *NAALADL2-AS2* would be a particularly strong prognostic marker in iCluster 2. To test this, TCGA-PRAD survival data were retrieved from cBioPortal and stratified by iCluster (iCluster 1–3) [16, 18]. Survival analyses were performed in RStudio; within each iCluster, a median expression cutoff was used to define high versus low *NAALADL2-AS2* expression. Five-year PFS Kaplan–Meier curves were

generated using the `survivalAnalysis` package. High *NAALADL2-AS2* expression was associated with poorer five-year PFS in iCluster 2 (HR = 4.23, $p = 0.0019$), but not in iCluster 1 (HR = 0.81, $p = 0.67$) or iCluster 3 (HR = 1.89, $p = 0.23$) (Figure 4.5).

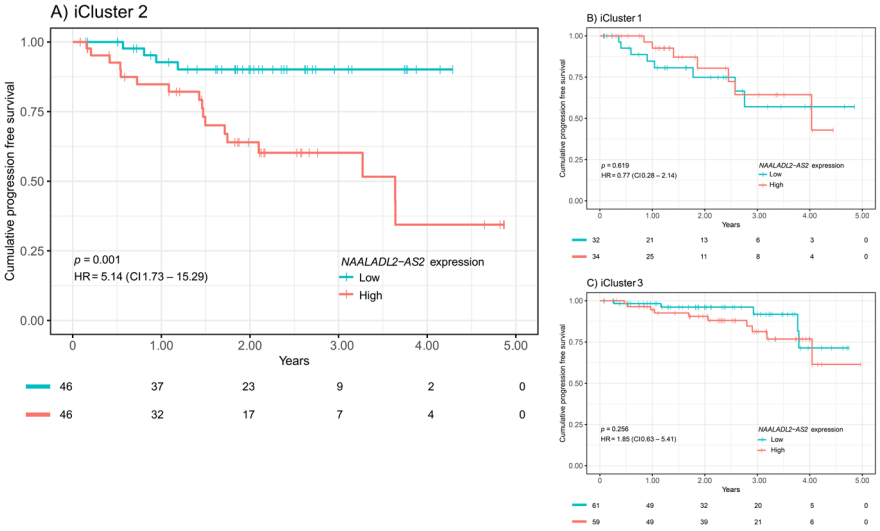

Figure 4.5: The prognostic value of *NAALADL2-AS2* in TCGA-iClusters.

Kaplan-Meier Survival Analysis of *NAALADL2-AS2* Expression Across TCGA-iClusters. (A) TCGA-iCluster 2 shows significant separation in cumulative PFS between low and high *NAALADL2-AS2* expression groups ($p = 0.001$, HR = 5.14 (95% CI: 1.73–15.29)). (B) TCGA-iCluster 1 shows no significant difference with cumulative PFS between low and high *NAALADL2-AS2* expression groups ($p = 0.619$, HR = 0.77 (95% CI: 0.28–2.14)). (C) TCGA-iCluster 3 shows no significant difference with cumulative PFS between low and high *NAALADL2-AS2* expression groups ($p = 0.256$, HR = 1.85 (95% CI: 0.63–5.41)). The number at risk for each group at selected time intervals is indicated in the risk tables below each Kaplan-Meier plot. The analysis period spans 5 years; a median cutoff was used to define low and high-expression groups.

4.3 Discussion

PCa is a clinically heterogeneous disease, with outcomes ranging from indolent, localized tumors to aggressive metastatic disease. Despite effective first-line treatment for many patients, PCa was projected to cause approximately 35,000 deaths in the U.S. in 2023, highlighting the need for improved molecular tools and subtyping strategies to enable more personalized therapeutic approaches [23].

The TCGA study "The Molecular Taxonomy of Prostate Cancer" highlighted the molecular heterogeneity of localized PCa and defined three integrated genomic–transcriptomic clusters (TCGA-iClusters) [17]. These TCGA-iClusters show distinct patterns of genomic alteration and pathway activity, with implications for patient stratification and personalized therapy. The *TMPRSS2–ERG* fusion is enriched in iCluster 2 (62%) and iCluster 3 (38%), but is absent in iCluster 1. Conversely, *SPOP* mutations (11% overall) occur predominantly in iCluster 1 (76%) and, less frequently, in iCluster 3 (24%); *FOXA1* mutations (3% overall) show a similar distribution (iCluster 1: 81%; iCluster 3: 19%). Notably, both *SPOP* and *FOXA1* alterations are absent in iCluster 2 [17].

These genomic patterns are consistent with a 2021 study linking ETS fusions and *SPOP* status to distinct luminal subtypes: ETS+/*SPOPmut*- luminal S and ETS-/*SPOPmut+* luminal A [19]. Accordingly, iCluster 1 most closely resembles luminal A, whereas iCluster 2 aligns with luminal S. Because androgen sensitivity distinguishes luminal from basal phenotypes, the enrichment of AR signaling genes in TCGA-iClusters 1 and 2 further supports a shared luminal origin. Transcriptomic scoring of TCGA-iClusters corroborated this interpretation: iCluster 1 associated with luminal A signatures, iCluster 2 with luminal S signatures, and iCluster 3 with basal gene expression. Overall, TCGA integrated omics subtypes appear to recapitulate epithelial PCa subtypes.

Epithelial differentiation is a major classifier across adenocarcinomas, including PCa, where approximately 90% of tumors can be assigned to luminal or basal subtypes. These subtypes reflect differences in androgen sensitivity, differentiation state, proliferation, and immune interactions, and they are associated with distinct clinical trajectories driven by subtype-specific oncogenic programs [6, 9–12]. Luminal tumors are typically androgen-responsive and rely on AR signaling to support survival and proliferation, which may confer a growth advantage in ADT-naive disease. In contrast, basal tumors appear less dependent on AR signaling and instead engage a broader set of oncogenic pathways, underscoring the need for subtype-tailored therapeutic strategies [6, 24, 25].

The androgen-regulated lncRNA *NAALADL2-AS2* is particularly relevant in the context of luminal PCa. Its expression shows a strong positive association with luminal S markers (e.g., *ERG*, *ALOX15*, *TOP2A*, and *COL2A1*), but not with luminal A or basal gene programs, consistent with a luminal S–specific expression pattern. This enrichment within TCGA-iCluster 2 supports *NAALADL2-AS2* as a candidate biomarker for luminal S PCa and suggests a functional role in the survival of androgen-sensitive cells [13].

Luminal subtypes comprise the majority of primary PCa and differ substantially in progression risk and treatment response, including variation in benefit from postoperative ADT [26]. In this context, *NAALADL2-AS2* expression in luminal tumors could serve as a prognostic biomarker and help stratify patients by likelihood of ADT response. By contrast, basal tumors, which are enriched in CRPC, tend to be less hormone-responsive and often require alternative treatment strategies such as chemotherapy and/or radiotherapy [5, 6, 11, 26]. The predominance of basal disease in CRPC may therefore help explain the limited prognostic utility of circulating *NAALADL2-AS2* in CRPC patients treated with enzalutamide or abiraterone [15].

In summary, integrating genomic and transcriptomic data provides a more nuanced view of PCa heterogeneity and reinforces the value of molecular

profiling for therapy selection. The distinct signatures of luminal and basal disease, including the enrichment of *NAALADL2-AS2* in luminal S PCa, offer insight into PCa pathogenesis and highlight opportunities for biomarker-driven, subtype-tailored interventions.

4.4 Methods

4.4.1 Study Design Overview

This study combines transcriptome-based in silico analyses of public PCa datasets with previously established experimental methodologies. Publicly available clinical, transcriptomic, and survival data were analyzed to assess epithelial subtype associations, differential expression, and prognostic relevance of *NAALADL2-AS2*. All computational analyses were performed independently of the experimental procedures described above.

4.4.2 Data Acquisition

Clinical, transcriptomic, and molecular subtype data were obtained from TCGA-PRAD [17]. Survival and gene expression data were retrieved from cBioPortal [18]. TCGA-iCluster assignments and ERG fusion status were derived from TCGA metadata.

4.4.3 Transcriptome Characterization of TCGA-iClusters

Gene signature scores were generated by aggregating log2-normalized expression values of predefined gene sets associated with luminal A, luminal S, basal differentiation, and androgen receptor (AR) pathway activity. Expression data were sourced from TCGA-PRAD [17]. Supervised clustering and visualization of gene signature scores across TCGA-iClusters were performed in RStudio.

4.4.4 Correlation Analysis

Pearson correlation coefficients were calculated using log2-normalized expression values of *NAALADL2-AS2* and selected gene signature components across the full TCGA-PRAD cohort ($n = 333$). Correlation matrices were generated using the `DESeq2` package in RStudio [20].

4.4.5 NAALADL2-AS2 Expression Analysis in TCGA-iClusters

Variance-stabilized expression values for *NAALADL2-AS2* were extracted and stratified by TCGA-iCluster membership. Subtype-specific expression was visualized using boxplots generated with `ggplot2`. Differential gene expression analysis was performed using `DESeq2`, comparing TCGA-iCluster 2 tumors with TCGA-iCluster 1 and TCGA-iCluster 3 combined. Results were visualized using the `EnhancedVolcano` package.

4.4.6 Survival Analysis

Patients were grouped according to TCGA-iCluster classification. Within each cluster, samples were dichotomized into high and low *NAALADL2-AS2* expression groups using a median expression cutoff. Kaplan–Meier progression-free survival analyses were conducted with a censoring threshold of 60 months (five years). Survival analyses were performed in RStudio using the `survivalAnalysis` package.

4.4.7 Software and Statistical Analysis

All computational analyses were conducted in RStudio (version 2022.07.2). Data processing, visualization, and statistical analyses employed the following R packages: `tidyverse`, `DESeq2`, `ggplot2`, `EnhancedVolcano`, `pheatmap`, `pvclust`, `RColorBrewer`, `ggpubr`, and `ggstatsplot`. Unless stated otherwise, statistical comparisons were performed using two-sided tests, and a p-value < 0.05 was considered statistically significant.

References

1. Egevad, L. *et al.* Identification of areas of grading difficulties in prostate cancer and comparison with artificial intelligence assisted grading. *Virchows Archiv* 477, 777–786 (Dec. 1, 2020).
2. Natrajan, R. & Weigelt, B. Risk Stratification and Intrinsic Subtype Classification of Breast Cancer: A Multiparameter Test to Rule Them All? *JNCI: Journal of the National Cancer Institute* 108, djw118 (Sept. 1, 2016).
3. Battaglin, F., Naseem, M., Lenz, H.-J. & Salem, M. E. Microsatellite Instability in Colorectal Cancer: Overview of Its Clinical Significance and Novel Perspectives. *Clinical advances in hematology & oncology : H&O* 16, 735–745 (Nov. 2018).
4. Gainor, J. F. *et al.* EGFR Mutations and ALK Rearrangements Are Associated with Low Response Rates to PD-1 Pathway Blockade in Non-Small Cell Lung Cancer (NSCLC): A Retrospective Analysis. *Clinical cancer research : an official journal of the American Association for Cancer Research* 22, 4585–4593 (Sept. 15, 2016).
5. Ge, Q. *et al.* Molecular classifications of prostate cancer: basis for individualized risk stratification and precision therapy. *Annals of Medicine* 55, 2279235 (2023).
6. Weiner, A. B. *et al.* A novel prostate cancer subtyping classifier based on luminal and basal phenotypes. *Cancer* 129, 2169–2178 (2023).
7. Yoon, J. *et al.* A comparative study of PCS and PAM50 prostate cancer classification schemes. *Prostate Cancer and Prostatic Diseases* 24, 733–742 (Sept. 2021).
8. Feng, F. Y.-C. *et al.* Luminal and basal subtyping of prostate cancer. *Journal of Clinical Oncology* 35, 3–3 (Feb. 20, 2017).
9. You, S. *et al.* Integrated Classification of Prostate Cancer Reveals a Novel Luminal Subtype with Poor Outcome. *Cancer Research* 76, 4948–4958 (Sept. 1, 2016).

10. Chua, M. L. K. *et al.* Transcriptomic analyses of localized prostate cancers of East Asian and North American men reveal race-specific luminal-basal and microenvironmental differences. *Cancer Communications* 43. _eprint: https://onlinelibrary.wiley.com/doi/pdf/10.1002/cac2.12467, 1164–1168 (2023).
11. Aggarwal, R. *et al.* Prognosis Associated With Luminal and Basal Subtypes of Metastatic Prostate Cancer. *JAMA Oncology* 7, 1644 (Nov. 1, 2021).
12. Zhao, S. G. *et al.* Clinical and Genomic Implications of Luminal and Basal Subtypes Across Carcinomas. *Clinical Cancer Research: An Official Journal of the American Association for Cancer Research* 25, 2450–2457 (Apr. 15, 2019).
13. Groen, L. *et al.* The Androgen Regulated lncRNA NAALADL2-AS2 Promotes Tumor Cell Survival in Prostate Cancer. *Non-Coding RNA* 8, 81 (Dec. 1, 2022).
14. Benoist, G. E. *et al.* Prognostic Value of Novel Liquid Biomarkers in Patients with Metastatic Castration-Resistant Prostate Cancer Treated with Enzalutamide: A Prospective Observational Study. *Clinical chemistry* 66, 842–851 (June 1, 2020).
15. Boerrigter, E. *et al.* RNA Biomarkers as a Response Measure for Survival in Patients with Metastatic Castration-Resistant Prostate Cancer. *Cancers* 13, 6279 (Dec. 14, 2021).
16. Tang, Z., Kang, B., Li, C., Chen, T. & Zhang, Z. GEPIA2: an enhanced web server for large-scale expression profiling and interactive analysis. *Nucleic Acids Research* 47, W556–W560 (W1 July 1, 2019).
17. Abeshouse, A. *et al.* The Molecular Taxonomy of Primary Prostate Cancer. *Cell* 163, 1011–1025 (Nov. 5, 2015).
18. Cerami, E. *et al.* The cBio Cancer Genomics Portal: An open platform for exploring multidimensional cancer genomics data. *Cancer Discovery* 2, 401–404 (May 2012).

19. Han, H. *et al.* Prostate epithelial genes define therapy-relevant prostate cancer molecular subtype. *Prostate Cancer and Prostatic Diseases* 24. Number: 4, 1080–1092 (Dec. 2021).
20. Love, M. I., Huber, W. & Anders, S. Moderated estimation of fold change and dispersion for RNA-seq data with DESeq2. *Genome Biology* 15 (Dec. 5, 2014).
21. Patil, I. Visualizations with statistical details: The 'ggstatsplot' approach. *Journal of Open Source Software* 6, 3167 (May 25, 2021).
22. Blighe K, Rana S & Lewis M. Publication-ready volcano plots with enhanced colouring and labeling. *Bioconductor* (2022).
23. *Key Statistics for Prostate Cancer | Prostate Cancer Facts* Key Statistics for Prostate Cancer | Prostate Cancer Facts. `https://www.cancer.org/cancer/types/prostate-cancer/about/key-statistics.html` (2023).
24. Ahmad, F., Cherukuri, M. K. & Choyke, P. L. Metabolic reprogramming in prostate cancer. *British Journal of Cancer* 125. Number: 9, 1185–1196 (Oct. 2021).
25. Coleman, I. M. *et al.* Therapeutic Implications for Intrinsic Phenotype Classification of Metastatic Castration-Resistant Prostate Cancer. *Clinical Cancer Research* 28, 3127–3140 (July 15, 2022).
26. Zhao, S. G. *et al.* Associations of Luminal and Basal Subtyping of Prostate Cancer With Prognosis and Response to Androgen Deprivation Therapy. *JAMA Oncology* 3, 1663–1672 (Dec. 1, 2017).

Chapter 5

Prognostic Transcriptome Profiling Using Circulating Tumor Cells in Advanced Prostate Cancer

Adapted from:
Groen, L. et al. Transcriptome Profiling of Circulating Tumor Cells to Predict Clinical Outcomes in Metastatic Castration-Resistant Prostate Cancer. IJMS 24, 9002 (2023).

5.1 Introduction

The discovery of oncogenes in the 1970s paved the way for targeted therapies and renewed hope for curative cancer treatment [1]. In metastatic castration-resistant prostate cancer (mCRPC), solid-tumor genotyping has since uncovered druggable oncogenic alterations that can contribute to therapy resistance, enabling new treatment modalities such as poly(ADP-ribose) polymerase inhibitors (PARPi) for tumors harboring loss-of-function alterations in DNA repair genes [2]. However, clinical responses to PARPi have been highly variable and difficult to predict [3].

Continued reliance on solid tissue biopsies to identify druggable alterations may be limiting progress. Conventional biopsies do not capture clonal heterogeneity and are constrained by invasiveness and the inaccessibility of certain lesions [4]. As a result, limited insight into dynamic spatiotemporal tumor evolution in prostate cancer (PCa) can restrict the clinical benefit of emerging therapies. In addition, the detection threshold of conventional diagnostic imaging is approximately one billion cells; below this level, malignant lesions are typically undetectable [5]. Collectively, such occult lesions may still contribute substantial tumor burden, increase overall heterogeneity, and harbor genetic aberrations associated with therapy resistance [6].

The prognostic value of circulating tumor cells (CTCs) has been recognized since the introduction of CellSearch in 2005; however, CTC enumeration has not been adopted as a routine prognostic or early-response biomarker in the clinical management of PCa [7]. Advances in molecular profiling and cell-sorting technologies have improved the sensitivity and reduced the cost of analyzing rare cells such as CTCs, making CTC molecular subtyping an increasingly viable route to precision diagnostics [8, 9]. Liquid biopsies (e.g., CTCs) can enable treatment stratification through biomarkers such as androgen receptor (AR) pathway activity and expression of DNA repair genes [10–12]. With longitudinal sampling, CTC transcriptome profiles can capture temporally resolved tumor phenotypes with clinically actionable

potential [13]. Despite rapid progress in biomarker discovery, therapeutic innovation has outpaced diagnostic implementation in PCa; consequently, patient stratification for personalized therapy remains an unmet clinical need.

This study combined label-free CTC enrichment with transcriptome analysis to characterize oncogenic signaling pathways in mCRPC patients initiating a new line of therapy. CTCs were enriched from whole blood using the Parsortix PR1 microfluidic system. The PR1 system employs the same technology as the Food and Drug Administration (FDA)-approved PC1 platform and captures CTCs based on physical properties such as increased size and reduced deformability relative to leukocytes [14]. This approach allows for the isolation of both epithelial and mesenchymal CTCs as single cells or aggregates (CTC clusters), resulting in CTC-enriched samples containing 200 to 800 leukocytes per mL of processed blood [14]. CTC gene expression was quantified using the HyCEAD™ (Hybrid Capture Enrichment Amplification and Detection) assay [15–17]. This multiplex assay has sufficient sensitivity and specificity to detect a single CTC target in a background of non-malignant circulating epithelial cells and leukocytes and has been used to predict malignancy in women with pelvic masses [16, 18].

The primary aim of this chapter is to evaluate the feasibility and prognostic utility of label-free CTC enrichment and transcriptome profiling in mCRPC. A secondary aim is to explore whether CTC transcriptome profiles can be used to predict therapeutic response in mCRPC.

5.2 Results

5.2.1 CTC Enrichment and Analysis Pipeline

Parsortix CTC-enriched samples contain a substantial leukocyte fraction, which can generate considerable background signal and complicate the design of gene panels for CTC transcriptome profiling. Using a proprietary microarray transcriptome dataset comprising PCa and leukocyte samples, we selected 64 genes that were highly expressed in PCa and showed minimal or no expression in peripheral blood cells. The leukocyte marker *PTPRC* was included to quantify background signal in each sample but was excluded from survival analyses. Hereafter, this 64-gene set is referred to as the "complete gene panel."

To evaluate feasibility, mock CTC samples were generated by spiking 10–1000 LNCaP cells into 8 mL of whole blood from young, healthy volunteers to approximate representative tumor–leukocyte mixtures. Tumor specificity of the complete gene panel was further assessed using blood from healthy volunteers, including age-matched males, young adult males, and females of various ages. Table 5.1 lists the genes in the panel and summarizes their relevance to PCa.

Table 5.1: PCa CTC transcriptome gene panel.

Gene	Relevance to PCa
ADAMTS9	Biomarker for liquid biopsies.
AGR2	Promotes metastasis.
AKR1C3	Androgen biosynthesis and AR activation.
AMACR	Upregulated in PCa (PRAD TCGA).
AOX1	Correlates with recurrence.
AR	Drives both castration-sensitive and insensitive PCa.
ARv7	Insensitive to ARSIs.
BIRC5	Upregulated in primary and metastatic PCa.
BMP6	Overexpressed, linked to invasiveness.
BRCA1/2	Tumor suppressor, DNA repair.
CCNE2	Promotes PCa proliferation.
DLX1	Biomarker for PCa.
EN2	Secreted in PCa, absent in normal tissue.
EPCAM	CTC detection target.
ERG	Drives PCa via transcription regulation.
EYA4	Promotes PCa progression.
FAM107A	Biomarker and therapeutic target.
FANCA	Germline alterations increase DNA repair sensitivity.
FAT1	Regulates apoptosis.
FOLH1	Expressed in AR+ but not AR− CRPC.
FOXA1	Facilitates AR-chromatin interactions.
GHR	Drives PCa progression.
GLYATL1	Androgen regulated, upregulated in PCa.
GNMT	Promotes proliferation via apoptosis.
GRHL2	AR coregulator in oncogenic AR axis.
HOXB13	Regulates AR/ARv7 binding in mCRPC.
HOXC6	Androgen-independent AR cofactor.
ITGBL1	Promotes EMT, invasion, and migration.
KIF11	Prognostic marker for mCRPC.
KIF20A	Drives mCRPC via AR activation.
KLK2/KLK3	Canonical AR targets.
KRT14	Marker for basal PCa cells.
KRT5	Androgen-independent PCa phenotype.
MYO6	Promotes motility and invasiveness.
NAALADL2	Promotes metastatic PCa.
NKX3-1	AR collaborator in androgen-dependent PCa.
PAX8-GLIS3	Fusion gene disrupts SHH signaling.
PCDHB2	Upregulated in PCa (PRAD TCGA).
PMEPA1	Biomarker and therapeutic target.
PPFIA2	Marker for aggressive PCa.
PRR16	Upregulated in PCa (PRAD TCGA).
PRSS8	Aberrantly expressed in PCa.
RORC	Upregulated in mCRPC.
RRM2	DNA repair, linked to poor outcomes.
SIM2	Promotes PCa onset and progression.
SLC25A33	Prevents mitochondrial dysfunction.
SOX2	Drives metastatic PCa.
SPOCK3	Correlates with PCa progression.
SRD5A1	Androgen biosynthesis and AR activation.
STEAP1	Overexpressed, immunotherapy target.
TDRD1	Overexpressed in PCa.
TERT	High expression linked to recurrence.
TFF1	Enhances metastasis and angiogenesis.
TLCD1	Upregulated in PCa (PRAD TCGA).
TMPRSS2	Drives ERG overexpression in PCa.
TMPRSS2-ERG	Fusion drives *ERG* overexpression.
TOP2A	AR collaborator in PCa progression.
TRPM8	Therapeutic target in androgen-dependent PCa.
TUSC3	Tumor suppressor.
VSTM2L	Prognostic, linked to immune infiltration.
WNT5A	Induces PCa dormancy.
WNT7B	AR-regulated, promotes CRPC.

5.2.2 Patient Characteristics

In total, 40 patients provided baseline CTC samples (i.e., prior to initiating a new line of therapy). Subsequent treatments included androgen receptor signaling inhibitors (ARSIs; abiraterone or enzalutamide; n=22), chemotherapy (docetaxel or cabazitaxel; n=9), immunotherapy (ipilimumab plus nivolumab; n=2), radioligand therapy (PSMA-Lu177 or radium-223; n=2), and PARPi (olaparib; n=2); two patients were managed with active surveillance until evidence of disease progression (i.e., no systemic therapy). Clinical trajectories, inclusion time points (CTC collection), and lines of therapy are summarized in Figure 5.1. For one patient receiving PARPi, two CTC samples were collected: RAD30 at baseline and RAD41 14 days later. RAD41 was excluded from the primary analysis because it was not a baseline sample. Baseline alkaline phosphatase and prostate-specific antigen (PSA) levels, age, de novo metastasis status, time since castration-resistant prostate cancer (CRPC) diagnosis, post-collection therapy, and 1-year survival by therapy group are reported in Table 5.2.

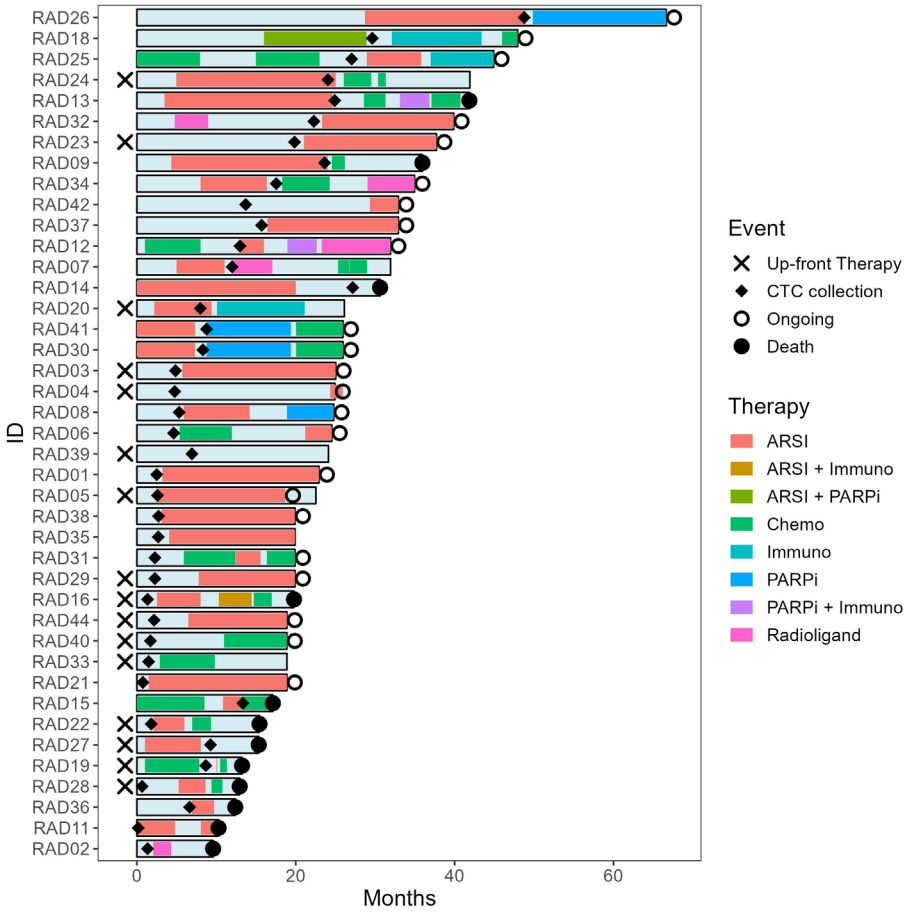

Figure 5.1: The clinical trajectories of study participants.

Patient IDs were anonymized and labeled RAD (Radboudumc) accompanied by a chronological number. Event legend: indicating whether patients received prior therapy for castrate-sensitive disease (Up-front Therapy), when CTCs were collected (CTC collection), whether therapy continued (ongoing), or if a patient had become deceased (death) at the last follow-up. Therapy legend: indicating lines of mono-therapy or combination therapy.

Table 5.2: Patient characteristics.

Number of patients	40
Age, median (range)	65 (45-85)
Years since CRPC, the median (range)	2 (0.8-5.5)
PSA (μg/L) at inclusion, median (range)	31.5 (1.2-1600)
De novo metastatic diseases, Num. (%)	
Yes	29 (72.5%)
No	11 (27.5%)
Alkaline phosphatase (U/L), median (range)	106 (54-1866)
Type of therapy following inclusion, Num. (%)	
ARSI	22 (54%)
Chemotherapy	9 (22%)
Immunotherapy	2 (5%)
Radioligand therapy	2 (5%)
PARPi therapy	2 (5%)
Active surveillance	3 (7%)
1-year survival per therapy, percentage (95% CI)	
Therapy-agnostic	82% (72-95%)
ARSI	86% (73-100%)
Chemotherapy	89% (71-100%)
Immunotherapy	50% (13-100%)
Radioligand	50% (13-100%)
PARPi	100%
Active surveillance	33% (6.7-100%)

Number of study participants, participants' age, years since CRPC diagnosis, median PSA level at the time of CTC collection, de novo metastasis at the time of PCa diagnosis, median alkaline phosphatase level at the time of CTC collection, type of therapy received following CTC collection, 1-year survival for each therapy group following CTC collection.

5.2.3 Genomic Alterations and CTC Transcriptomes

Next-generation DNA sequencing of solid-tissue biopsies was successful in 38 patients (95%). *AR* alterations were detected in 11 patients (29%) and comprised nine amplifications and three mutations; one patient harbored both an amplification and a mutation. *TP53* alterations were observed in 10 patients (26%; nine mutations and one shallow deletion), and *PTEN* alterations in seven patients (18%; four mutations and three shallow deletions). Alterations in DDR genes were identified in nine patients (24%), involving *BRCA2*, *MSH2*, *RAD51B*, *CHEK2*, and *FANCL*. *BRCA2* was the most frequently altered DDR gene (three mutations and two shallow deletions). Other recurrent mutations, each present at lower frequencies (2.6–5%), affected *PPP2R2A*, *CDK12*, *MSH2*, *RAD51B*, *CHEK2*, *RB1*, *PIK3CA*, *AKT1*, *SPOP*, and *FANCL* (Figure 5.2).

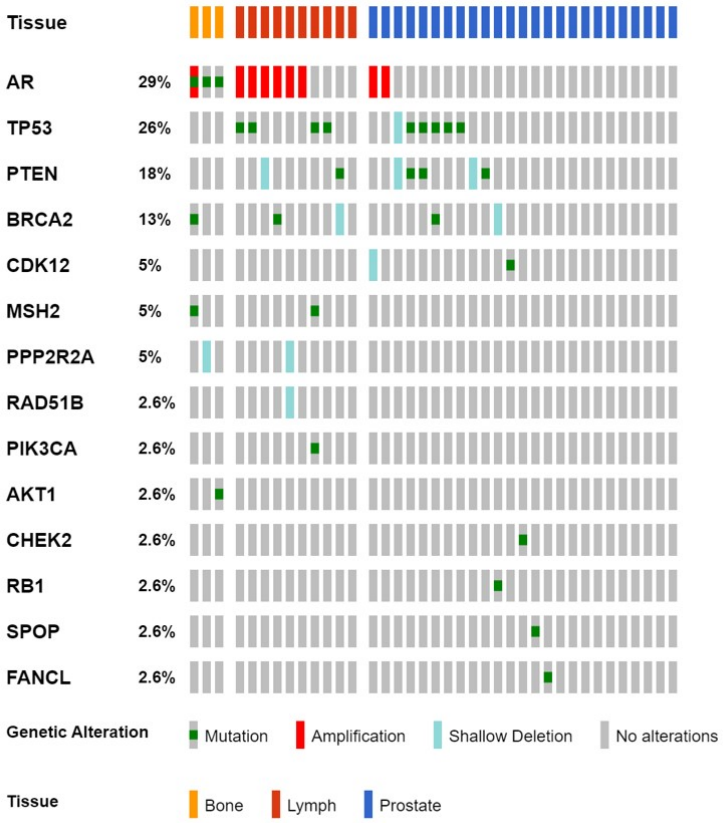

Figure 5.2: Genetic alterations in solid tissue biopsies.

Genetic alterations identified through next-generation DNA sequencing in the PROMPT trial. Genetic alterations: Mutation, inframe, missense, splice, or truncal mutations; Amplification, copy number amplification; Shallow Deletion, heterogeneous deletion; No alterations, wildtype. Tissue; Bone, metastatic bone biopsy; Lymph, metastatic lymph-node biopsy; Prostate, prostate tissue biopsy.

Because the DNA sequencing and CTC transcriptome panels overlapped, we assessed whether *AR* and *BRCA2* alterations identified in solid-tissue biopsies were reflected at the transcript level in matched CTCs. Among nine patients with *AR* amplification, eight showed increased expression of AR signaling genes (*AR*, *KLK3*, *ARv7*, and/or *FOXA1*) in CTCs (Figure 5.3A), suggesting strong concordance between solid-tissue and CTC-based profiling [19]. By contrast, the patient with both *AR* amplification and mutation did not show increased CTC expression of AR signaling genes (Figure 5.3A). For *BRCA2*, two patients harbored shallow deletions; in one of these cases, *BRCA2* and related DDR genes (*BRCA1*, *FANCA*, *RRM2*, *TOP2A*) remained expressed in matched CTCs (Figure 5.3B). These findings suggest that *BRCA2* loss may be less consistently concordant between solid-tissue and CTC biopsies [20].

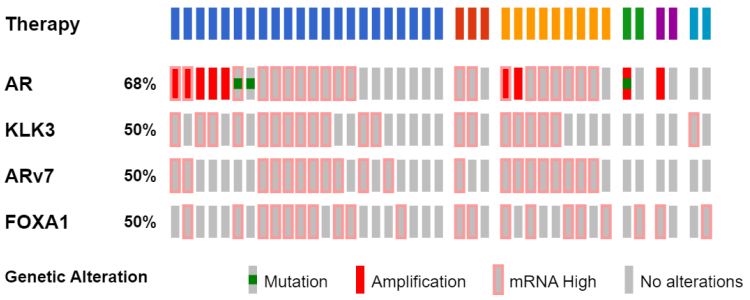

(a) AR signaling gene alterations and expression.

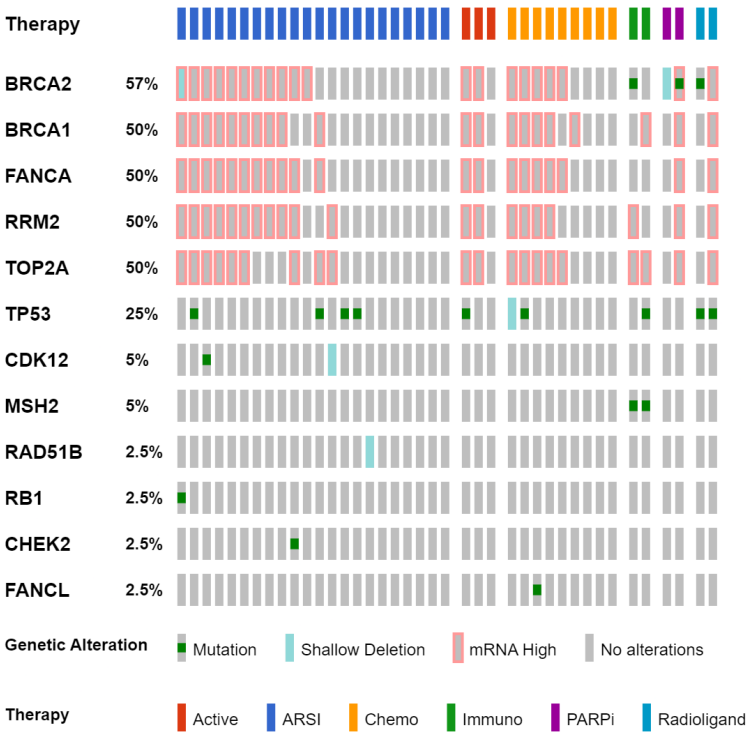

(b) DNA repair gene alterations and expression.

Figure 5.3: Concordance between tumor genomic alterations and CTC gene expression.

Genetic alterations in tissue biopsies and high gene expression in matched CTC samples of AR signaling genes (A) and DDR genes (B). Genetic alterations: Mutation, inframe, missense, splice, or truncal mutations in tissue biopsies; Amplification, copy number amplification in tissue biopsies; Shallow Deletion, heterogeneous deletion in tissue biopsies; mRNA High, high expression in CTC samples; No alterations, wildtype gene in tissue biopsies. Therapy: Active, active surveillance; ARSI, ARSI therapy; Chemo, chemotherapy; Immuno, immunotherapy; PARPi, PARPi therapy; Radioligand, radioligand therapy.

5.2.4 The prognostic value of CTC transcriptome profiling

Hierarchical clustering with the complete gene panel, independent of treatment modality (the "therapy-agnostic cohort"), identified two transcriptionally distinct groups (Figure 5.4A). The group with higher expression of AR signaling genes (*ARv7*, *DLX1*, *HOXB13*, and *KLK3*), DDR genes (*BRCA1*, *BRCA2*, *FANCA*, and *TOP2A*), and oncogenes (*ERG* and *GRHL2*) showed shorter PFS (HR=1.99, p=0.076) and significantly shorter OS (HR=5.1, p=0.007) (Figure 5.4B/C). Genes with limited prognostic value were removed from subsequent clustering to improve risk stratification.

To quantify the relative prognostic contribution of each gene in the complete panel, we performed a multivariate analysis of PFS and ranked genes by HR (Supplementary Figure 5.1). Notably, the epithelial marker *EPCAM* was not a top-ranked prognosticator in this cohort, despite prior evidence that *EPCAM*-positive CTCs are prognostically relevant across malignancies [7, 21]. In contrast, genes related to AR signaling (*KLK3*, *HOXB13*, and *GRHL2*) and metastasis (*MYO6* and *TRPM8*) were more informative [22, 23]. Guided by these rankings and the literature, and refined through iterative clustering and survival analyses, we defined a tailored panel comprising *AR*, *ARv7*, *FOLH1* (PSMA), *KLK2*, *KLK3*, and *TMPRSS2* (the "agnostic gene panel") [24].

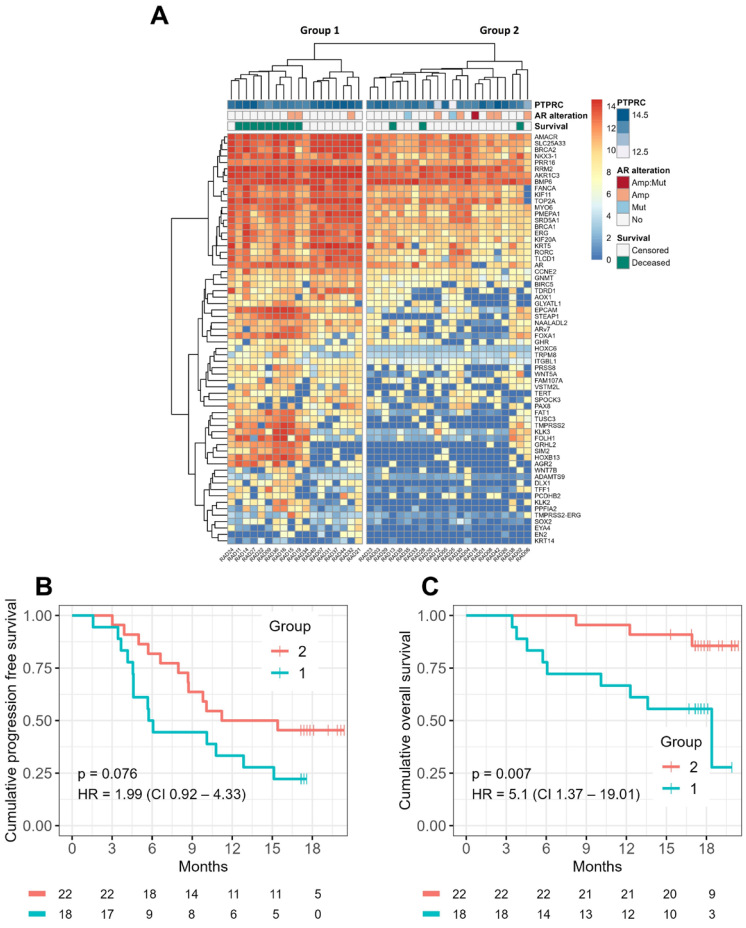

Figure 5.4: Hierarchical clustering of CTC transcriptomes in PCa.

Hierarchical clustering of the therapy-agnostic cohort using the complete gene panel (A). Cluster *p*-values are p=0.26 for Group 1 and p=0.27 for Group 2. PFS (B) and OS (C) of patients with either Group 1 or Group 2 profiles. Expression annotation: log2 expression values. Heatmap annotation: PTPRC: leukocyte background signal in each sample, AR alteration: Amp:Mut, AR amplification and mutation: Amp, AR amplification, Mut: AR mutation, No: no alteration; Survival, Censored: alive at last follow-up, Deceased: deceased at last follow-up. Survival statistics: HR, Hazard ratio; CI, 95% confidence interval; p, *p*-value.

Hierarchical clustering with the agnostic gene panel separated patients into two transcriptionally distinct groups: Group 1 and Group 2 (Figure 5.5A). These groups had no significant differences in *PTPRC* levels (Supplementary Figure 5.2). At baseline, Group 1 patients (n=16) had lower mean leukocyte counts (6.7 vs. 9.2×10^9/L), and higher mean alkaline phosphatase (334.5 vs. 103.6 U/L), and PSA (215.8 vs. 40.8 μg/L) than Group 2 patients (n=24) (Supplementary Table 5.1). *AR* amplification prevalence was similar between groups and was not prognostic for PFS or OS (Figure 5.5A; Supplementary Figure 5.3). Group 1 had a significantly higher risk of progression (HR=4.28, p<0.001) (Figure 5.5B) and death (HR=10.78, p<0.001); at last follow-up, 63% of Group 1 patients were deceased compared with 8% of Group 2 (Figure 5.5C; Supplementary Figure 5.4A). In univariate analyses, the Group 1 profile was the strongest predictor of both PFS (HR=4.28, p<0.001) and OS (HR=10.78, p<0.002) relative to PSA, *ARv7* expression, and age (Figure 5.5D/E; Supplementary Figure 5.4B). The Group 1 profile remained the strongest predictor in multivariate models for PFS (HR=3.83, p<0.002) and OS (HR=9.99, p<0.005) that included age (HR=1.00, p<0.850) and PSA (HR=1.00, p<0.045) (Supplementary Figure 5.4C). Likewise, the Group 1 profile was highly prognostic for OS (HR=9.99, p<0.005) in a multivariate model containing age (HR=1.04, p<0.199) and PSA (HR=1.00, p<0.214) (Supplementary Figure 5.4D).

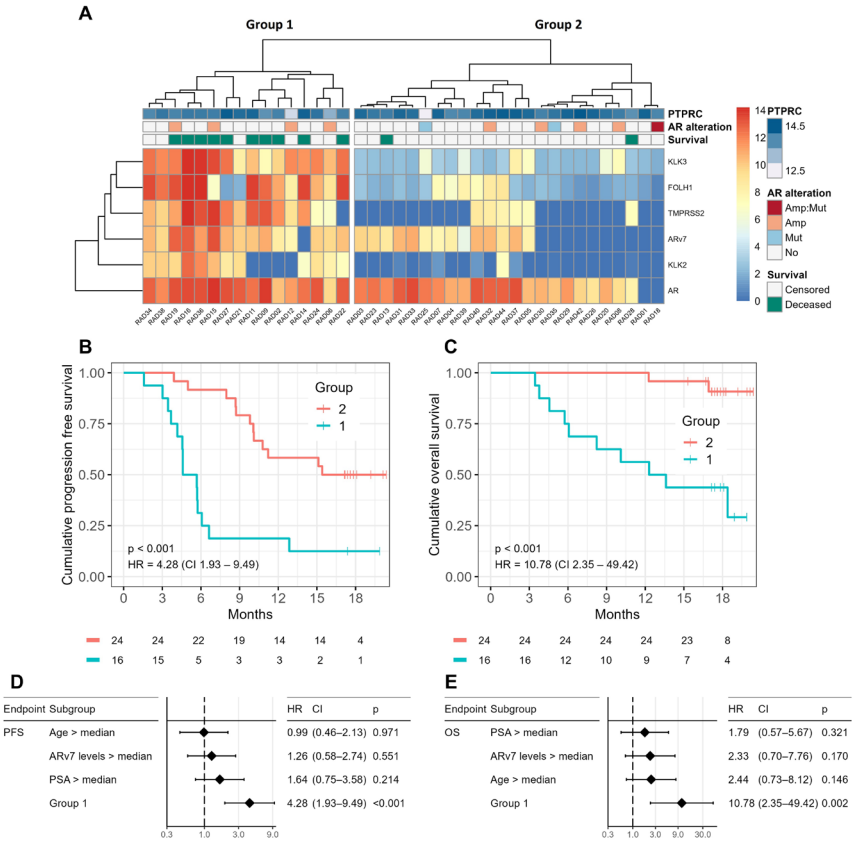

Figure 5.5: Targeted CTC transcriptome profiles stratify clinical outcomes in PCa.

Hierarchical clustering of the therapy-agnostic cohort using the agnostic gene panel (A). Expression of *KLK3*, *FOLH1*, *TMPRSS2*, *ARv7*, *KLK2*, and *AR* clustered into two groups: Group 1 (p=0.06) and Group 2 (p=0.07). Kaplan-Meier plots show Group 1 and Group 2 survival (PFS (B) and OS (C)). Age, *ARv7* levels, Group 1, and PSA for independent surval on PFS (D), and OS (E). Expression annotation: expression is shown in log2 values, from 0 (dark blue) to 14 (deep red). Heatmap annotation: PTPRC: leukocyte background signal in each sample, AR alteration: Amp:Mut: AR amplification and mutation, Amp: AR amplification, Mut: AR mutation, No: no alteration. Survival: Censored: alive at last follow-up, Deceased: deceased at last follow-up. Survival statistics: HR, hazard ratio; CI, 95% confidence interval; p, p-value.

5.2.5 CTC Transcriptomes Predict Therapy Response

Patients were stratified by subsequent therapy to assess whether targeted CTC transcriptome profiling could predict treatment response.

To identify transcripts associated with response to ARSIs, we performed a multivariate analysis of PFS in the ARSI-treated subset (n=22) using the complete gene panel. Genes were ranked by HR (Supplementary Figure 5.5). Among the highest-ranked genes, most were involved in AR signaling, including *GRHL2*, *KLK3*, *HOXB13*, *FOXA1*, and *AGR2*. Unsupervised clustering and survival analysis using the complete gene panel separated ARSI-treated patients into two groups with significantly different OS, but not PFS (Figure 5.6).

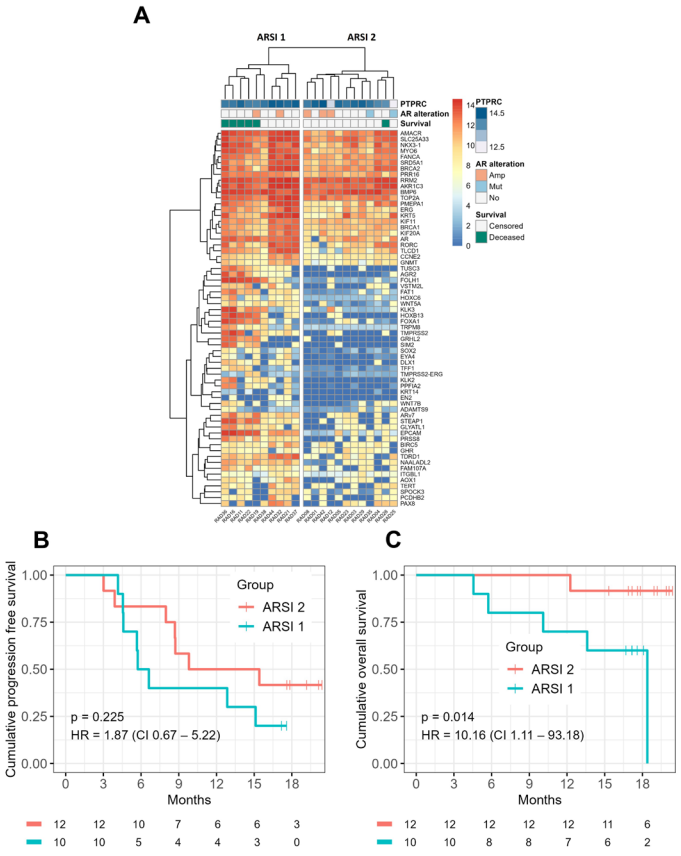

Figure 5.6: The feasibility of using CTC transcriptome profiles predict ARSI response.

Hierarchical clustering of the ARSI cohort using the agnostic gene panel (A). Cluster p-values are p=0.26 for ARSI 1 and p=0.3 for ARSI 2. PFS (B) and OS (C) of patients with either ARSI 1 or ARSI 2 profiles visualized in Kaplan–Meier plots. Expression annotation: expression is shown in log2 values, from 0 (dark blue) to 14 (deep red). Heatmap annotation: PTPRC: leukocyte background signal in each sample, AR alteration: Amp: AR amplification, Mut: AR mutation, No: no alteration. Survival: Censored: alive at last follow-up, Deceased: deceased at last follow-up. Survival statistics: HR, hazard ratio; CI, 95% confidence interval; p, p-value.

After iterative clustering and survival analyses, we defined a reduced gene set with improved prognostic performance relative to the complete panel (the "ARSI gene panel"; Figure 5.7).

Hierarchical clustering using the ARSI gene panel identified two transcriptionally distinct groups, ARSI 1 and ARSI 2 (Figure 5.7A). *PTPRC* levels did not differ significantly between groups (Supplementary Figure 5.6). At baseline, patients in ARSI 1 (n=6) had lower mean leukocyte counts (7 vs. 10.3×10^9/L) and higher mean alkaline phosphatase (255.3 vs. 99.9 U/L) and PSA (130.1 vs. 39.8 μg/L) than patients in ARSI 2 (n=16) (Supplementary Table 5.2). *AR* amplification was more prevalent in ARSI 2, but amplification status was not prognostic for PFS or OS (Figure 5.7A; Supplementary Figure 5.7).

Compared with ARSI 2, patients in ARSI 1 had a significantly higher risk of progression (HR=13.05, p<0.001) and death (HR=21.56, p<0.001) (Figure 5.7C). At last follow-up, 88% of ARSI 1 patients had died versus 6% of ARSI 2 patients (Supplementary Figure 5.8A). In univariate models, the ARSI 1 profile was the strongest prognosticator of PFS (HR=13.05, p=0.002) compared with ARv7 expression (HR=1.76, p=0.282), PSA (HR=1.35, p=0.566), and age (HR=0.78, p=0.636) (Figure 5.7D). The ARSI 1 profile remained associated with progression in a multivariate model including age and PSA (HR=11.59, p=0.006) (Supplementary Figure 5.8C). Notably, the prognostic value of *ARv7* expression for OS was higher in the ARSI cohort than in the therapy-agnostic cohort (HR=6.90 vs. 2.33) (Figure 5.5E; Figure 5.7E; Supplementary Figure 5.8B), whereas this pattern was not observed for PFS (Figure 5.5D; Figure 5.7D). For OS, ARSI 1 was again the strongest prognosticator in univariate analyses (HR=21.56, p=0.005) relative to *ARv7* expression (HR=6.90, p=0.080), PSA (HR=2.53, p=0.291), and age (HR=1.76, p=0.518) (Figure 5.7E). In a multivariate model including age and PSA, ARSI 1 remained the strongest prognosticator of OS (HR=27.36, p=0.005).

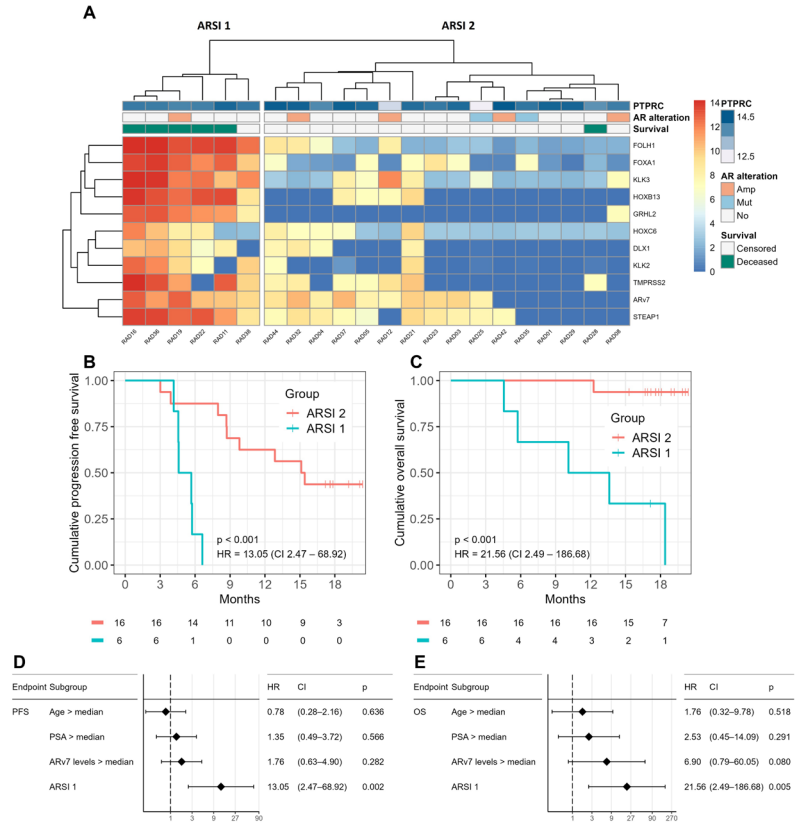

Figure 5.7: CTC transcriptome profiles predict ARSI response.

Hierarchical clustering of the ARSI cohort using the ARSI gene panel (A). Cluster p-values are p=0.12 for ARSI 1, and p=0.14 for ARSI 2. PFS (B) and OS (C) of patients with either ARSI 1 or ARSI 2 profiles visualized in Kaplan–Meier plots. Independent prognostic values of age, *ARv7* levels, ARSI 1, and PSA on PFS (D) and OS (E). Expression annotation: expression is shown in log2 values, from 0 (dark blue) to 14 (deep red). Heatmap annotation: PTPRC: leukocyte background signal in each sample, AR alteration: Amp: AR amplification, Mut: AR mutation, No: no alteration. Survival: Censored: alive at last follow-up, Deceased: deceased at last follow-up. Survival statistics: HR, hazard ratio; CI, 95% confidence interval; p, p-value.

To explore predictors of chemotherapy response, we performed a multivariate

analysis of PFS in the chemotherapy-treated subset (n=9) using the complete gene panel and ranked genes by HR (Supplementary Figure 5.9). *AKR1C3*, *DLX1*, *HOXC6*, and *MYO6* were among the highest-ranked genes. Kaplan–Meier curves for PFS and OS based on *ARv7* levels, age, PSA, and these genes are shown in Figure 5.8 and Figure 5.9. Expression of *AKR1C3*, *DLX1*, *HOXC6*, and *MYO6* were equally strong prognosticators of PFS (HR=10.97, p=0.011) and ranked above age (HR=0.8, p=0.806), *ARv7* (HR=2.45, p=0.320), and PSA (HR=0.91, p=0.923) (Figure 5.8A–G). For OS, *ARv7* levels ranked above all other considered variables in this cohort (HR=6.82, p=0.081) (Figure 5.9A–G). Given the small sample size and associated statistical limitations, we did not pursue further analyses in this cohort.

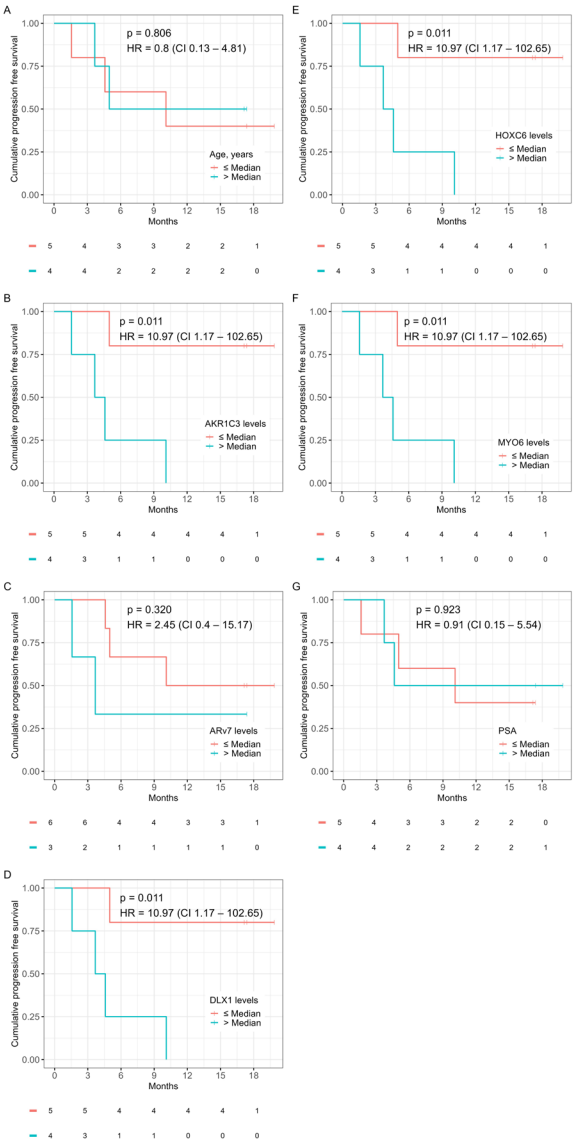

Figure 5.8: CTC transcriptome profiles prognosticate chemotherapy-specific PFS.

Kaplan–Meier plots for PFS in the chemotherapy cohort for age (A), *AKR1C3* levels (B), *ARv7* levels (C), *DLX1* levels (D), *HOXC6* levels (E), *MYO6* levels (F), and PSA (G). Survival statistics: HR, hazard ratio; CI, 95% confidence interval; p, *p*-value.

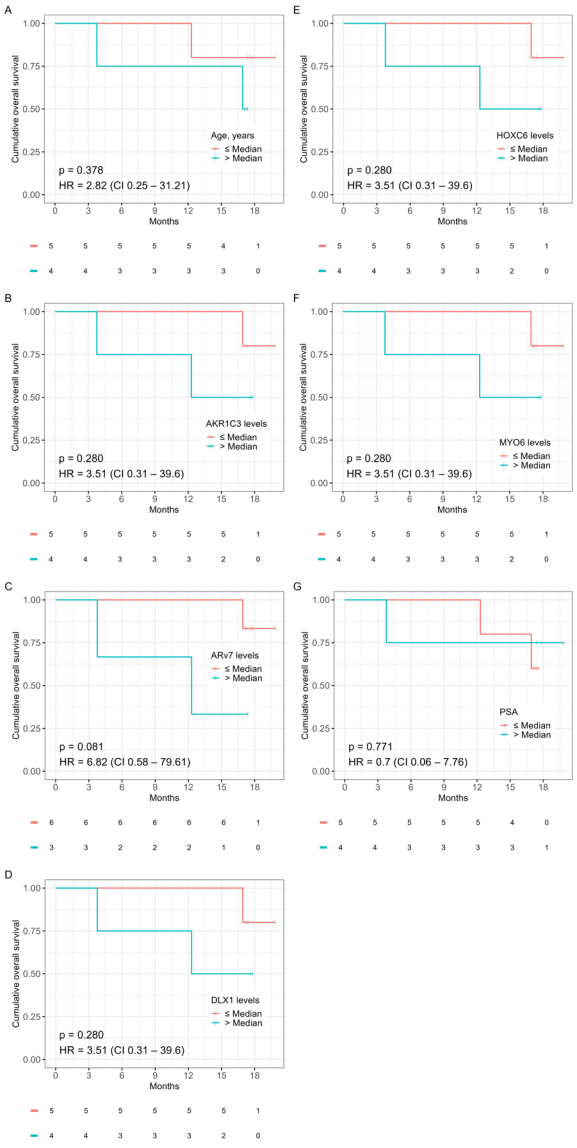

Figure 5.9: CTC transcriptome profiles prognosticate chemotherapy-specific OS.

Kaplan–Meier plots for OS in the chemotherapy cohort for age (A), *AKR1C3* levels (B), *ARv7* levels (C), *DLX1* levels (D), *HOXC6* levels (E), *MYO6* levels (F), and PSA (G). Survival statistics: HR, hazard ratio; CI, 95% confidence interval; p, *p*-value.

5.2.6 Longitudinal CTC Profiling–A Case Discussion

Deviating from the main protocol, one patient was sampled twice: at baseline (RAD30) and again 14 days after initiating PARPi therapy (RAD41). The two samples showed comparable *PTPRC* levels and broadly similar CTC transcriptome profiles, with several notable differences. Relative to RAD30, RAD41 showed upregulation of *SOX2*, *TRPM8*, *NAALADL2*, *ARv7*, *DLX1*, *TUSC3*, *GHR*, *FOXA1*, *FOLH1*, and *HOXC6*, alongside downregulation of *WNT5A*. A modest but discernible increase in *EPCAM* expression suggests that the epithelial cell fraction may have been higher in RAD41 than in RAD30 (Figure 5.10). Many of the upregulated genes are associated with AR signaling, suggesting increased AR pathway activity relative to baseline, either due to transcriptional changes within CTCs or increased CTC burden.

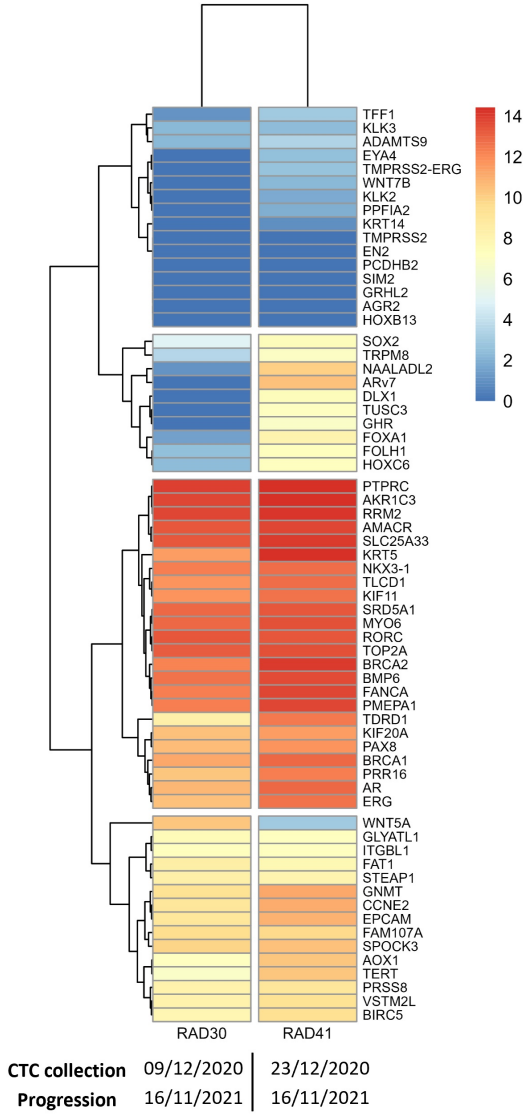

Figure 5.10: Longitudinal CTC profiling.

CTC profiles of samples RAD30 and RAD41 based on the complete gene panel. Samples were collected from a patient receiving PARPi, RAD30 at baseline followed by RAD41 14 days later. Expression annotation: log2 expression values.

5.3 Discussion

The data presented here highlight the prognostic value of CTC transcriptome profiling in advanced PCa. Using transcriptome analyses of tumor tissue and leukocyte samples, I selected 64 genes for targeted CTC profiling. Within this panel, AR signaling genes were among the strongest prognostic markers, separating patients into two transcriptionally distinct groups with divergent clinical trajectories. These observations are consistent with a prospective study by Sperger *et al.* [24]. Although the present work focuses on advanced PCa, Sperger *et al.* included a substantial proportion of hormone-sensitive patients (28%). The notable overlap between the Sperger gene panel and the therapy-agnostic panel further supports the central role of AR signaling in both CSPC and mCRPC progression. *ARv7* has received considerable attention as a PCa biomarker [11, 25] and, given its capacity to sustain AR signaling in the absence of ligand, might be expected to have prognostic utility in mCRPC [25]. However, in the therapy-agnostic cohort, CTC *ARv7* expression was not an independent predictor of survival, potentially reflecting the contribution of alternative resistance mechanisms [26].

In patients receiving ARSI therapy, CTC *ARv7* expression was prognostic for OS but not PFS. Consistent with this, AR signaling genes remained strong predictors of survival in the ARSI cohort, and stratifying patients with an AR pathway–focused gene panel substantially improved the prognostic performance of CTC profiling (Figure 5.6 and Figure 5.7). AR pathway activity scoring has also been used to stratify response to combined androgen blockade in AR-positive salivary duct carcinoma (SDC) [27]. Notably, in SDC, *SRD5A1* expression outperformed AR pathway activity as a prognostic marker [27]. *SRD5A1* increases intracellular DHT, consistent with canonical (androgen-dependent) AR signaling [28]. In contrast, *SRD5A1* did not stratify ARSI response in this study, underscoring the prevalence of non-canonical AR signaling in mCRPC (Supplementary Figure 5.5) [29]. Similarly, *AR*/*ARv7* lacked prognostic utility as independent biomarkers for

PFS in the ARSI cohort. *AR/ARv7* expression alone does not capture AR nuclear translocation, a prerequisite for genomic signaling [30]. Although *AR* amplification is considered an important driver of AR signaling, it was not prognostic for survival or ARSI response in this study [31]. Instead, prognostication of PFS required co-expression of AR co-factors and downstream transcriptional targets, highlighting the value of a multifaceted approach to profiling AR pathway activity when stratifying ARSI response in mCRPC.

In patients receiving chemotherapy, CTC transcriptome profiling identified a distinct set of prognostic genes compared with patients receiving ARSIs (Supplementary Figures 5.5 and 5.9). In this cohort, *AKR1C3*, *DLX1*, *HOXC6*, and *MYO6* were the strongest predictors of survival.

DLX1 and *HOXC6* are key biomarkers in the SelectMDx liquid biopsy test for identifying high-risk localized PCa [32]. *HOXC6* is upregulated across localized, advanced, and metastatic disease and promotes proliferation [33]. As an androgen-independent AR co-factor, HOXC6 can support non-canonical AR signaling under castrate conditions and may promote *DLX1* expression in ERG-negative mCRPC [33–35]. This biology may underlie the consistent prognostic value of *HOXC6* and *DLX1* across both CTC- and urine-based liquid biopsy studies [36]. In chemotherapy-treated mCRPC, the two genes may act synergistically to drive progression, consistent with evidence that *DLX1* upregulation promotes metastasis in mouse models of advanced PCa [35].

AKR1C3 transcribes an androgenic enzyme that is highly expressed in mCRPC. By promoting intracellular DHT biosynthesis, AKR1C3 can sustain canonical AR signaling even in the absence of testosterone [37]. Notably, *AKR1C3* is also highly expressed in AR-negative mCRPC, suggesting additional AR-independent oncogenic functions [37]. Supporting this possibility, in esophageal adenocarcinoma AKR1C3 has been shown to regulate AKT phosphorylation and promote chemotherapy resistance [38].

MYO6 transcribes an actin motor protein that is central to cell motility [39].

In PCa, *MYO6* is upregulated and promotes proliferation of CRPC cells [40]. Its potential role in metastasis is supported by evidence that *MYO6* mRNA knockdown in PCa cell lines impairs cellular migration [41]. Accordingly, CTC *MYO6* expression may reflect metastatic potential. In this study, *MYO6* was uniquely prognostic in patients receiving chemotherapy, a cohort with high metastatic burden as suggested by elevated alkaline phosphatase levels (Supplementary Table 5.3).

Because CTC counts could not be determined, the extent to which CTC burden influenced the observed transcriptome profiles cannot be directly assessed. Nevertheless, *EPCAM*, a cell-adhesion marker used for prognostic CTC enumeration with the CellSearch platform, was not a strong prognostic marker in this study (Supplementary Figures 5.1, 5.5, and 5.9) [7]. Together, these findings suggest that CTC transcriptome profiling provides prognostic information beyond enumeration alone.

AR pathway activity was prognostic across treatment modalities, underscoring its broad oncogenic relevance in mCRPC. Consistent with this, prior studies have reported synthetic lethality between AR and PARP inhibition, implicating AR in DDR [42, 43]. PARP inhibition has been shown to reduce genomic stability and inhibit AR nuclear translocation in PCa [42–44]. In contrast, in one patient receiving PARPi, several AR signaling genes were upregulated in CTCs relative to baseline (Figure 5.10). This patient harbored a *BRCA2* mutation, which has been associated with increased Src signaling [45]. Src-mediated phosphorylation of AR can promote AR nuclear translocation and may represent a mechanism of PARPi resistance [45]. These observations suggest that longitudinal monitoring of CTC AR pathway activity could serve as an early response biomarker in *BRCA2*-mutant patients receiving PARPi; however, further work is required to substantiate this hypothesis.

Thus far, this discussion has emphasized the clinical utility of CTC transcriptome profiling in mCRPC. However, key determinants of CTC fitness,

including survival, invasiveness, and resistance to vascular stressors, are unlikely to be specific to mCRPC [46, 47]. In multiple cancer types, CTC clusters are associated with poorer outcomes, consistent with their enhanced resilience to vascular stress and high metastatic potential [47]. Cluster formation has been linked to expression of the basal cell marker *KRT14* in ovarian and breast cancer [47, 48]; notably, basal PCa cells also exhibit an aggressive phenotype [49]. The ion channel TRPM8 has been implicated in tumor cell invasiveness across several cancers [50], and *MYO6* upregulation has been associated with metastasis and disease progression in several cancers including PCa [39, 40, 51]. Accordingly, the prognostic value of *KRT14*, *TRPM8*, and *MYO6* in the present study suggests that they may serve as markers of CTC metastatic potential (Supplementary Figures 5.1 and 5.9).

CTC transcriptomes can provide temporal insight into emerging therapy resistance and metastatic potential. Label-free CTC enrichment combined with tailored transcriptome profiling therefore represents a promising strategy for stratifying treatment response in mCRPC. A limitation of this work is that our approach did not allow CTC quantification, precluding direct assessment of the relationship between CTC burden and transcriptome profiles.

5.4 Methods

5.4.1 Gene Panel Development

An in-house microarray transcriptome dataset containing PCa and leukocyte samples was used to select a panel of 64 genes [36] (Table 5.1). The panel consists of genes that are highly expressed in localized PCa and mCRPC, with limited or no expression in peripheral blood cells, and/or have known roles in PCa biology. A leukocyte-specific gene, *PTPRC*, was included to assess the leukocyte background signal. *PTPRC* expression was excluded from survival analyses. The 64-gene panel will be referred to as the "complete gene panel" hereafter. Mock CTC samples containing representative fractions of PCa cells and leukocytes (i.e., 10–1000 LNCaP cells spiked in 8 mL whole

blood of young and healthy volunteers) were used to test the feasibility of our approach (ATCC, Manassas, VA, USA). Tumor-specificity of the complete gene panel was tested using healthy volunteer blood from age-matched males, young adult males, and age-agnostic females.

5.4.2 Patient Recruitment

Patients were recruited from a single-center observational study at Radboudumc (Nijmegen, the Netherlands; PROMPT, NCT04746300). Eligible participants were men with confirmed mCRPC who were either therapy naive or had received at most one line of systemic therapy in the castrate setting. Prior treatment in the castrate-sensitive setting with up to six cycles of docetaxel or an ARSI was permitted. All participants provided written informed consent for study participation and for biobanking of blood and urine for pre-defined biomarker studies.

5.4.3 Healthy Donor Recruitment

EDTA blood samples from healthy volunteers were collected at the Sanquin blood bank in Nijmegen, Netherlands. In total, 29 donors participated, including 9 age-matched males ($\geq$50 years), 10 young adult males ($<$50 years), and 10 females. Healthy donor demographics are shown in the supplementary table 5.4.

5.4.4 Next-Generation DNA Sequencing

Tumor molecular profiling was performed for all PROMPT participants using next-generation DNA sequencing with the TruSight Oncology 500 (TSO500; Illumina, San Diego, CA, USA) panel. Sequencing was carried out on formalin-fixed, paraffin-embedded prostate or metastatic biopsy tissue, preferably obtained in the castrate state. A virtual PCa-specific diagnostic panel was applied, restricting the analysis to 44 genes with prognostic and/or actionable potential in PCa (Supplementary table 5.5).

5.4.5 Presentation of Genomic Alterations

Genomic alterations from solid tissue biopsies and matched transcriptomic alterations from liquid CTC biopsies were presented in an oncoprint using the online OncoPrinter tool from cBioPortal [52, 53].

5.4.6 Sample Processing

Blood was drawn into 8 mL EDTA vacutainers at inclusion and processed within 48 h. When required, whole blood was stored at 4 °C until processing. Samples were passed through a 6.5 μm filtration cassette at 50 mbar using the Parsortix PR1 system, according to the manufacturer's instructions (CelLBxHealth plc, Guildford, UK). After filtration, trapped cells were harvested by pulsatile backflush with PBS into HyCEAD lysis buffer, following the manufacturer's protocol. Lysates were stored at −80 °C and shipped on dry ice to CelLBxHealth plc laboratories in Toronto, ON, Canada for transcriptome profiling.

5.4.7 Transcriptome Profiling

Lysed samples were analyzed using sense-strand HyCEAD probes on Ziplex® Flow-Thru Chip® (CelLBxHealth plc, Guildford, UK) [15, 16, 54]. Raw expression values were floored at 1 and $\log_2$ transformed before analysis. Transcriptome profiles were generated by hierarchical clustering as described in Section 5.4.9.

5.4.8 Clinical Follow-Up and Data Collection

Patient inclusion started in September 2020 and ended in January 2021. Baseline clinical parameters and genomic alterations in metastatic tissue or prostate biopsies were recorded at the time of CTC collection. Clinical and genomic data were prospectively collected, and clinical outcomes were updated following inclusion until May 2022 or death.

5.4.9 Statistical Analysis

Clinical trajectories were visualized using swimmer plots generated in RStudio (version 4.2.2) with `tidyverse` and `swimplot` [55].

Unsupervised hierarchical clustering of $\log_2$-transformed expression values was performed in RStudio using `tidyverse`, `pheatmap`, `pvclust`, `RColorBrewer`, and `grid` [55]. CTC transcriptome profiles were clustered using Euclidean distance and complete linkage. Cluster support was assessed by multiscale bootstrap resampling with 10^4 iterations. The prognostic value of CTC gene expression, sPSA, and age was evaluated by survival analyses using the cohort median as the cut-off.

Univariate and multivariate survival analyses were performed in RStudio using `tidyverse`, `survivalAnalysis`, `ggpubr`, and `ggstatsplot` [55, 56].

5.5 Supplementary Figures

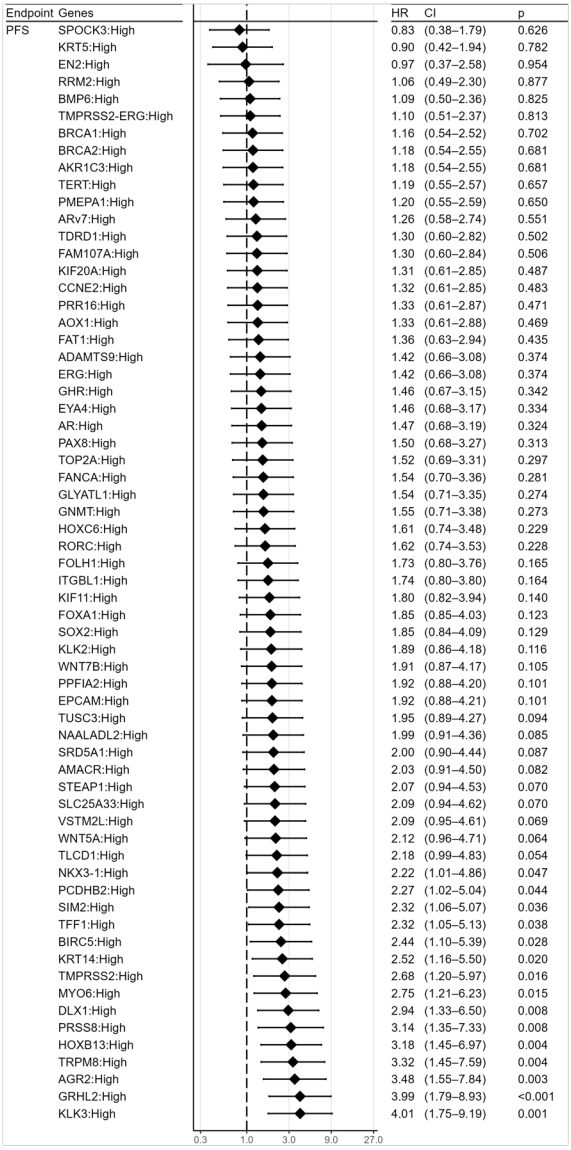

Supplementary Figure 5.1: The prognostic value of genes from the complete gene panel on PFS in the therapy-agnostic cohort. A multivariate model was used to determine risk for progression (HR), 95% confidence intervals, and statistical significance (p). Survival statistics: HR: Hazard ratio, CI: Confidence interval, p: *p*-value.

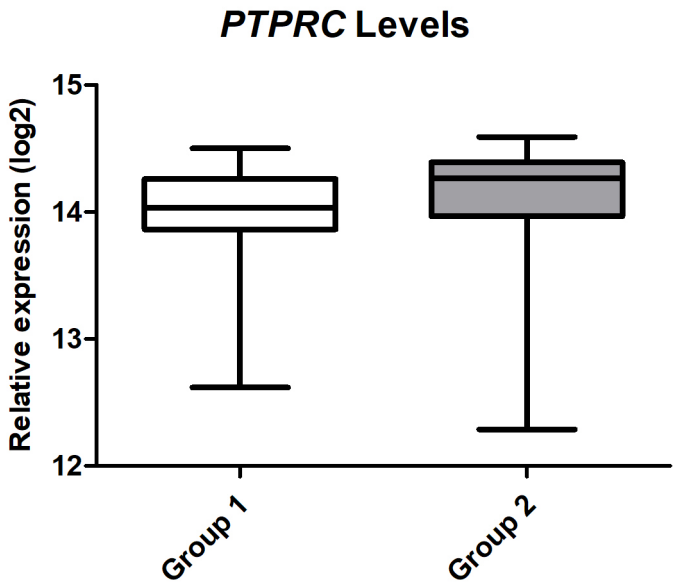

Supplementary Figure 5.2: PTPRC levels in Group 1 (n=16) and Group 2 (n=24) patients from the therapy-agnostic cohort. Patients were grouped via unsupervised hierarchical clustering using the agnostic gene panel (Figure 5.5A).

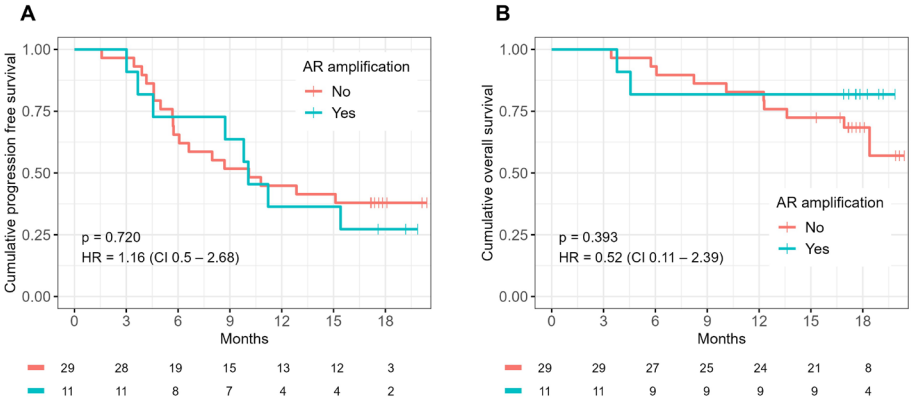

Supplementary Figure 5.3: *AR* gene amplification status on PFS (A) and OS (B) in the therapy agnostic cohort. Survival statistics: HR, hazard ratio; CI, 95% confidence interval; p, *p*-value.

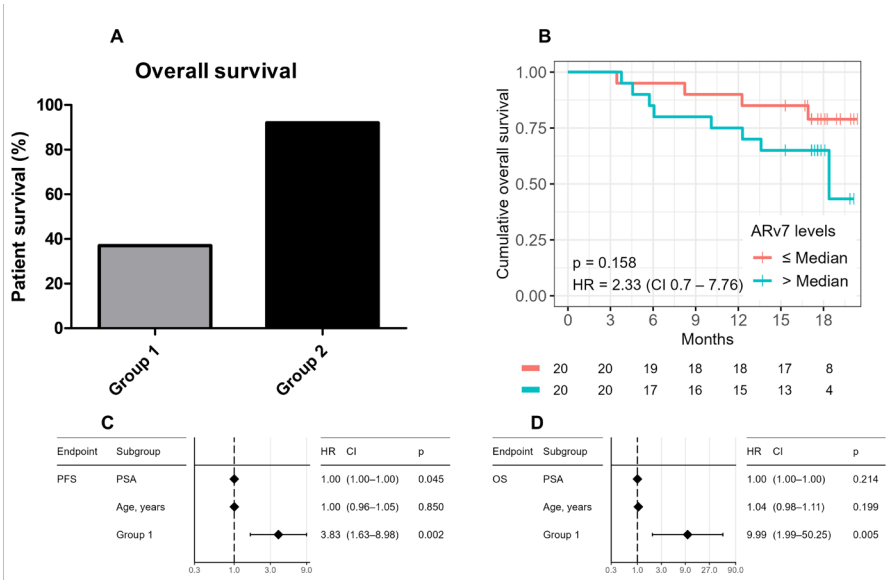

Supplementary Figure 5.4: *AR* gene amplification status on PFS (A) and OS (B) in the therapy agnostic cohort. Survival statistics: HR, hazard ratio; CI, 95% confidence interval; p, *p*-value.

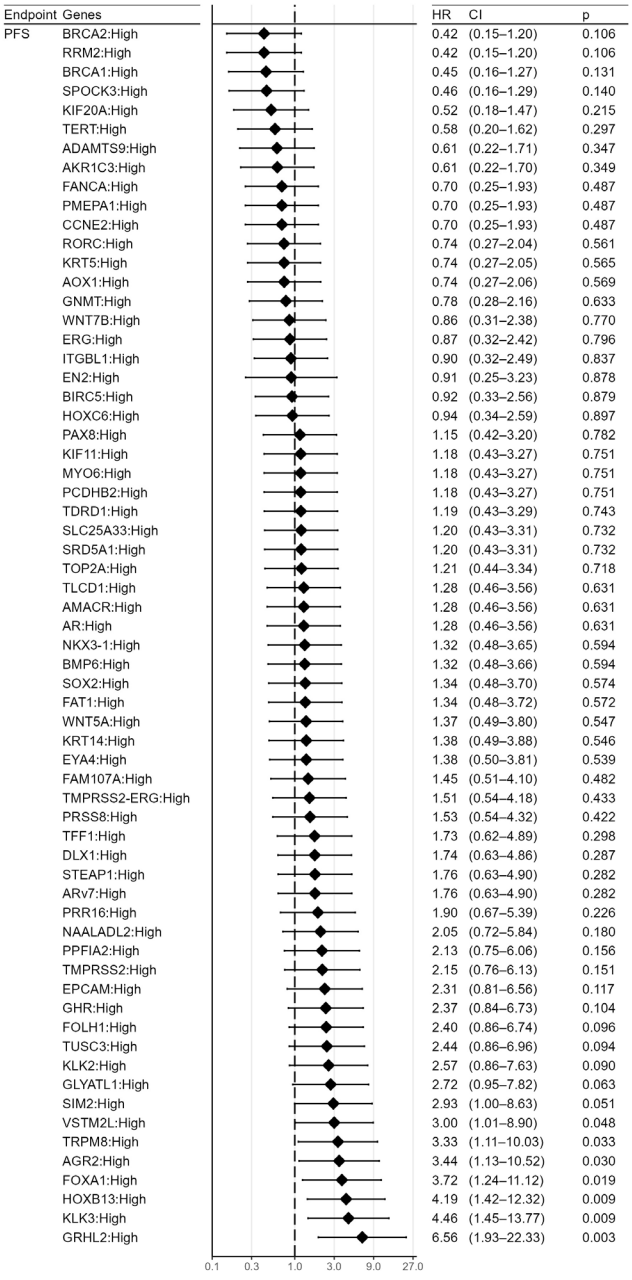

Supplementary Figure 5.5: The prognostic value of genes from the complete gene panel on PFS in the ARSI cohort. A multivariate model was used to determine risk for progression (HR), 95% confidence intervals, and statistical significance (p). Survival statistics: HR: Hazard ratio, CI: Confidence interval, p: *p*-value.

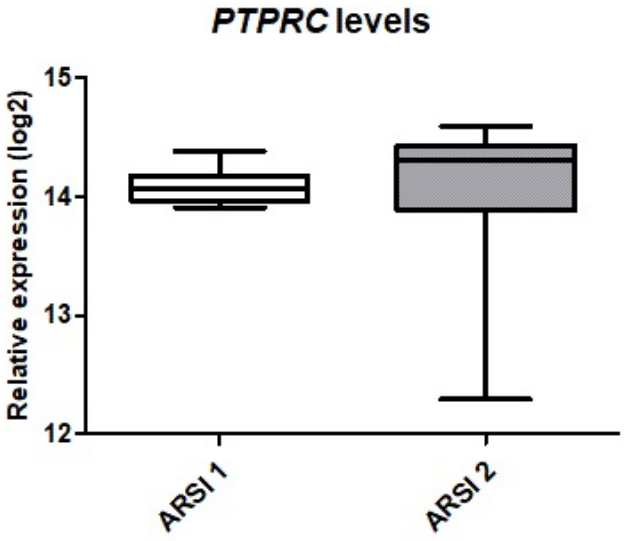

Supplementary Figure 5.6: *PTPRC* levels in ARSI 1 (n=6) and ARSI 2 (n=16) patients. Patients were grouped via unsupervised hierarchical clustering using the ARSI gene panel (Figure 5.7A).

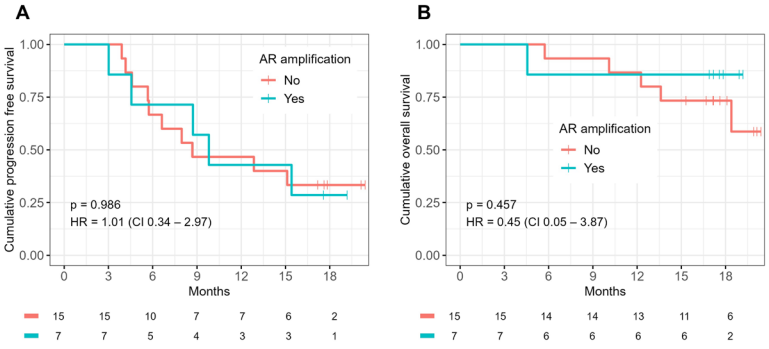

Supplementary Figure 5.7: *AR* gene amplification status on PFS (A) and OS (B) in the ARSI cohort. Survival statistics: HR, hazard ratio; CI, 95% confidence interval; p, p-value.

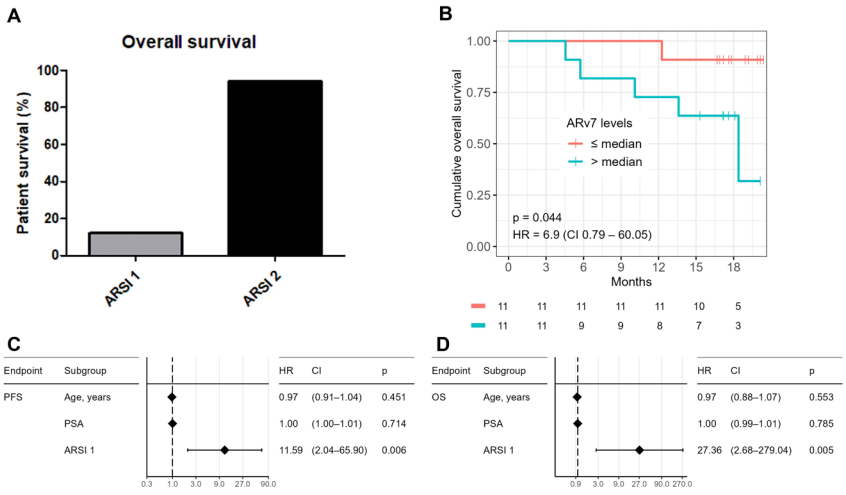

Supplementary Figure 5.8: Survival of ARSI 1 (n=6) and ARSI 2 (n=16) patients in the ARSI cohort at last follow-up (A). The independent prognostic value of *ARv7* levels on OS in the ARSI cohort (B). Multivariate analysis on PFS (C) and OS (D) including variables: PSA, age, and the ARSI 1 profile in the ARSI cohort. Survival statistics: HR, hazard ratio; CI, 95% confidence interval; p, p-value.

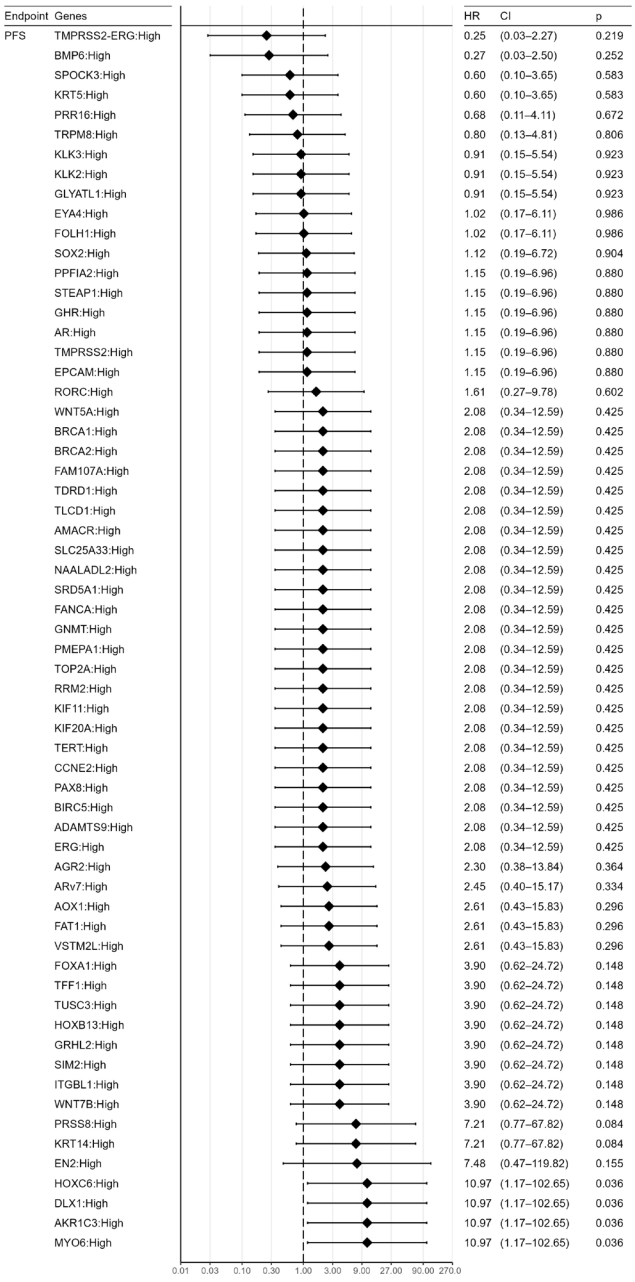

Supplementary Figure 5.9: The prognostic value of genes from the complete gene panel on PFS in the chemotherapy cohort. A multivariate model was used to determine risk for progression (HR), 95% confidence intervals, and statistical significance (p). Survival statistics: HR: Hazard ratio, CI: Confidence interval, p: *p*-value.

5.6 Supplementary Tables

Supplementary Table 5.1: Baseline blood parameters of Group 1 and Group 2 patients.

Characteristic, mean (range)	Group 1	Group 2
Lymphocytes (10^9/L)	1.3 (0.6-2.2)	1.5 (0.7-2.6)
Leukocytes (10^9/L)	6.7 (3-11.5)	9.2 (5-11.5)
Neutrophils (10^9/L)	4.7 (2.1-9.6)	4.4 (2.5-9.6)
Thrombocytes (10^9/L)	234.6 (116-359)	250 (119-359)
Alkaline phosphatase (U/L)	334.5 (67-1866)	103.6 (54-229)
Hb (mmol/L)	8.0 (6.6-9.4)	8.3 (6.7-9.2)
LD (U/L)	283.5 (123-663)	202.2 (111-663)
PSA μg/L	215.8 (3.6-1600)	40.8 (1.2-130)
Testosterone nmol/L	<0.4	<0.4 (0.4-0.7)

Supplementary Table 5.2: Baseline blood parameters of ARSI 1 and ARSI 2 patients.

Characteristic, mean (range)	ARSI 1	ARSI 2
Lymphocytes (10^9/L)	1.3 (0.6-2)	1.8 (0.9-3.1)
Leukocytes (10^9/L)	7 (4.9-9.5)	10.3 (4.8-68)
Neutrophils (10^9/L)	4.9 (2.7-8.1)	4 (2.5-6.1)
Thrombocytes (10^9/L)	251.7 (186-323)	257.2 (190-418)
Alkaline phosphatase (U/L)	255.3 (79-701)	99.9 (54-229)
Hb (mmol/L)	8.2 (7.3-9.4)	8.3 (6.7-9.2)
LD (U/L)	254.5 (188-317)	188.9 (111-257)
PSA μg/L	130.1 (6.7-470)	39.8 (1.2-180)
Testosterone nmol/L	0.<4	<0.4

Supplementary Table 5.3: Baseline alkaline phosphatase and PSA per therapy.

Cohort	Alkaline phosphatase (U/L)	PSA (μg/L)
Therapy agnostic, mean (range)	195.9 (54-1866)	110.8 (1.2-1600)
ARSI, mean (range)	142.3 (54-701)	64.4 (1.2-470)
Chemotherapy, mean (range)	208.1 (54-1016)	81.5 (4.8-450)
Immuno, mean (range)	120 (103-137)	82 (44-120)
Radioligand	110.3 (82-178)	81 (39-160)
PARPi, mean (range)	99 (94-104)	120 (110-130)
Active surveillance	715.7 (63-1866)	557.3 (24-1600)

Supplementary Table 5.4: Healthy volunteer demographics.

Characteristic	Statistics
Num. of samples	29
Age, median (range)	50 (22–71)
Sex, Num. (%)	
Male	19 (66%)
Female	10 (34%)
Men aged $>$ 50, Num. (%)	9 (47%)
Men aged $<$ 50, Num. (%)	10 (53%)

Supplementary Table 5.5: TSO500 PCa gene panel.

AKT1	*AKT2*	*AKT3*	*AR*
ATM	*ATR*	*BARD1*	*BRAF*
BRCA1	*BRCA2*	*BRIP1*	*CCND1*
CDK12	*CDK4*	*CDK6*	*CDKN2A*
CHEK1	*CHEK2*	*ERCC2*	*FANCL*
MAP2K1	*MAP2K2*	*MAP2K4*	*MAP3K1*
MLH1	*MSH2*	*MSH6*	*NBN*
PALB2	*PIK3CA*	*PIK3CB*	*PIK3R1*
PMS2	*POLE*	*PPP2R2A*	*PTEN*
RAD51B	*RAD51C*	*RAD51D*	*RAD54L*
RAF1	*RB1*	*SPOP*	*TP53*

References

1. Bister, K. Discovery of oncogenes: The advent of molecular cancer research. *Proceedings of the National Academy of Sciences of the United States of America* 112, 15259–15260 (Dec. 15, 2015).
2. Peyraud, F. & Italiano, A. Combined parp inhibition and immune checkpoint therapy in solid tumors. *Cancers* 12, 1–28 (June 1, 2020).
3. Teyssonneau, D. *et al.* Prostate cancer and PARP inhibitors: progress and challenges. *Journal of Hematology and Oncology* 14 (Dec. 1, 2021).
4. Gilson, P., Merlin, J. L. & Harlé, A. Deciphering Tumour Heterogeneity: From Tissue to Liquid Biopsy. *Cancers* 14 (Mar. 1, 2022).
5. Frangioni, J. V. New technologies for human cancer imaging. *Journal of Clinical Oncology* 26, 4012–4021 (2008).
6. Braun, S. *et al.* A Pooled Analysis of Bone Marrow Micrometastasis in Breast Cancer. *New England Journal of Medicine* 353, 793–802 (Aug. 25, 2005).
7. Riethdorf, S., O'Flaherty, L., Hille, C. & Pantel, K. Clinical applications of the CellSearch platform in cancer patients. *Advanced Drug Delivery Reviews* 125, 102–121 (Feb. 1, 2018).
8. Lambros, M. B. *et al.* Single-cell analyses of prostate cancer liquid biopsies acquired by apheresis. *Clinical Cancer Research* 24, 5635–5644 (Nov. 15, 2018).
9. Rushton, A. J., Nteliopoulos, G., Shaw, J. A. & Coombes, R. C. A review of circulating tumour cell enrichment technologies. *Cancers* 13, 1–33 (Mar. 1, 2021).
10. Casanova-Salas, I. *et al.* Quantitative and Qualitative Analysis of Blood-based Liquid Biopsies to Inform Clinical Decision-making in Prostate Cancer. *European Urology* 79, 762–771 (June 1, 2021).
11. Li, H. *et al.* Androgen Receptor Splice Variant 7 Predicts Shorter Response in Patients with Metastatic Hormone-sensitive Prostate Cancer Receiving Androgen Deprivation Therapy. *European Urology* 79, 879–886 (June 1, 2021).

12. Sorrentino, C. & Di Carlo, E. Molecular Targeted Therapies in Metastatic Prostate Cancer: Recent Advances and Future Challenges. *Cancers* 15. Number: 11, 2885 (Jan. 2023).
13. Pereira-Veiga, T. *et al.* Longitudinal CTCs gene expression analysis on metastatic castration-resistant prostate cancer patients treated with docetaxel reveals new potential prognosis markers. *Clinical and Experimental Metastasis* 38, 239–251 (Apr. 1, 2021).
14. Miller, M. C., Robinson, P. S., Wagner, C. & O'Shannessy, D. J. The Parsortix™ Cell Separation System—A versatile liquid biopsy platform. *Cytometry Part A* 93, 1234–1239 (Dec. 1, 2018).
15. ENGLERT DAVID FREDERICK & SETO KELLY KAI YIN *US Patent* 2021/0230670 A1 (US) (2021).
16. Englert, D. *et al.* Multiplex gene expression using the HyCEAD assay in CTCs isolated with the Parsortix™ system. 79 (2019).
17. Farhang Ghahremani, M. *et al.* Novel method for highly multiplexed gene expression profiling of circulating tumor cells (CTCs) captured from the blood of women with metastatic breast cancer. *Journal of Translational Medicine* 21, 414 (June 26, 2023).
18. Moore, R. G. *et al.* Malignancy assessment using gene identification in captured cells algorithm for the prediction of malignancy in women with a pelvic mass. *Obstetrics and gynecology (New York. 1953. Online)/Obstetrics and gynecology* 140, 631–642 (Sept. 2022).
19. Podolak, J. *et al.* Androgen receptor amplification is concordant between circulating tumor cells and biopsies from men undergoing treatment for metastatic castration resistant prostate cancer. *Oncotarget; Vol 8, No 42* (2017).
20. Barnett, E. *et al.* Prevalence and tissue concordance of BRCA2 copy number loss evaluated by single-cell, shallow whole genome sequencing of circulating tumor cells (CTCs) in castration-resistant prostate cancer (CRPC). *Journal of Clinical Oncology* 38, 5531–5531 (May 20, 2020).

21. Franken, A. *et al.* Comparative analysis of EpCAM high-expressing and low-expressing circulating tumour cells with regard to their clonal relationship and clinical value. *British Journal of Cancer* (2023).
22. Di Donato, M. *et al.* Therapeutic potential of TRPM8 antagonists in prostate cancer. *Scientific Reports* 11, 23232 (2021).
23. Ouderkirk, J. L. & Krendel, M. Non-muscle myosins in tumor progression, cancer cell invasion, and metastasis. *Cytoskeleton* 71, 447–463 (Aug. 1, 2014).
24. Sperger, J. M. *et al.* Prospective Evaluation of Clinical Outcomes Using a Multiplex Liquid Biopsy Targeting Diverse Resistance Mechanisms in Metastatic Prostate Cancer. *Journal of Clinical Oncology* 39, 2926–2937 (Sept. 10, 2021).
25. Wang, Z. *et al.* The characteristics of androgen receptor splice variant 7 in the treatment of hormonal sensitive prostate cancer: A systematic review and meta-analysis. *Cancer Cell International* 20 (May 6, 2020).
26. Dahiya, V. & Bagchi, G. Non-canonical androgen signaling pathways and implications in prostate cancer. *Biochimica et Biophysica Acta - Molecular Cell Research* 1869 (Dec. 1, 2022).
27. Lassche, G. *et al.* Predictive and prognostic biomarker identification in a large cohort of androgen receptor-positive salivary duct carcinoma patients scheduled for combined androgen blockade. *Cancers* 13 (July 2, 2021).
28. Enna, S. J. & Bylund, D. B. Dihydrotestosterone. *xPharm: The Comprehensive Pharmacology Reference.* ISBN: 9780080552323, 1–2 (2007).
29. He, Y. *et al.* A noncanonical AR addiction drives enzalutamide resistance in prostate cancer. *Nature Communications* 12 (Dec. 1, 2021).
30. Tien, A. H. & Sadar, M. D. Keys to unlock androgen receptor translocation. *Journal of Biological Chemistry* 294, 8711–8712 (May 31, 2019).
31. Jamroze, A., Chatta, G. & Tang, D. G. Androgen receptor (AR) heterogeneity in prostate cancer and therapy resistance. *Cancer Letters* 518, 1–9 (Oct. 10, 2021).

32. Matuszczak, M., Schalken, J. A. & Salagierski, M. Prostate cancer liquid biopsy biomarkers' clinical utility in diagnosis and prognosis. *Cancers* 13 (July 1, 2021).
33. Hamid, A. R. A. *et al.* The role of HOXC6 in prostate cancer development. *Prostate* 75, 1868–1876 (Dec. 1, 2015).
34. Luo, Z. & Farnham, P. J. Genome-wide analysis of HOXC4 and HOXC6 regulated genes and binding sites in prostate cancer cells. *PLoS ONE* 15 (Feb. 1, 2020).
35. Goel, S. *et al.* Transcriptional network involving ERG and AR orchestrates Distal-less homeobox-1 mediated prostate cancer progression. *Nature Communications* 12, 5325 (Sept. 7, 2021).
36. Leyten, G. H. *et al.* Identification of a candidate gene panel for the early diagnosis of prostate cancer. *Clinical Cancer Research* 21, 3061–3070 (July 1, 2015).
37. Wang, B. *et al.* AKR1C3, a crucial androgenic enzyme in prostate cancer, promotes epithelial-mesenchymal transition and metastasis through activating ERK signaling. *Urologic Oncology: Seminars and Original Investigations* 36, 472.e11–472.e20 (Oct. 1, 2018).
38. Zhou, C. *et al.* Aldo-keto reductase 1c3 mediates chemotherapy resistance in esophageal adenocarcinoma via ros detoxification. *Cancers* 13 (May 2, 2021).
39. Majewski, Ł., Sobczak, M., Wasik, A., Skowronek, K. & Rędowicz, M. J. Myosin VI in PC12 cells plays important roles in cell migration and proliferation but not in catecholamine secretion. *Journal of Muscle Research and Cell Motility* 32, 291–302 (2011).
40. Wang, D. *et al.* MYO6 knockdown inhibits the growth and induces the apoptosis of prostate cancer cells by decreasing the phosphorylation of ERK1/2 and PRAS40. *Oncology Reports* 36, 1285–1292 (Sept. 1, 2016).
41. Dunn, T. A. *et al.* A novel role of myosin VI in human prostate cancer. *American Journal of Pathology* 169, 1843–1854 (2006).

42. Asim, M. *et al.* Synthetic lethality between androgen receptor signalling and the PARP pathway in prostate cancer. *Nature Communications* 8 (Dec. 1, 2017).
43. Nizialek, E., Haffner, M., Bhamidipati, A. & Yegnasubramanian, S. The effect of PARP inhibition on androgen receptor localization and activity in castration resistant prostate cancer. *Journal of Clinical Oncology* 40, e17037–e17037 (June 1, 2022).
44. Congregado, B., Rivero, I., Osmán, I., Sáez, C. & López, R. M. PARP Inhibitors: A New Horizon for Patients with Prostate Cancer. *Biomedicines* 10 (June 1, 2022).
45. Ehsani, M., David, F. O. & Baniahmad, A. Androgen receptor-dependent mechanisms mediating drug resistance in prostate cancer. *Cancers* 13 (Apr. 1, 2021).
46. Au, S. H. *et al.* Clusters of circulating tumor cells: A biophysical and technological perspective. *Current Opinion in Biomedical Engineering* 3, 13–19 (Sept. 1, 2017).
47. Castro-Giner, F. & Aceto, N. Tracking cancer progression: From circulating tumor cells to metastasis. *Genome Medicine* 12 (Mar. 19, 2020).
48. Bilandzic, M. *et al.* Keratin-14 (KRT14) positive leader cells mediate mesothelial clearance and invasion by ovarian cancer cells. *Cancers* 11 (Sept. 1, 2019).
49. Simper, N. B. *et al.* Basal cell carcinoma of the prostate is an aggressive tumor with frequent loss of PTEN expression and overexpression of EGFR. *Human Pathology* 46, 805–812 (June 1, 2015).
50. Fels, B., Bulk, E., Pethő, Z. & Schwab, A. The role of TRP channels in the metastatic cascade. *Pharmaceuticals* 11 (June 1, 2018).
51. Zhan, X. J., Wang, R., Kuang, X. R., Zhou, J. Y. & Hu, X. L. Elevated expression of myosin VI contributes to breast cancer progression via MAPK/ERK signaling pathway. *Cellular Signalling* 106 (June 1, 2023).

52. Cerami, E. *et al.* The cBio Cancer Genomics Portal: An open platform for exploring multidimensional cancer genomics data. *Cancer Discovery* 2, 401–404 (May 2012).
53. Gao, J. *et al.* Integrative analysis of complex cancer genomics and clinical profiles using the cBioPortal. *Science Signaling* 6 (Apr. 2, 2013).
54. Quinn, M. C. *et al.* The chemiluminescence based Ziplex® automated workstation focus array reproduces ovarian cancer Affymetrix GeneChip® expression profiles. *Journal of Translational Medicine* 7 (July 6, 2009).
55. Wickham, H. *et al.* Welcome to the Tidyverse. *Journal of Open Source Software* 4, 1686 (Nov. 21, 2019).
56. Patil, I. Visualizations with statistical details: The 'ggstatsplot' approach. *Journal of Open Source Software* 6, 3167 (May 25, 2021).

Chapter 6

Discussion

6.1 Liquid Biopsies in Advanced PCa

6.1.1 Minimal Intervention, Maximum Impact

Between 2014 and 2019, the incidence of prostate cancer (PCa) increased by 3% annually [1]. As the baby boomer generation enters retirement, the growing burden of chronic disease will strain national healthcare systems, particularly in developing countries, underscoring the need for novel, cost-effective diagnostic, prognostic, and personalized protocols [2]. In urology, prostate-specific antigen (PSA) testing and Gleason grading remain foundational [3], but both have well-recognized limitations. The clinical application of biomarkers, in general, is guided by clinical insights from randomized controlled trials (RCTs). Although RCTs are designed to generate the strongest evidence for efficacy at the population level, they primarily estimate average treatment effects [4]. RCTs therefore offer little guidance for individual decision-making in biologically heterogeneous diseases such as PCa [5]. This limitation becomes especially important when multiple treatments are known to improve outcomes (e.g., androgen deprivation therapy (ADT), next-generation androgen receptor signaling inhibitors (ARSIs)), yet robust predictive biomarkers for selecting optimal treatment approaches are lacking. For example, population-wide PSA screening in the 1990s and early 2000s reduced the incidence of metastatic PCa at diagnosis but also produced substantial overdiagnosis and overtreatment of indolent tumors [6]. Extrapolating population-averaged PSA thresholds to individual patients is akin to using body mass index (BMI) to diagnose obesity: both are useful correlates but lack sensitivity to discriminate between a true positive (cancer/obesity) and a false one (benign prostatic hyperplasia (BPH)/muscular person). Gleason grade groups are established from similar population-derived evidence and, in the hands of even the best pathologist, are vulnerable to sampling error and misclassification, leading to potential false-negative diagnoses [7]. Diagnostic imaging is an example of a diagnostic approach that attempts to incorporate patient-level data [8]. This is reflected in the high sensitivity of

magnetic resonance imaging (MRI) and prostate-specific membrane antigen positron emission tomography/computed tomography (PSMA PET/CT) for lesion detection [9]. Although highly sensitive, diagnostic imaging lacks specificity to discriminate clinically relevant lesions from irrelevant "incidentalomas" [10].

Incorporating additional patient-level data is critical to the performance of any biomarker. PSA-based screening can be an effective approach for identifying early-stage PCa, but the United States Preventive Services Task Force (USPSTF) recommendation against its use reflects, in part, the limited utility of PSA as a standalone diagnostic test [11]. By contrast, PSA velocity (i.e., the rate of change in PSA concentration over time) provides valuable prognostic insight in castration-resistant disease [12]. It may be worth considering whether analogous trajectory-based measures (e.g., BMI velocity) could improve prediction of aggressive obesity.

What PSA velocity achieves with regard to the prognostic value of PSA as a clinical indicator of cancer is that it anchors measurements to a personalized baseline [12]. This small difference in how we sample and interpret PSA changes can transform its value from a biomarker with low sensitivity into a remarkably effective prognostic instrument. Transcriptomics, or the study of gene expression, aims to take this step further by grounding evidence that links biological phenomena (e.g., high PSA) to changes in gene expression (e.g., *KLK3*) in an undifferentiated prostate epithelial cell. Liquid biopsies enable high-throughput collection of patient-level biomolecular data. Whereas tissue biopsies sample small and potentially unrepresentative regions of a tumor, liquid biopsies capture tumor-derived material in the bloodstream, offering a broader view of tumor biology. By interrogating circulating biomarkers, they provide a minimally invasive, high-throughput approach for monitoring disease progression. Circulating biomarkers are typically present as "free" molecules or are encapsulated within exosomes or circulating tumor cells (CTCs), as described in Chapter 2. By enabling molecular characterization of CTCs, they support the study of metastatic

dissemination and the identification of candidate therapeutic targets [13]. Liquid biopsies therefore represent a promising strategy for characterizing PCa and for detecting emerging therapy resistance, as demonstrated in Chapter 5. Liquid biopsies do come with their own sampling bias, as discussed in Chapter 2. However, with liquid sampling the bias becomes a known (and adjustable) variable, whereas in solid biopsies sampling bias is largely uncontrolled because it depends on operator handling. Although better equipped to handle sampling bias, the low abundance of circulating biomarkers compared to solid-tissue biomarkers poses a significant technical challenge. In addition, inter-patient biological variation can affect the quantity and integrity of circulating biomarkers. For example, release of tumor-derived material (e.g., circulating tumor DNA (ctDNA)) depends strongly on proliferation and cell-death rates, biasing detection toward more rapidly turning over tumors. Among Tier 1 cancers, PCa typically exhibits a comparatively low tumor mutational burden (TMB; median 3.6 mutations/Mb), whereas skin and lung cancers show higher medians (47.3 and 12.2 mutations/Mb, respectively) [14]. Despite this, PCa is heterogeneous at both histological and molecular levels, likely reflecting dysregulated transcriptional programs. Taken together, RNA-based biomarkers may be better suited to map disease drivers and uncover druggable targets in PCa than genomic biomarkers, particularly with regard to liquid biopsies.

This thesis describes a novel approach to PCa subtyping based on circulating transcriptomic biomarkers [15]. This minimally invasive strategy enables longitudinal monitoring of tumor dynamics and can facilitate earlier detection of therapy resistance and disease progression, advancing personalized care. Profiling circulating RNA species derived from CTCs and tumor-associated extracellular vesicles (e.g., exosomes) provides near real-time insight into oncogenic programs linked to resistance and progression. By tracking patient-specific expression signatures over time, liquid-biopsy transcriptomics can support timely treatment adaptation by identifying early molecular indicators of resistance.

6.1.2 Needle in a Haystack

A primary aim of this thesis was to assess whether molecular characterization of CTCs can stratify therapy response and prognosticate clinical outcomes in castration-resistant prostate cancer (CRPC). Achieving this requires three steps: enrichment, isolation, and molecular characterization. Among these, enrichment of tumor content is required to satisfy signal-to-background thresholds for molecular assessment of tumor biology. For example, a standard 7.5 mL blood sample used for CTC enumeration contains approximately 40 billion blood cells but may only contain a dozen CTCs in patients with metastatic disease [16, 17]. Thus, prior to enrichment, the expected signal-to-background ratio in advanced PCa is:

$$\text{CTC concentration before enrichment} = \frac{0.3266\ CTC}{1\ billion\ blood\ cells}$$

Molecular profiling by sequencing, microarray, or hybridization typically requires up-front enrichment to achieve tumor fractions on the order of one CTC per 100,000 blood cells [18]. A widely used strategy is positive selection, in which ferrofluid-coated antibodies bind epithelial cell adhesion molecule (EpCAM) to capture CTCs [16, 19–21]. First commercialized by CellSearch in 2005, this approach helped catalyze the development of higher-resolution CTC platforms [22, 23]. Current systems span (i) positive selection, (ii) negative selection, which enriches CTCs by depleting blood cells, and (iii) label-free methods that exploit physical differences between tumor and blood cells [16, 24, 25].

Regardless of the approach, enrichment criteria can introduce selection bias, a concern in metastatic disease, where phenotypic heterogeneity and epithelial–mesenchymal programs may reduce EpCAM expression and limit recovery by EpCAM-based capture. Accordingly, while positive selection remains widely used, it preferentially recovers EpCAM-positive CTCs and can undersample phenotypes that have attenuated epithelial markers. This matters

because the clinical question is often about "state," not merely "presence." Under treatment pressure (e.g., ADT and ARSIs), resistant disease may be represented by rare subpopulations with altered differentiation programs, stress responses, or lineage plasticity that are precisely the cells most likely to evade EpCAM-based capture.

Accordingly, while positive selection remains widely used, negative selection and label-free approaches can mitigate this bias. One example is the Parsortix PC1 system, which uses a microfluidic chamber for size-based cell separation enabling both CTC enumeration and downstream molecular characterization [15, 25]. However, label-free enrichment also encodes assumptions (e.g., size, deformability), and no single platform can be assumed to recover an unbiased representation of the full metastatic compartment. In practice, platform choice becomes part of the biomarker definition.

6.1.3 Recognizing Metastasis Before It's Too Late

Most epithelial cancers behave as chronic diseases, in other words, they are "slow" causes of death. A primary tumor becomes life-threatening only when its burden compromises essential organ function. Unless cancer arises in anatomically constrained, high-value tissues such as, brain or hematologic cancers, it typically must acquire the capacity to metastasize to distant organs to become lethal [26]. As such, PCa mortality typically reflects a prolonged course of metastatic dissemination. Reducing PCa-related deaths therefore requires mechanistic insight into the processes that enable metastasis. This is also why biomarkers in advanced disease must do more than detect cancer: they must track evolving tumor composition and function under therapy.

Recent advances in CTC enrichment methods and high-throughput assays now enable integrated interrogation of metastatic biology across multiple omic layers. Genomics and transcriptomics, in principle, offer complementary perspectives on the same process. Genomics captures relatively stable alterations that steer tumor biology, while transcriptomics reveals the underlying

dynamic signaling programs and cellular states that constitute tumor biology. Transcriptomics, therefore, enables real-time assessment of the evolutionary selection pressures imposed by the tumor microenvironment and systemic therapy.

Historically, oncology has prioritized genomics, an approach that has yielded effective targeted therapies (e.g., PARP inhibition in tumors with DNA damage–repair defects), but genomic biomarkers have been less informative in cancers with low TMB, such as PCa. In PCa, the clinical utility of genomics often lies less in mutational burden and more in identifying specific liabilities (e.g., DNA repair defects) and structural alterations that drive tumor evolution. At the same time, a key limitation of genomic profiling is that the presence of an alteration does not guarantee it is an active driver of disease progression at the time of measurement. A tumor can carry an alteration consistent with AR dependence (e.g., AR amplification), while its transcriptional program suggest functional escape through partial AR bypass (e.g., GR pathway activation), lineage plasticity (e.g., epithelial–mesenchymal transition (EMT)), or activation of compensatory survival pathways (e.g., phosphatidylinositol 3-kinase/protein kinase B/mechanistic target of rapamycin (PI3K/AKT/mTOR) pathway activation).

Transcriptomics (gene-expression profiling) complements genomics by capturing oncogenic signaling programs linked to metastasis and therapy resistance in PCa [27, 28]. Because transcriptional states are cell-type and context specific, RNA profiles provide sensitive biomarkers for prognosis, including real-time assessment of tumor aggressiveness and treatment response. This is particularly relevant in the setting of ARSIs, where resistance can arise through changes in AR pathway output that are better reflected at the RNA level than by single genomic events. The key tradeoff is that RNA is less stable and more sensitive to sampling, and cellular admixture, making standardization and clinical translation more challenging.

Integrating transcriptome profiling with CTC enrichment can therefore

better tackle heterogeneity in metastatic castration-resistant prostate cancer (mCRPC), support personalized therapy, and improve prediction of clinical outcomes [27, 29]. As such, CTC transcriptomics should not be seen as an alternative to traditional genomics but as a novel strategy for longitudinal assessment of tumor biology. At the same time, researchers must acknowledge that the enrichment of circulating biomarkers itself can shape how this biology is perceived.

6.1.4 Long Non-Coding Yet Highly Specific RNA

Improving clinical outcomes for patients with advanced PCa requires an accurate understanding of the molecular mechanisms driving progression [28, 30]. Long non-coding RNAs (lncRNAs) have emerged as key players in cancer biology and have the potential to act as biomarkers to predict clinical outcomes and stratify therapy response in PCa [30]. Compared to the coding genome, the non-coding genome is not well characterized and therefore represents a largely untapped source of potential biomarkers. Importantly, non-coding biology can be interrogated through both a genomic lens by identifying regulatory and structural alterations in noncoding regions, and a transcriptomic lens by directly measuring noncoding RNA output as a readout of cell state.

The expression of non-coding RNAs, particularly lncRNAs, is highly specific to the cell type and molecular context, making them ideal for use as circulating biomarkers in clinical settings. This specificity is a practical advantage in liquid biopsy contexts, where tumor-derived signal must be distinguished from a large background of normal blood-cell RNA. With the advancement of omics technologies, the accessibility of high-throughput sequencing assays has led to the discovery of many novel PCa-associated lncRNAs such as *SCHLAP1* and *MALAT1*. Due to their transcript lengths ($\geq$200 nucleotides), lncRNAs are capable of folding into complex tertiary structures that allow molecular interactions with DNA, RNA, and proteins. Subsequently, lncRNAs can regulate gene expression at various levels that impact critical cellular processes

such as proliferation, apoptosis, migration, and metastasis [31]. From a biomarker perspective, lncRNAs occupy an attractive middle ground as they can be highly tissue- and context-specific (supporting discrimination) while also reflect pathway activity and cellular state (supporting dynamic monitoring). These reasons also drove my interest in the utility of lncRNAs to study resistance biology and identify novel biomarkers in CRPC, eventually leading to the discovery of *NAALADL2-AS2* as a novel PCa-associated lncRNA.

NAALADL2-AS2 is located in region 26 of the long arm of chromosome 3 (3q26) [30]. Copy number gains in the 3q26 amplicon have been identified in 20% of human tumors [32]. In CRPC, amplifications of *NAALADL2* and *TBL1XR1* in the 3q26.31-32 genetic locus have been associated with aggressiveness [33]. Furthermore, a germline single nucleotide polymorphism (SNP) within the *NAALADL2* genetic locus is associated with aggressive and high-grade localized PCa [32]. In recurrent PCa, copy number gains of *TBL1XR1* have been reported in two out of seven patients [34]. These findings highlight the extensive genetic instability in the 3q26 region and could be potential drivers of *NAALADL2-AS2* upregulation in androgen-sensitive PCa.

While these genomic observations provide a plausible structural context for dysregulation at 3q26, the key contribution of *NAALADL2-AS2* in this thesis is not simply that it is altered, but that its expression captures a biologically and clinically meaningful epithelial state. In Chapter 4, *NAALADL2-AS2* expression was shown to be enriched in The Cancer Genome Atlas (TCGA)-iCluster 2 and to align with a luminal S transcriptional program. This association was supported by its positive correlation with luminal S and AR-associated genes [30]. These results underscore a broader point about transcriptomics in PCa: gene expression readouts can resolve subtype identity and pathway activity that are not fully captured by genomic subclassification alone, even when genomic subtypes provide important etiologic anchors (e.g., *TMPRSS2-ERG*/*SPOP* status).

The subtype specificity of *NAALADL2-AS2* also clarifies why its biomarker performance differs across disease contexts. In localized epithelial PCa, high *NAALADL2-AS2* expression was associated with early progression risk within luminal S tumors, consistent with a role in identifying a higher-risk state inside an otherwise androgen-responsive compartment. By contrast, in CRPC, exploratory trial data suggested that circulating *NAALADL2-AS2* did not behave as a robust adverse prognostic marker and may even associate with more favorable outcomes [35, 36]. This divergence is likely a function of stage-dependent biology where disease progression under therapeutic selection pressures can diminish the relative abundance of luminal AR-active epithelial states while alternative phenotypes become more prevalent. In this setting, circulating *NAALADL2-AS2* may no longer track tumor aggressiveness but instead reflect the proportion of tumor burden that remains within a luminal S transcriptional program. In other words, *NAALADL2-AS2* may function as a marker of epithelial state, and the prognostic interpretation of such a marker depends on which state dominates the disease at the time of measurement.

This state-dependence illustrates both the promise and limitation of transcriptomic biomarkers in advanced PCa. The promise is that transcriptomics can report on pathway output and phenotype in real time, which is central to understanding therapy resistance. The limitation is that RNA-based biomarkers are inherently context-specific and are influenced by what biological compartments are sampled and shed into circulation. These considerations motivate longitudinal transcriptomic monitoring in liquid-biopsy settings, particularly through CTC-based assays, where intact tumor cells can be profiled to interrogate transcriptional programs linked to progression and resistance.

References

1. Siegel, R. L., Miller, K. D., Fuchs, H. E. & Jemal, A. Cancer statistics, 2022. *CA: A Cancer Journal for Clinicians* 72, 7–33 (Jan. 2022).
2. Groen, L. & Schalken, J. Liquid Biopsy for Prostate and Bladder Cancer: Progress and Pitfalls. *European Urology Focus* 8, 904–906 (July 2022).
3. Shah, R. B. & Zhou, M. Recent advances in prostate cancer pathology: Gleason grading and beyond. *Pathology International* 66, 260–272 (May 2016).
4. Braga, L. H. *et al.* Randomized controlled trials – The what, when, how and why. *Journal of Pediatric Urology* 21, 397–404 (Apr. 1, 2025).
5. Efstathiou Eleni, C. L. Prostate Cancer Therapy in Evolution: Time to Rethink and Redirect? *The ASCO Post* (June 25, 2018).
6. Bangma, C. H., Roemeling, S. & Schröder, F. H. Overdiagnosis and overtreatment of early detected prostate cancer. *World Journal of Urology* 25, 3–9 (Mar. 2007).
7. Quintana, L. *et al.* Gleason Misclassification Rate Is Independent of Number of Biopsy Cores in Systematic Biopsy. *Urology* 91, 143–149 (May 2016).
8. Doan, L. M. T. *et al.* Bridging modalities with AI: a review of AI advances in multimodal biomedical imaging. *Communications Engineering* 5, 30 (Feb. 13, 2026).
9. Sitharthan, D. *et al.* The Sensitivity and Specificity of Multiparametric Magnetic Resonance Imaging and Prostate-Specific Membrane Antigen Positron Emission Tomography/Computed Tomography for Predicting Seminal Vesicle Invasion in Clinically Significant Prostate Cancer: A Multicenter Retrospective Study. *Journal of Clinical Medicine* 13, 4424 (Jan. 2024).
10. Mannas, M. P., Lee, T., Pourghiasian, M., Wilson, D. C. & Black, P. C. Incidentalomas of the prostate detected by 18-fluoro-2-deoxy-D-glucose

positron emission tomography/computed tomography. *Canadian Urological Association Journal* 14, E180–E184 (May 2020).

11. A. Moyer, V. & Force*, o. b. o. t. U. S. P. S. T. Screening for Prostate Cancer: U.S. Preventive Services Task Force Recommendation Statement. *Annals of Internal Medicine* (July 17, 2012).
12. Cui, F. *et al.* Prostate-specific antigen velocity as a predictor of survival outcomes in patients with prostate cancer: a meta-analysis. *Frontiers in Oncology* 16 (Feb. 10, 2026).
13. Assi, T. *et al.* Overview of the role of liquid biopsy in cancer management. *Translational Oncology* 34, 101702 (May 31, 2023).
14. Chalmers, Z. R. *et al.* Analysis of 100,000 human cancer genomes reveals the landscape of tumor mutational burden. *Genome Medicine* 9, 34 (Apr. 19, 2017).
15. Groen, L. *et al.* Transcriptome Profiling of Circulating Tumor Cells to Predict Clinical Outcomes in Metastatic Castration-Resistant Prostate Cancer. *International Journal of Molecular Sciences* 24, 9002 (May 19, 2023).
16. Allard, W. J. *et al.* Tumor Cells Circulate in the Peripheral Blood of All Major Carcinomas but not in Healthy Subjects or Patients With Nonmalignant Diseases. *Clinical Cancer Research* 10, 6897–6904 (Oct. 22, 2004).
17. Brihi, J. E. & Pathak, S. in *StatPearls [Internet]* (StatPearls Publishing, June 8, 2024).
18. Song, Y. *et al.* Enrichment and single-cell analysis of circulating tumor cells. *Chemical Science* 8, 1736–1751 (2017).
19. Franken, A. *et al.* Comparative analysis of EpCAM high-expressing and low-expressing circulating tumour cells with regard to their clonal relationship and clinical value. *British Journal of Cancer* (2023).
20. Gradilone, A. *et al.* Circulating tumor cells and "suspicious objects" evaluated through CellSearch® in metastatic renal cell carcinoma. *Anticancer Research* 31, 4219–4221 (2011).

21. Zavridou, M. *et al.* Direct comparison of size-dependent versus EpCAM-dependent CTC enrichment at the gene expression and DNA methylation level in head and neck squamous cell carcinoma. *Scientific Reports* 10 (Dec. 1, 2020).
22. Castro-Giner, F. & Aceto, N. Tracking cancer progression: From circulating tumor cells to metastasis. *Genome Medicine* 12 (Mar. 19, 2020).
23. Aceto, N. *et al.* Circulating Tumor Cell Clusters Are Oligoclonal Precursors of Breast Cancer Metastasis. *Cell* 158, 1110–1122 (Aug. 28, 2014).
24. Chalmers, J. J., Lustberg, M., Jatana, K. R. & Zborowski, M. Emerging Technologies for CTC Detection Based on Depletion of Normal Cells. 195. ISBN: 978-3-642-28159-4, 1–13 (2012).
25. Templeman, A. *et al.* Analytical performance of the FDA-cleared Parsortix® PC1 system. *Journal of Circulating Biomarkers* 12, 26–33 (Aug. 7, 2023).
26. Fares, J., Fares, M. Y., Khachfe, H. H., Salhab, H. A. & Fares, Y. Molecular principles of metastasis: a hallmark of cancer revisited. *Signal Transduction and Targeted Therapy* 5. Number: 1, 1–17 (Mar. 12, 2020).
27. You, S. *et al.* Integrated Classification of Prostate Cancer Reveals a Novel Luminal Subtype with Poor Outcome. *Cancer Research* 76, 4948–4958 (Sept. 1, 2016).
28. Ge, Q. *et al.* Molecular classifications of prostate cancer: basis for individualized risk stratification and precision therapy. *Annals of Medicine* 55, 2279235 (2023).
29. Weiner, A. B. *et al.* A novel prostate cancer subtyping classifier based on luminal and basal phenotypes. *Cancer* 129, 2169–2178 (2023).
30. Groen, L. *et al.* The Androgen Regulated lncRNA NAALADL2-AS2 Promotes Tumor Cell Survival in Prostate Cancer. *Non-Coding RNA* 8, 81 (Dec. 1, 2022).

31. Solé, C. *et al.* The Circulating Transcriptome as a Source of Biomarkers for Melanoma. *Cancers* 11, 70 (Jan. 10, 2019).
32. Fields, A. P., Justilien, V. & Murray, N. R. The chromosome 3q26 OncCassette: A multigenic driver of human cancer. *Advances in Biological Regulation* 60, 47–63 (Jan. 2016).
33. Simpson, B. S. *et al.* Genetic alterations in the 3q26.31-32 locus confer an aggressive prostate cancer phenotype. *Communications Biology* 3 (Dec. 1, 2020).
34. Heselmeyer-Haddad, K. M. *et al.* Single-Cell Genetic Analysis Reveals Insights into Clonal Development of Prostate Cancers and Indicates Loss of PTEN as a Marker of Poor Prognosis. *The American Journal of Pathology* 184, 2671–2686 (Oct. 1, 2014).
35. Benoist, G. E. *et al.* Prognostic Value of Novel Liquid Biomarkers in Patients with Metastatic Castration-Resistant Prostate Cancer Treated with Enzalutamide: A Prospective Observational Study. *Clinical chemistry* 66, 842–851 (June 1, 2020).
36. Boerrigter, E. *et al.* RNA Biomarkers as a Response Measure for Survival in Patients with Metastatic Castration-Resistant Prostate Cancer. *Cancers* 13, 6279 (Dec. 14, 2021).

Chapter 7

Future Perspectives

7.1 The Next Paradigm Shift in PCa Management

Currently, tissue biopsies and imaging modalities, including multiparametric magnetic resonance imaging (mpMRI) and prostate-specific membrane antigen computed tomography/positron emission tomography (PSMA-CT/PET), are routinely used to monitor therapy response and disease progression in patients with prostate cancer (PCa). However, these approaches come with considerable limitations: biopsies are invasive and carry procedural risk, while advanced imaging is diagnostically robust but can be prohibitively expensive [1–3]. The integration of liquid biopsies into existing diagnostic and prognostic frameworks offers substantial advantages, particularly through repeatable sampling that enables longitudinal disease monitoring. Prostate-specific antigen (PSA) testing represents one of the earliest and most impactful implementations of a liquid biopsy in oncology. Its widespread adoption across Western countries in the 1990s coincided with a reduction in prostate cancer–specific mortality of roughly 25% [2, 4, 5], illustrating how a liquid biopsy–based diagnostic test can drive a paradigm shift in urologic practice and PCa management. Furthermore, recent advancements have demonstrated the effectiveness of urine-derived biomarkers for PCa detection and for reducing overtreatment, reinforcing the clinical utility of liquid biopsies across the disease course [6]. Despite the scientific evidence and technical availability, the clinical adoption of liquid biopsies continues to encounter significant barriers, including pre-analytical variability, assay standardization, prospective demonstration of clinical utility, and integration into reimbursement pathways and clinical guidelines.

7.2 Decoding the Oncotranscriptome

Although the development of diagnostic and prognostic tools has largely plateaued, there has been a marked expansion in novel targeted treatment options, including next-generation androgen receptor inhibitors (ARSIs), peroxisome proliferator-activated receptor (PPAR) inhibitors, immune checkpoint inhibitors, and PSMA-directed radioligand therapies. Despite these therapeutic advances, clinicians still rely primarily on PSA measurements to inform prognosis and guide treatment decisions. While PSA is sensitive, it has limited specificity and therefore does not reliably stratify therapy response, particularly in patients with CRPC [7–10]. Transcriptomic profiling of circulating biomarkers may represent the next step in this trajectory, evolving the PSA paradigm from single-analyte testing toward pathway-level, real-time characterization of tumor biology. Yet, the relative instability of RNA compared with DNA presents substantial technical hurdles [11, 12]. Molecular analysis of circulating tumor cells (CTCs) offers a practical workaround, protecting nucleic acids and other biomolecules within the cell's phospholipid membrane and thus capturing a real-time molecular snapshot of the tumor [13, 14]. In this light, the emergence of multi-omics research is a highly promising development and offers numerous opportunities for actionable clinical discoveries.

Therapeutic progress in PCa has outpaced advances in diagnostic platforms, underscoring the urgent need for more refined and dependable stratification tools to enable truly personalized care. Within this framework, a multi-omics approach that integrates data from CTCs, circulating tumor DNA (ctDNA), and tumor-derived exosomes has shown clear benefits over traditional single-marker strategies for key clinical applications, including early detection, longitudinal surveillance, and treatment selection [15]. Although standard tissue biopsies, interpreted through histopathology by expert pathologists, will remain central to clinical practice, the integration of artificial intelligence (AI) with comprehensive multi-omics datasets promises to reshape

PCa management. This integration could hasten the identification of new druggable pathways, improve the accuracy of prognostic and predictive models, and enable the continual refinement of treatment algorithms across all stages of disease [16, 17]. Transcriptomics has been aptly described as a "language" through which the body communicates its internal state [18]. From this perspective, large language models (LLMs) may be uniquely suited to "read," interpret, and systematically decode the oncotranscriptome, potentially uncovering patterns and regulatory networks that remain obscure to conventional analytical methods. Prospective validation and transparent model interpretation will be essential to translate these approaches into clinical decision-making.

References

1. Zhu, M. *et al.* Up-to-Date Imaging and Diagnostic Techniques for Prostate Cancer: A Literature Review. *Diagnostics* 13. Number: 13, 2283 (Jan. 2023).
2. Hao, S. *et al.* Cost-Effectiveness of Magnetic Resonance Imaging in Prostate Cancer Screening: A Microsimulation Study. *Value in Health* 24, 1763–1772 (Dec. 2021).
3. Messina, E. *et al.* Design of a magnetic resonance imaging-based screening program for early diagnosis of prostate cancer: preliminary results of a randomized controlled trial-Prostate Cancer Secondary Screening in Sapienza (PROSA). *European Radiology* 34, 204–213 (Jan. 2024).
4. Schröder, F. H. *et al.* Screening and prostate cancer mortality: results of the European Randomised Study of Screening for Prostate Cancer (ERSPC) at 13 years of follow-up. *The Lancet* 384, 2027–2035 (Dec. 2014).
5. Xu, L. *et al.* Comparison of clinical and survival characteristics between prostate cancer patients of PSA-based screening and clinical diagnosis in China. *Oncotarget* 9, 428 (Sept. 8, 2017).
6. Groen, L. & Schalken, J. Liquid Biopsy for Prostate and Bladder Cancer: Progress and Pitfalls. *European Urology Focus* 8, 904–906 (July 2022).
7. Marshall, C. H. *et al.* Randomized phase II trial of sipuleucel-T with or without radium-223 in men with bone-metastatic castration-resistant prostate cancer. *Clinical cancer research : an official journal of the American Association for Cancer Research* 27, 1623 (Jan. 15, 2021).
8. Armstrong, A. J. *et al.* Prognostic Association of Prostate-specific Antigen Decline with Clinical Outcomes in Men with Metastatic Castration-resistant Prostate Cancer Treated with Enzalutamide in a Randomized Clinical Trial. *European Urology Oncology* 2, 677–684 (Nov. 1, 2019).

9. Armstrong, A. J. *et al.* Association of Declining Prostate-specific Antigen Levels with Clinical Outcomes in Patients with Metastatic Castration-resistant Prostate Cancer Receiving [177Lu]Lu-PSMA-617 in the Phase 3 VISION Trial. *European Urology* (Sept. 5, 2024).
10. Mendonça Macedo, A., Gameiro Marques, R., Cunha André, M., Silva Figueira, N. & Leal Carvalho, M. Prostate-specific antigen response after Abiraterone treatment in mCRPC: PSA as a predictor of overall survival. *Archivio Italiano Di Urologia, Andrologia: Organo Ufficiale [di] Societa Italiana Di Ecografia Urologica E Nefrologica* 95, 11052 (Feb. 22, 2023).
11. Benoist, G. E. *et al.* Prognostic Value of Novel Liquid Biomarkers in Patients with Metastatic Castration-Resistant Prostate Cancer Treated with Enzalutamide: A Prospective Observational Study. *Clinical chemistry* 66, 842–851 (June 1, 2020).
12. Boerrigter, E. *et al.* RNA Biomarkers as a Response Measure for Survival in Patients with Metastatic Castration-Resistant Prostate Cancer. *Cancers* 13, 6279 (Dec. 14, 2021).
13. Lambros, M. B. *et al.* Single-cell analyses of prostate cancer liquid biopsies acquired by apheresis. *Clinical Cancer Research* 24, 5635–5644 (Nov. 15, 2018).
14. Rushton, A. J., Nteliopoulos, G., Shaw, J. A. & Coombes, R. C. A review of circulating tumour cell enrichment technologies. *Cancers* 13, 1–33 (Mar. 1, 2021).
15. Keup, C., Kimmig, R. & Kasimir-Bauer, S. Combinatorial Power of cfDNA, CTCs and EVs in Oncology. *Diagnostics* 12, 870 (Mar. 31, 2022).
16. Weinstein, J. N. *et al.* The cancer genome atlas pan-cancer analysis project. *Nature Genetics* 45, 1113–1120 (Oct. 1, 2013).
17. Cerami, E. *et al.* The cBio Cancer Genomics Portal: An open platform for exploring multidimensional cancer genomics data. *Cancer Discovery* 2, 401–404 (May 2012).

18. *The Molecular Language of Cancer* in collab. with Ramu, H. Eikbosserweg 276, Hilversum, Feb. 7, 2026.

Chapter 8

Summary

8.1 English Summary

8.1.1 Introduction

Prostate cancer (PCa) is the second most diagnosed cancer in men worldwide, with an estimated 1.4 million diagnoses annually. In 2020, over 375,000 men worldwide died from PCa. The initial steps for diagnosing PCa include a serum prostate-specific antigen (PSA) test and a digital rectal examination (DRE). If PCa is suspected, tissue biopsies are performed for pathological confirmation. Today, magnetic resonance imaging (MRI) is increasingly utilized for diagnosing PCa due to its high sensitivity and specificity in identifying and localizing prostate abnormalities. The shift toward personalized healthcare has led to the emergence of novel PCa-specific therapies, such as targeted radioligand therapies, which deliver radiation directly to cancer cells with minimal impact on surrounding healthy tissue. Advances in immunotherapy, including checkpoint inhibitors and cancer vaccines, are also promising avenues for the clinical management of PCa. Additionally, new generations of hormone therapies are significantly more effective at disrupting androgen signaling, a critical pathway for PCa growth. These treatments aim to tailor clinical intervention by using patient-specific genetic, molecular, and cellular characteristics. As such, there is a clear clinical need to develop novel diagnostic tests to measure therapy-specific treatment responses in patients with PCa.

8.1.2 Chapter Summaries

Chapter 1 examines both the historical and current clinical challenges associated with PCa. It addresses the initial effectiveness and eventual limitations of first-line hormone therapy, emphasizing the crucial role that PSA screening has played in transforming PCa diagnostics and decreasing mortality rates. This chapter also outlines the drawbacks of traditional solid tissue biopsies and highlights the potential advantages of liquid biopsies in providing real-time assessments of PCa. Furthermore, it discusses the clinical challenges in

distinguishing between clinically significant and indolent PCa, emphasizing the need for improved diagnostic methodologies to mitigate the risks of overdiagnosis and overtreatment.

Liquid biopsies, which analyze tumor-derived components in biofluids, provide a less invasive alternative to traditional solid tissue biopsies for cancer diagnosis. Although tumor biopsies offer crucial diagnostic and prognostic insights, their use is often constrained by the risks associated with surgical interventions in the pelvic region. Liquid biopsies facilitate continuous evaluation of biomarkers such as PSA, enabling monitoring of disease progression and treatment responses. In the past decade, several novel tumor-specific molecular biomarkers, including proteins, RNA, and DNA, have been identified in the urine and blood of patients with PCa. Chapter 2 explores the clinical utility of novel urine and blood biomarkers and compares their diagnostic and prognostic efficacy with traditional methods such as serum PSA screening.

Urine has proven to be a valuable source of diagnostic, prognostic, and predictive biomarkers for PCa due to its anatomical connection to the prostate and its lower content of non-malignant cells compared with other biofluids such as blood. The clinical implementation of urine-based tests has enhanced PCa diagnostics by differentiating between indolent disease (or benign prostatic hypertrophy) and clinically significant disease. Although urine-based tests are highly effective in a diagnostic setting, they are less suitable for PCa prognosis.

Epithelial cells can release molecular signals into the bloodstream through both passive processes, such as cell death, and active ones, such as exosome secretion. Oncogenic processes, such as proliferation, dedifferentiation, and metastasis, are major sources of circulating tumor material in epithelial cancers, making blood an effective medium for liquid biopsies in localized and metastatic PCa. Circulating biomarkers can indicate disease progression, survival, and therapy response in PCa, supporting treatment stratification

and monitoring. However, routine clinical use is hindered by the low concentration of tumor-derived material in blood and the need for highly sensitive detection technologies.

Chapter 3 highlights the untapped potential of long non-coding RNAs (lncRNAs) in PCa as a source of biomarkers with high specificity for disease stage and grade. Transcriptome analysis of lncRNAs in benign and clinically significant PCa revealed several uncharacterized lncRNAs linked to high-grade PCa. In silico analyses highlighted *NAALADL2-AS2* as a cancer-specific antisense lncRNA, prominently expressed in PCa and associated with resistance to hormone therapy. Additionally, *NAALADL2*, a sense-strand neighbor and established oncogene, was observed to be co-expressed with *NAALADL2-AS2*. In vitro experiments showed that *NAALADL2-AS2* expression increases with exposure to hormone therapy and supports tumor-cell survival by modulating glycogen metabolism and inhibiting apoptosis. These findings imply that *NAALADL2-AS2* may play a role in PCa progression and could be a promising biomarker or therapeutic target for hormone-sensitive PCa.

Developing a molecular grading system for PCa could revolutionize traditional tumor grading, enhancing diagnostics, therapy selection, and monitoring. Chapter 4 reveals that *NAALADL2-AS2*, an androgen-regulated lncRNA, strongly correlates with luminal PCa subtypes. Most primary PCa cases are luminal, showing significant differences in disease progression and response to postoperative hormone therapy. Therefore, *NAALADL2-AS2* expression levels could serve as a biomarker for luminal tumors, offering crucial insights into PCa pathogenesis and guiding therapy selection.

Although the prognostic value of circulating tumor cells (CTCs) in advanced PCa is evident, these cells are primarily utilized as surrogate biomarkers for tumor burden in clinical trials and have not yet been widely adopted in clinical practice. Chapter 5 examines the prognostic utility of molecular profiling of CTCs in clinically significant and metastatic PCa through

multiplex RNA hybridization analysis. Tumor cells were captured using a Food and Drug Administration (FDA)-approved, label-free CTC microfluidic system to minimize selection bias and facilitate the capture of molecularly diverse CTCs. This enabled the assessment of multiple distinct oncogenic pathways in patients undergoing hormone and/or chemotherapy. CTC transcriptome profiling successfully prognosticated disease progression and survival in therapy-specific and therapy-agnostic cohorts, indicating that CTC transcriptomes could be predictive of therapy response in PCa.

In conclusion, this thesis demonstrates the added value of liquid biopsies and transcriptome profiling in the diagnosis and clinical management of PCa. The identification of *NAALADL2-AS2* as a novel biomarker for hormone-sensitive luminal PCa not only highlights the clinical relevance of lncRNAs but also opens avenues for further investigation into their therapeutic potential.

8.2 Nederlandse Samenvatting

8.2.1 Introductie

Prostaatkanker (PCa) is wereldwijd de op één na meest gediagnosticeerde kanker bij mannen, met naar schatting 1,4 miljoen diagnoses per jaar. In 2020 overleden wereldwijd meer dan 375.000 mannen aan PCa. De eerste stappen voor het diagnosticeren van PCa omvatten een serum-PSA-test en een DRE. Als PCa wordt vermoed, worden weefselbiopsieën uitgevoerd voor pathologisch onderzoek. Tegenwoordig wordt MRI steeds vaker gebruikt voor het diagnosticeren van PCa vanwege de hoge gevoeligheid en specificiteit bij het identificeren en lokaliseren van afwijkingen in de prostaat. De verschuiving naar gepersonaliseerde gezondheidszorg heeft geleid tot de opkomst van nieuwe PCa-specifieke therapieën, zoals gerichte radioligandtherapieën, die straling rechtstreeks naar kankercellen brengen met minimale impact op omliggend gezond weefsel. Vooruitgang in immunotherapie, waaronder checkpoint-remmers en kankervaccins, vormt een veelbelovende mogelijkheid voor de klinische behandeling van PCa. Daarnaast zijn nieuwe generaties hormoontherapieën significant effectiever in het verstoren van androgeensignalering, een cruciale groeifactor voor PCa. Deze behandelingen zijn gericht op het aanpassen van klinische interventies door gebruik te maken van patiëntspecifieke genetische, moleculaire en cellulaire kenmerken. Er is ook een duidelijke klinische behoefte aan de ontwikkeling van nieuwe diagnostische testen om therapie-specifieke behandelingsresponsen bij PCa-patiënten te meten.

8.2.2 Samenvatting per Hoofdstuk

Hoofdstuk 1 onderzoekt zowel de historische als huidige klinische uitdagingen bij PCa. Het behandelt de initiële effectiviteit en uiteindelijke beperkingen van eerstelijns hormoontherapie en benadrukt de cruciale rol die PSA-screening heeft gespeeld bij het verbeteren van de PCa-diagnostiek en het

verlagen van sterftecijfers. Dit hoofdstuk schetst ook de nadelen van traditionele vaste weefselbiopsieën en belicht de potentiële voordelen van vloeibare biopsieën bij het bieden van een real-time beeld van PCa. Verder bespreekt het de klinische uitdagingen bij het onderscheiden van klinisch significante en indolente PCa en benadrukt het de noodzaak van verbeterde diagnostische methoden om de risico's van overdiagnose en overbehandeling te verminderen.

Vloeibare biopsieën, die tumor-afgeleide componenten in biofluïda analyseren, bieden een minder invasief alternatief voor traditionele vaste weefselbiopsieën voor kankerdiagnose. Hoewel tumorbiopsieën cruciale diagnostische en prognostische inzichten bieden, wordt hun gebruik vaak beperkt door de risico's die gepaard gaan met chirurgische ingrepen in het bekkengebied. Vloeibare biopsieën vergemakkelijken de continue evaluatie van biomarkers zoals PSA, waardoor monitoring van ziekteprogressie en behandelingsresponsen mogelijk wordt. In het afgelopen decennium zijn verschillende nieuwe tumorspecifieke moleculaire biomarkers, waaronder eiwitten, RNA en DNA, geïdentificeerd in de urine en het bloed van PCa-patiënten. Hoofdstuk 2 onderzoekt de klinische bruikbaarheid van nieuwe biomarkers in urine en bloed en vergelijkt hun diagnostische en prognostische effectiviteit met traditionele methoden zoals serum PSA-screening.

Urine is een waardevolle bron van diagnostische, prognostische en voorspellende biomarkers voor PCa vanwege de anatomische verbinding met de prostaat en de lagere inhoud van niet-malignante cellen in vergelijking met andere biofluïda zoals bloed. De klinische implementatie van op urine gebaseerde tests heeft PCa-diagnostiek verbeterd door onderscheid te maken tussen indolente of goedaardige prostaathypertrofie en klinisch significante ziekte. Hoewel op urine gebaseerde tests zeer effectief zijn in een diagnostische setting, zijn ze minder geschikt voor de prognose van PCa. Epitheelcellen kunnen moleculaire signalen in de bloedbaan afgeven via zowel passieve processen, zoals celdood, als actieve processen, zoals exosoomafscheiding. Oncogene processen, zoals proliferatie, dedifferentiatie en metastase, zijn belangrijke bronnen van circulerend tumormateriaal bij epitheliale kankers,

waardoor bloed een geschikt medium is voor vloeibare biopsieën bij zowel gelokaliseerde als gemetastaseerde PCa. Circulerende biomarkers zijn goede indicatoren voor ziekteprogressie, overleving en therapierespons bij PCa, wat behandelingsstrategieën en -resultaten kan verbeteren. Routinematig klinisch gebruik wordt echter belemmerd door de lage concentratie van tumor-afgeleid materiaal in bloed en de behoefte aan zeer gevoelige detectietechnologieën. Hoofdstuk 3 bespreekt de analyse van lncRNA-expressiedata in goedaardige en klinisch significante PCa, wat leidde tot de ontdekking van verschillende ongekarakteriseerde lncRNA's die gekoppeld zijn aan significante PCa. In silico analyses identificeerden *NAALADL2-AS2* als een kankerspecifieke antisense lncRNA, sterk uitgedrukt bij PCa en geassocieerd met castratieresistentie. NAALADL2, sense-strand verwante en bekende oncogen, bleek co-uitgedrukt te zijn met *NAALADL2-AS2*. In vitro experimenten suggereren dat *NAALADL2-AS2* expressie toeneemt bij blootstelling aan ADT (bijv. hormoontherapie), wat de overleving van tumorcellen bevordert door glycogeenmetabolisme te moduleren en apoptose te remmen. Deze bevindingen impliceren dat *NAALADL2-AS2* een rol kan spelen bij de progressie van PCa en mogelijk een doelwit is voor toekomstige therapieën.

Het ontwikkelen van een moleculair gradatiesysteem voor PCa zou de traditionele tumorgraad revolutioneren, waardoor diagnostiek, therapiekeuze en monitoring worden verbeterd. Hoofdstuk 4 onthult dat *NAALADL2-AS2*, een door androgenen gereguleerd lncRNA, sterk correleert met luminale PCa-subtypes. De meeste primaire PCa-gevallen zijn luminaal, met aanzienlijke verschillen in ziekteprogressie en respons op postoperatieve hormoontherapie. Daarom kunnen *NAALADL2-AS2*-expressieniveaus een biomarker zijn voor luminale tumoren, wat cruciale inzichten biedt in de pathogenese van PCa en therapiekeuze leidt.

Hoewel CTC's bij PCa duidelijke prognostische waarde hebben, met name bij gevorderde ziekte, zijn ze nog niet breed geadopteerd in de klinische behandeling van PCa en dienen ze voornamelijk als surrogaat biomarker voor tumorlast in klinische onderzoeken. Hoofdstuk 5 onderzoekt de prognostische waarde

van moleculaire profilering van CTC's bij klinisch significante en gemetastaseerde PCa door middel van multiplex RNA-hybridisatieanalyse. Door gebruik te maken van het label-vrije microfluïdische CTC-verrijkingssysteem Parsortix PC1 werd selectie-bias verminderd, wat resulteerde in een representatiever tumormonster, dan die verzameld met EpCAM-gebaseerde positieve-selectie CTC-verrijkingsplatformen zoals CellSearch. Deze benadering gebruikt vloeibare biopsieën en high-throughput moleculaire subtypering om de beoordeling van oncogene routes mogelijk te maken bij patiënten die hormoontherapie en/of chemotherapie ondergaan. CTC-transcriptome profiling gaf met succes progressie- en overlevingspercentages aan, wat potentieel biedt voor het voorspellen van therapierespons.

Concluderend, hoewel verder onderzoek nodig is, tonen de bevindingen van deze thesis duidelijk de toegevoegde waarde van vloeibare biopsieën en tumortranscriptoomprofilering aan voor de diagnose en therapeutische toepassingen in PCa. In het bijzonder benadrukt het onderzoek de relatie tussen de expressieniveaus van het lncRNA *NAALADL2-AS2* en luminale PCa-subtypes.

Chapter 9

Appendices: List of Publications, Portfolio, Curriculum Vitae, and Acknowledgments

9.1 List of Publications

1. Groen, L. et al. The Expression of NAALADL2-AS2 Associates with Androgen-sensitive Luminal Prostate Cancer Subtypes. *IJMS* under peer review, (2025).
2. Groen, L. et al. Transcriptome Profiling of Circulating Tumor Cells to Predict Clinical Outcomes in Metastatic Castration-Resistant Prostate Cancer. *IJMS* 24, 9002 (2023).
3. Groen, L. et al. The Androgen-Regulated lncRNA NAALADL2-AS2 Promotes Tumor Cell Survival in Prostate Cancer. *Non-coding RNA* 8, 81 (2022).
4. Groen, L. et al. Liquid Biopsy for Prostate and Bladder Cancer: Progress and Pitfalls. *EU Focus* 8, 904–906 (2022).
5. Groen, L. et al. RNA Biomarkers as a Response Measure for Survival in Patients with Metastatic Castration-Resistant Prostate Cancer. *Cancers* 13, 6279 (2021).
6. Groen, L. et al. Liquid biopsy reveals KLK3 mRNA as a prognostic marker for progression-free survival in patients with metastatic castration-resistant prostate cancer undergoing first-line abiraterone acetate and prednisone treatment. *Molecular Oncology* 15, 2453–2465 (2021).
7. Groen, L. et al. Clinical utility of emerging biomarkers in prostate cancer liquid biopsies. *Expert Review of Molecular Diagnostics* 20, 219–230 (2020).
8. Groen, L. et al. Prognostic Value of Novel Liquid Biomarkers in Patients with Metastatic Castration-Resistant Prostate Cancer Treated with Enzalutamide: A Prospective Observational Study. *Clinical Chemistry* 66, 842–851 (2020).

9.2 Portfolio

To be included from hora finita...

9.3 Research Data Management

All human studies included in this thesis were conducted according to the principles outlined in the Declaration of Helsinki and comply with Dutch national regulations regarding the ethical use of human samples. The medical and ethical review board "Committee on Research Involving Human Subjects Region Arnhem-Nijmegen, Nijmegen, the Netherlands" granted approval for conducting the described studies.

Data obtained throughout this PhD research have been managed and archived in compliance with the Findable, Accessible, Interoperable, and Reusable (FAIR) principles. Laboratory experiments and related procedures performed during this thesis were comprehensively documented using digital laboratory notebooks stored centrally and securely backed up on the Radboudumc server.

Specifically, data utilized for Chapters 1 and 2, derived from published review articles (Groen & Schalken, 2022 and Boerrigter et al., 2020), are accessible through their respective journal repositories and are cited accordingly in the manuscript. Sequencing data and associated transcriptomic analyses described in Chapter 3 are securely stored on the local server infrastructure of the Department of Urology at Radboudumc and deposited in the designated public repository as specified in the corresponding publication.

Data supporting the research findings of Chapter 4, currently under peer review (Groen, submitted), were obtained from the online repository The Cancer Genome Atlas (TCGA) Program. For Chapter 5, which describes transcriptome profiling of circulating tumor cells, all primary data generated are stored digitally at Radboudumc and are publicly accessible through the International Journal of Molecular Sciences (IJMS) open-access framework (Chapter 5).

De-identified clinical data integrated within Chapters 3, 4, and 5 have

been systematically captured and maintained within the electronic data-capture system Castor, ensuring confidentiality and compliance with privacy regulations. All research data related to this thesis will remain securely archived and available for 15 years post-study completion, in accordance with Radboudumc guidelines. Additional supporting data may be requested from the corresponding author upon reasonable request.

9.4 Curriculum Vitae

Levi Groen was born on May 9, 1992, in Leusden, The Netherlands. Raised in California, he began high school in Dana Point, USA, and later completed it at the International School Hilversum, where he graduated with an International Baccalaureate diploma. He pursued a Bachelor of Science in pre-medical studies at Roosevelt University College in Middelburg, part of Utrecht University, graduating in 2014. Levi then completed a master's degree in the Biology of Disease at Utrecht University in 2017. That same year, Levi began his graduate research on "Discovering Actionable Alterations Through Liquid Biopsies and Transcriptomics in Prostate Cancer" at Radboud University Medical Center (Radboudumc) in Nijmegen, The Netherlands, under the guidance of Professor Dr. Jack Schalken. From 2022 to 2024, he further expanded his focus, working on a bladder cancer research project alongside Dr. Niven Mehra at Radboudumc. Since 2018, his research has culminated in eight published peer-reviewed articles to which he has contributed.

9.5 Acknowledgments

I am immensely grateful to the patients and volunteers whose participation was crucial to this research. Their contributions have been invaluable and made this work possible. I hope that this research can contribute to a better prognosis for newly diagnosed prostate cancer (PCa) patients. I owe a debt of gratitude to my supervisors for their expert guidance and support throughout this journey. Jack Schalken provided me with the opportunity to pursue a doctorate in molecular life sciences, giving me the freedom to explore and conduct my research. His supervision of the molecular aspects of this study has been instrumental in shaping the direction and execution of my work. Niven Mehra enabled essential collaborations with the medical oncology department, facilitating the clinical translation of our findings. His insights and supervision on the medical side of the research were crucial for integrating clinical perspectives with molecular sciences, creating a balanced approach to our study. I would also like to thank Gerald Verhaegh, who, as my daily supervisor, provided continuous guidance and support. His expertise and mentorship were vital in helping me navigate the challenges of this project and ultimately bring it to fruition. Furthermore, I must acknowledge my colleagues at the Experimental Urology lab. The technicians, in particular, have provided an indispensable foundation for my work. Their support and assistance enabled me to pursue various research interests and gave me a shoulder to lean on during challenging times. Each of these individuals has left a significant mark on my work, and I am thankful for their contributions to my academic and personal growth.

I would like to extend my thanks to Frank Smit and the MDxHealth team for their technical support and for introducing me to the Experimental Urology lab. Access to specialized analytical equipment greatly streamlined my research, cutting down on both the time and costs involved in my experiments.

Special thanks to Peter Collins, Chief Executive Officer of CelLBxHealth plc,

and the CelLBxHealth team for providing crucial equipment that supported completion of my PhD thesis (Parsortix PR1 system). I would also like to thank Paul Smith, David Englert, and Kelly Seto for their technical and analytical assistance.

In addition, I would like to express gratitude to my students, whose contributions were essential to the study of lncRNAs in PCa. Their dedication, hard work, and insight enabled the discovery of a novel lncRNA, *NAALADL2-AS2*, and shed light on its molecular function in PCa.

I would like to thank my parents, Jan Groen and Charlotte Burgmans, for their support throughout this challenging journey. A special thanks to my friends and family for supporting me throughout this transformative phase of my life.

Finally, I would like to thank the members of the manuscriptcommissie for their patience and contribution toward this special moment.

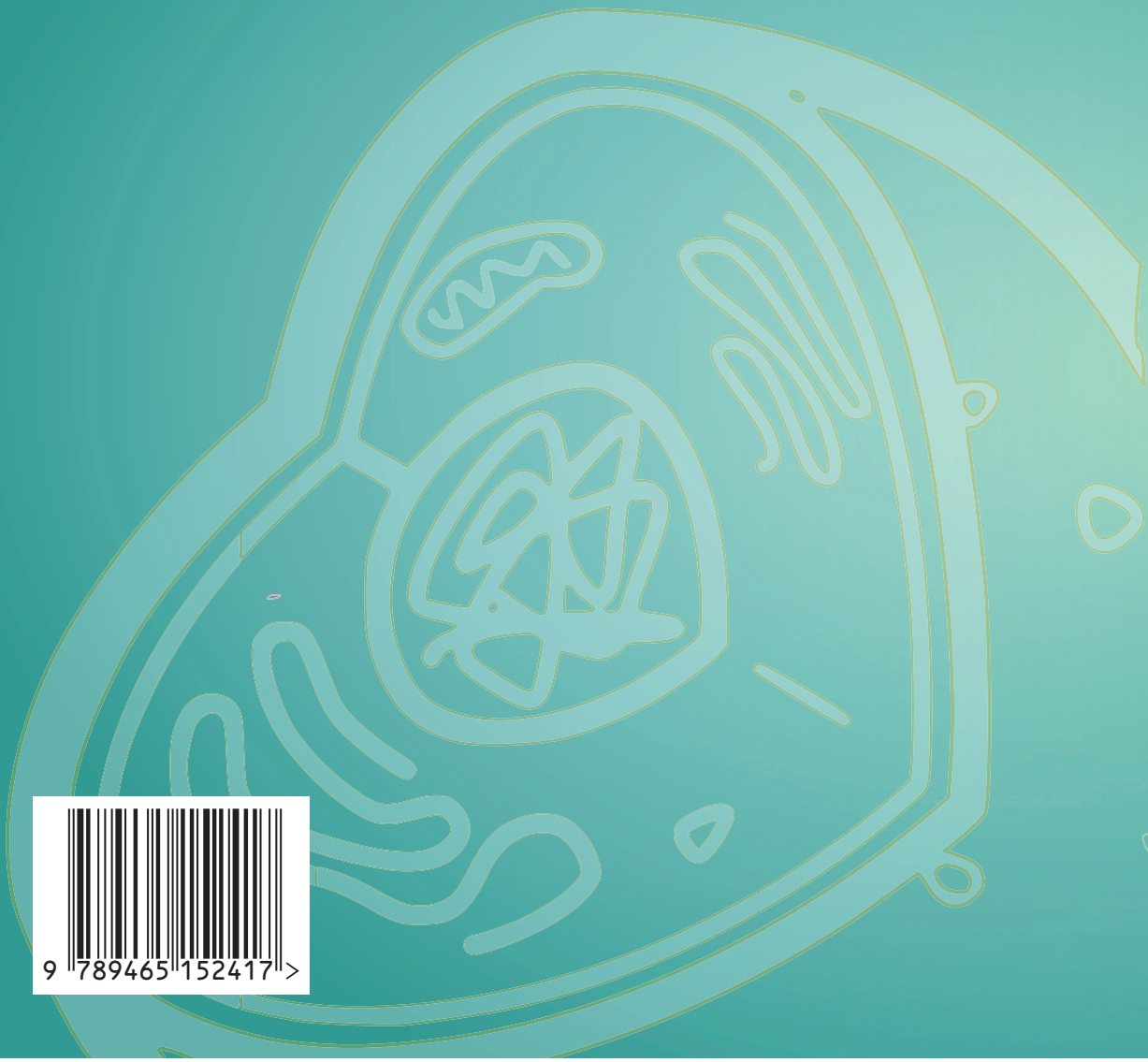

9 789465 152417 >

Radboudumc university medical center

IN DEI NOMINE FELICITER

Radboud University